RESEARCH ON
ENVIRONMENTAL RADIOACTIVITY

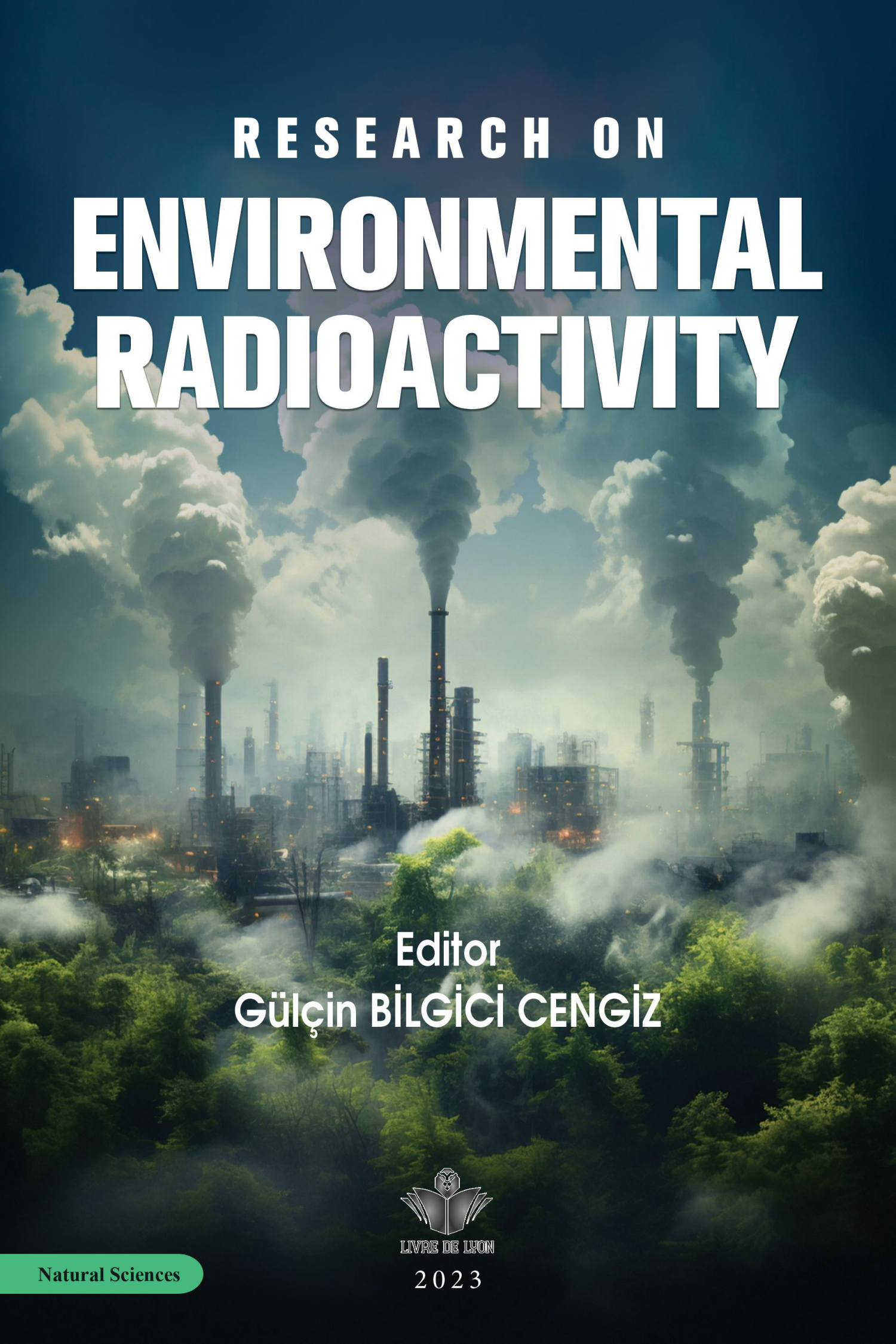

Editor
Gülçin BİLGİCİ CENGİZ

LIVRE DE LYON
2023

Natural Sciences

Research on Environmental Radioactivity

Editor
Gülçin BİLGİCİ CENGİZ

LIVRE DE LYON
Lyon 2023

Research on Environmental Radioactivity

Editor
Gülçin BİLGİCİ CENGİZ

LIVRE DE LYON
Lyon 2023

Research on Environmental Radioactivity

Editor • Assoc. Prof. Dr. Gülçin Bilgici Cengiz • Orcid: 0000-0002-6164-3232
Cover Design • Motion Graphics
Book Layout • Motion Graphics

First Published • December 2023, Lyon

e-ISBN: 978-2-38236-641-7

DOI:10.5281/zenodo.10442949

Publisher • Livre de Lyon
Address • 37 rue marietton, 69009, Lyon France
website • http://www.livredelyon.com
e-mail • livredelyon@gmail.com

LIVRE DE LYON

PREFACE

The natural or artificial radiation that people are exposed to in their environment creates the natural background radiation level. Every substance existing on Earth contains even a small amount of radioactive atoms. The natural contribution to environmental radiation comes from radioactive substances present in trace amounts in the earth's crust, inhaled air, drinking water and food, and space-borne cosmic radiation. In addition, artificial radioactive substances are used in medicine and industry, and nuclear weapon tests, leaks, and accidents in nuclear power plants also cause an increase in environmental radiation levels. Living organisms are generally continuously exposed to cosmic and other terrestrial ionizing radiation. However, exposures vary between localities due to altitude and geological characteristics. Other human activities also contribute to increased exposure to ionizing radiation.

Regarding radiation protection, there are many international organizations such as the United Nations Scientific Committee on the Effects of Atomic Radiation (UNSCEAR), the International Atomic Energy Agency (IAEA), the World Health Organization (WHO), and the International Standards Organization (ISO). The first institution working on this subject was the International Commission on Radiological Protection (ICRP), which was established in Stockholm in 1928.

In Turkey, this task was undertaken by the Turkish Atomic Energy Agency (TAEK), which operated between 1956 and 2020 and was established to guide Turkey's radiation and nuclear energy policies. The Turkish Energy Nuclear and Mining Research Institute (TENMAK), which includes the Turkish Atomic Energy Agency, the National Boron Research Institute, and the Rare Earth Elements Research Institute under the Ministry of Energy and Natural Resources, was established in 2020, replacing TAEK.

Environmental radiation, whether natural or human-induced, can cause potential harm to living things in the environment. It is known that ionizing radiation can cause genetic mutations and cancer. It can also cause thermal damage due to the heating effect. It may have negative effects on living species and habitats in ecosystems.

Routine implementation of environmental radioactivity monitoring programs to determine natural radiation levels to which humans are exposed and to detect significant changes in environmental radiation levels also prepares and supports and enhances existing capacity to deal with radiological emergencies.

In the first chapter of the book, information is given about radioactivity, natural and artificial environmental radioactivity, and the effects of the resulting environmental radiation on living things. The radiation protection system, which aims to minimize radiation exposure and reduce potential health risks, is also explained in detail in this section.

Building materials made of stone and soil may contain low levels of radioactivity. Thus, people can be exposed to radiation inside buildings and outside their living spaces. In the second chapter of the book, the results of research conducted in Turkey to determine the activity of gamma radiation emitted from ^{226}Ra, ^{232}Th, and ^{40}K radioactive isotopes contained in building materials frequently used in various regions of Turkey were compiled.

Cancer is one of the most serious health problems that threaten human life. When the 2020 data of the International Agency for Research on Cancer (IARC) is examined; A significant proportion of deaths worldwide are reported to be due to cancer, with an estimated millions of new cancer cases occurring. It is observed that 18% of all cancer deaths in 2020 were caused by lung cancer. Epidemiological studies conducted to date show that there is a direct relationship between radon exposure and lung cancer occurrence (ICRP, 2010). In the third chapter of the book, radon, which is among the most dangerous carcinogenic substances, and the variation in indoor atmospheric radon concentration depending on altitude, where we spend most of our time, are investigated.

It is known that increased reactive oxygen (ROS) levels and the products of oxidative stress are associated with cancer. Many factors lead to an increase in ROS levels in cells. Scientific research reports that oxidative stress is highly intertwined with various cancers (such as lung cancer, colorectal cancer, breast cancer, hepatocellular cancer, and cervical cancer). To identify more effective therapeutics against cancer, it is necessary to know the ROS mechanism in carcinogenesis. In the fourth chapter of this book, information is given about ROS and its relationship with cancer.

ALARA (As Low As Reasonably Achievable) is a safety policy designed to minimize radiation doses and release of radioactive material. Individual monitoring of workers exposed to external ionizing radiation is essential to allow the application of the ALARA principle and to follow official dose limits. In the fifth chapter, an electronic dosimeter system, which has been used by the radiation safety division of TARLA (Turkish Accelerator and Radiation Laboratory in Ankara), was introduced.

In the sixth chapter of the book, the radiation absorption behaviours of various chemotherapy drugs used in cancer treatment are compiled from various

research articles in the literature. Additionally, it has been emphasized that the differences in the types of elements in drugs and the number of atoms in the elements greatly impact the photon interaction parameters.

Today, from the discovery of radiation, radiation technology, energy production, medical applications, space technologies, etc. It is widely used in many areas such as. However, since radiation exposure has inevitable bad consequences for humans, many materials are used as shielding materials to protect against the harmful effects of radiation. Research on non-toxic, light, flexible, and cost-effective radiation protection materials that will replace traditional protective materials is continuing in the world and Turkey. In chapters seven and eight, two studies are given on the effect of Nd_2O_3 doping on the radiation protection properties of tungsten tellurium glasses and the synthesis of some antimony-based glasses' gamma radiation protection properties.

I hope this book will be useful to academicians and readers who want to be informed about the current situation in environmental radioactivity and environmental radiation studies. Assoc. Prof. Dr. Gülçin Bilgici Cengiz would like to thank all the authors who contributed to bringing this book to its current state by giving their valuable time, knowledge, and interest, as well as the Livre de Lyon publishing team.

Assoc. Prof. Dr. Gülçin Bilgici Cengiz

CONTENTS

CHAPTER I

ENVIRONMENTAL RADIATION AND ITS EFFECTS ON PEOPLE

Gülçin BİLGİCİ CENGİZ

(Assoc. Prof. Dr.) Kafkas University, Faculty of Science and Letters, Department of Physics, Kars, Turkey
E-mail:gulcincengiz@kafkas.edu.tr,
ORCID: 0000-0002-6164-3232

1. Introduction

Environmental radiation is the ubiquitous presence of radiation from natural or artificial sources. Natural radiation sources include the sun, earth, water, cosmic radiation from space, and natural radioactive materials found underground. Artificial radiation sources include radiation from human activities such as medical applications, nuclear power plants, industrial activities, and nuclear weapons testing.

Today's nuclear weapons tests and nuclear accidents cause a global increase in the level of environmental radioactivity. Due to increased radioactivity, all living organisms are inevitably and continuously irradiated by these radiation sources. The local increase in environmental radioactivity may reach dimensions that will harm the ecosystem in that region.

This article provides information about natural and artificial environmental radioactivity and the effects of the resulting environmental radiation on living things.

2. Natural Radiation Sources

Natural sources of radiation refer to the types of radiation naturally found in our environment and associated with the normal functioning of nature. As seen in Figure 1, these sources are caused by factors such as sunlight, cosmic rays, radioactive substances found in underground and aboveground rocks, drinking water, and radioactive isotopes found in some foods (Issa et al.,2014).

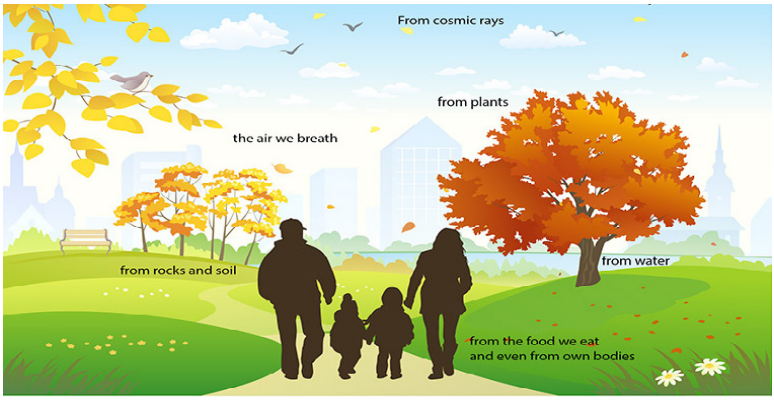

Figure 1. Natural radiation sources (Retrieved from Canadian Nuclear Safety Commission)

2.1. Cosmic Rays

Sunlight is the most important source of natural radiation. The sun provides energy by emitting radiation in different parts of the electromagnetic spectrum. This radiation includes ultraviolet (UV), visible light, and infrared rays of various wavelengths and frequencies. Sunlight plays an important role in the photosynthesis of plants, the synthesis of vitamin D, and the warming of air and water (Neville et al., 2020; Caridi et al., 2019).

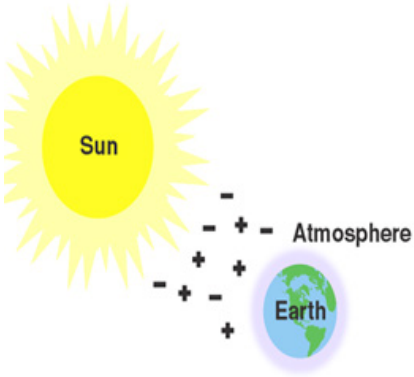

Figure 2. Cosmic Radiation

Cosmic rays are high-energy particles from outer space. These particles usually come from outside the Solar System and are absorbed by our atmosphere. High-energy cosmic rays collide in the upper layers of the atmosphere, transferring energy to atoms and molecules in the atmosphere. As a result of these interactions, radioactive particles are formed in the atmosphere and radiation is naturally emitted (Figure 2) (UNSCEAR, 2000; Safarov et al., 2023).

2.2. Terrestrial Radiation

Terrestrial radiation originates from radioisotopes of the natural radioactive series present in the earth's crust. It is estimated that many isotopes were radioactive when the universe was just beginning to form. It is accepted that this situation lasts for several million years and that radionuclides with short half-lives become extinct because they complete their lives during this period. Since the half-lives of currently existing radionuclides are long enough to be compared to the lifespan of the universe (at least 10^{10} years), decay continues (NRC, 1999; Vuruş, 2013). The decay of radioactive elements found naturally on Earth causes irradiation. Therefore, it would not be wrong to say that the earth itself is a source of radiation. Rocks and minerals, soil, and earth contain radioactive nuclei. (Yachiso et al., 2023)

Radioactive materials found in underground and aboveground rocks are also natural sources of radiation. Due to its geological structure, Turkey has rich radioactive mineral resources in many regions. For example, radioactive gases (such as radon) are released in coal mines in the provinces of the Black Sea region. (Baldık, 2006). In addition, rocks containing radioactive minerals such as granite are found in the Taurus Mountains and Eastern Anatolia Region. These radioactive substances are released into the environment through groundwater and soil (Aykamış and Kılıç, 2009; Turhan et al., 2018; Bilgici Cengiz and Çağlar, 2022).

2.3. Radon Gas

Radon, which is colorless, odorless, and tasteless and is in the noble gases class of the periodic table with atomic number 86, is formed as a result of the radioactive decay of natural uranium found in rocks, soil, and water. The main atoms of this degradation chain can be found in all-natural materials. For this reason, radon is released into the environment from all rock and soil fragments and building materials on the surface (UNSCEAR, 2008). Since radon's reactivity is weak, it does not chemically bind to tissues when inhaled. Although its solubility in tissues is very low, radon decay products bind to dust and other particles and form radioactive aerosols. Therefore, they can be transported and taken into the living body by breathing. (WHO, 2009).

Decomposition continues until the degradation products become stable; Radiation is released at every stage of the decay process. As a result of deterioration in the respiratory tract, the radiation dose to the bronchial epithelium increases. The biological effects of alpha radioactivity become important because some of its decay products are alpha emitters. Radon gas undergoes radioactive decay

and turns into particles that can be captured by the lungs when inhaled. When the decay of these particles continues, the energy released causes damage to lung tissue and, over time, cancer. However, this does not mean that everyone exposed to high doses of radon will develop lung cancer. (Kaur and Singh, 2019). Since people generally spend almost 90% of their time indoors, radon exposure is a significant problem. Most sources of radon in buildings are the soil and rocks at the building's foundation. Most radon enters buildings through soil or underlying rocks. Radon and other gases rise from the soil and become trapped under the building (Kürkçüoğlu, and Çine, 2017). These trapped gases create pressure. Air pressure in homes is usually lower than the pressure on the ground. Due to this high pressure under the building, gases leak into the building from the floor and walls, mostly through cracks and gaps, as shown schematically in Figure 3 (Kürkçüoğlu, and Bayraktar, 2014). Radon can also dissolve in water, especially groundwater. Typically, 1/10,000 of the radon in tap water is released into the air. As the amount of radon in the water increases, the radon level inside the building will also increase. Trace amounts of uranium found in building materials used in the construction industry are one of the factors that increase the radon level in buildings. Some of the factors that cause differences in radon gas concentration in homes include local geology, permeability of the soil, construction material, and ventilation of buildings (UNEP, 2016; Bilgici Cengiz et al., 2017).

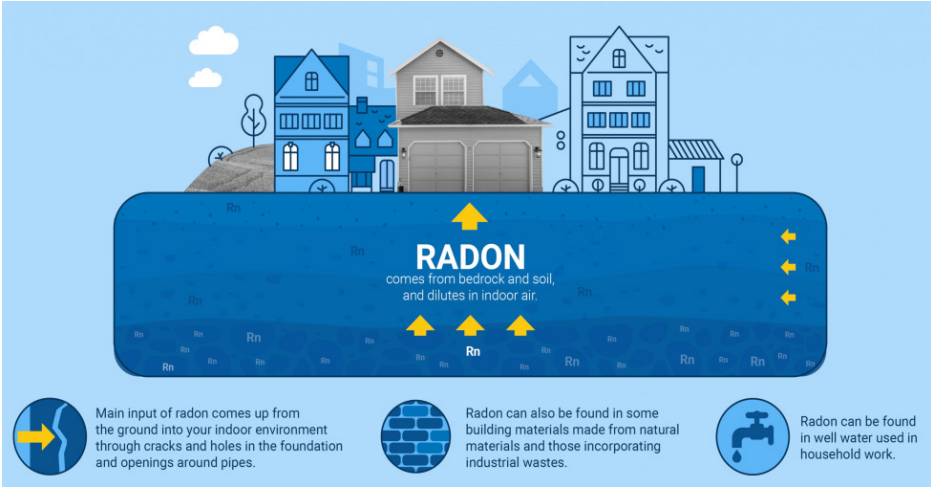

Figure 3. Ways of radon entry into buildings (Adapted from Ref. UNEP 2016; Open-source content for public information)

As a result of heating houses, especially in cold weather, the pressure inside the house decreases and the pressure outside increases, and therefore the radon rate inside increases. Since the same situation applies in windy weather, the radon rate increases indoors. In summer months, in well-ventilated workplaces and homes, the radon level in the environment decreases as there will be no pressure difference from the outside (Küçükönder, 2021).

2.4. Natural Radioactivity in Food

Drinking water and some foods also naturally contain radioactive isotopes. For example, radioactive isotopes originating from basalt rocks may pass into groundwater and be found in drinking water (Caridi et al., 2023). Likewise, some minerals can be taken up by soils and plants, causing the build-up of radioactive isotopes in food (Al-Hamarneh, et al., 2016; Nguyen, et al., 2018). In Turkey, research and measurements on this subject are carried out, potential risk areas are determined in terms of radioactive isotopes and precautions are taken (Bilgici Cengiz and Caglar, 2022; Canbazoğlu and Doğru, 2013; Görür et al., 2012).

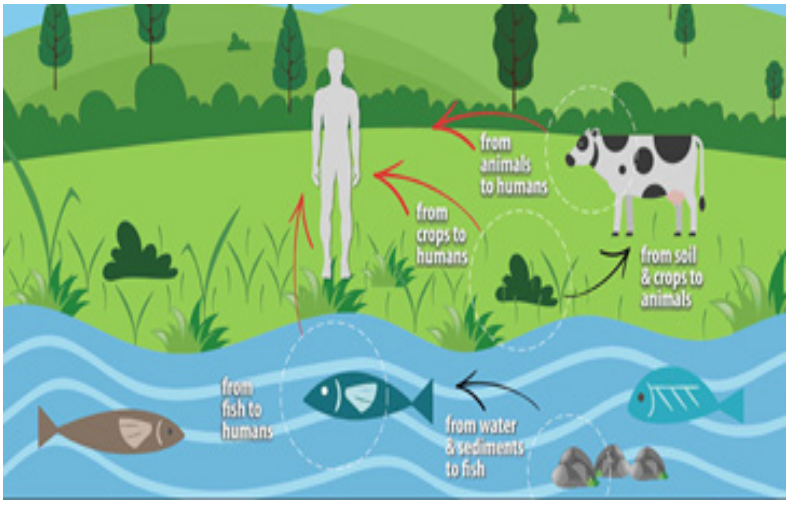

Figure 4. Natural radioactivity in food

All foods contain natural radionuclides, which are transferred from the soil to the crops on land and from water to fish in rivers, lakes, and the sea. Figure 4 shows the pathways of natural radionuclides in food to humans through ingestion. Levels of natural radionuclides in food and drinking water are generally very low and safe for human consumption. However, they can vary

considerably depending on local geology, climate, and agricultural practices (Peli´c et al., 2023; Howard, 2021; Bilgici Cengiz, 2020)

2.5. Internal Radiation

All humans are exposed to radiation due to isotopes such as Potassium-40 and Carbon-14 that are naturally present in their bodies. Although dose amounts vary from person to person, the dose amounts resulting from internal radiation are much less than the Cosmic and Earth-based doses (Hutchison and Hutchison, 1997).

3. Artificial (Man-Made) Radiation Sources

Radiation is used in many areas of our lives, such as medical, industrial, research, education, security applications, and consumer products. These and similar artificial sources increase the radiation dose from natural sources for both individuals and the world population (Wielopolski, 2013).

3.1. Medical Applications

Most of the radiation received from artificial sources is of medical origin. Medically derived radiation is of particular concern for patients exposed to diagnostic X-rays or radiotherapy and nuclear medicine used for diagnosis and treatment. Doses obtained from medical applications are higher than doses obtained from other man-made sources (UNSCEAR, 2000).

In the field of Nuclear Medicine, in order to examine the functions of organs or tissues in the body, some radioactive substances are combined with a chemical substance that will cause the radioactive substance to temporarily accumulate in the tissue to be examined and is administered to the body. The distribution or flow of radioactive material in the body is obtained by devices capable of detecting gamma rays released from radioactive material entering the body (UNSCEAR, 2000).

Radiography is a technique for imaging the internal structure of objects with opaque and heterogeneous structures, such as the human body, by using electromagnetic radiation with higher energy than visible light. The most used type of electromagnetic radiation is X-rays, after X-rays, gamma rays are the most used. The most commonly used radiography methods are X-ray, tomography, and computed tomography (Watson et al.,2005).

X-ray devices used in the diagnosis of diseases or injuries send X-rays to the area to be examined. The x-ray passes through the patient's body and images the area of interest. X-ray sources have the largest share in the amount of radiation exposure from medical sources.

Radiotherapy is used in cancer treatment. Gamma rays originating from the cobalt-60 isotope are frequently used in radiotherapy applications. In radiotherapy, high amounts of radiation must be applied to the tissue to kill tumors or neutralize harmful cells in cancerous tissue. This irradiation can be hazardous to healthy tissues in the body of the patient receiving treatment. Therefore, radiotherapy is used only in the most serious cases or when no other treatment method is possible or effective (Mehta et al., 2010). Just like X-ray imaging devices, radiotherapy devices are being developed day by day. Studies are being carried out to expose only the relevant tissue to radiation and minimize surrounding healthy cells' irradiation (IAEA, 2018).

3.2. Industrial Applications

Radiation sources are frequently used in industry. Some of the applications involving the use of radiation sources in industry are listed below:

• Pipe, steam boiler, etc. radiography technique is used to check whether there are any defects in machine parts.

• Appropriate radionuclides are used in tests related to component wear in the automotive industry.

• Iron, steel, rubber, yarn, glass, etc. Radiation sources are used to measure properties such as density, level, thickness, and weight during the production of materials.

• Nuclear measuring devices are used to determine the density and chemical elements of rocks. Oil and mineral searches are also carried out with similar devices.

• Radiation sources are also used in other industrial applications such as monitoring groundwater movements, measuring flow in streams, and detecting water leaks in dams.

• Radiation is also used to preserve food after it is produced. In many countries, including Turkey, different foods are irradiated to prevent them from spoiling. In our country, the packages of irradiated products must contain warnings stating that they are irradiated (Vaz, 2015).

3.3. Nuclear Energy Production

Uranium is used as fuel raw material in nuclear power plants. Nuclear energy is the huge amount of energy that emerges as a result of the disintegration of heavy radioactive substances such as uranium or the combination of light radioactive atoms to form heavier atoms.

A very small amount of radioactive material is released into the environment during the mining, processing, and use of uranium, which is a nuclear power plant fuel, and its storage after it becomes waste. The annual average dose exposure in the world from these emissions is 0.008 mSv. In addition, some radioactive material may be released into the environment as a result of accidents that may occur in nuclear power plants (Hashimoto et al., 2022).

3.4. Research and Laboratories

Radiation sources are used for research purposes at universities and other research centers. Some of the fields where research on radiation sources is carried out are physics, mining, metallurgy, biology, medicine, agriculture, environment, geology, and chemistry. As a result of research, new methods and even new products that may include radiation applications can be developed (www.epa.gov).

3.5. Consumer Products

Some products such as lightning rods, smoke detectors, phosphorescent clocks, x-ray security systems, fuels such as gas and coal, and building construction materials contain radioactive substances, albeit in small amounts. Even optical lenses and porcelain teeth contain traces of thorium and uranium, a radioactive substance (Shaw et al., 2007). The world average annual radiation dose exposed to these sources is 0.0005 mSv. The amount of radiation in these products is almost negligible compared to medical sources. Figure 5 shows that natural sources of radiation account for approximately 82% of all public exposure, while man-made sources account for the remaining 18% (NCRP, 1987).

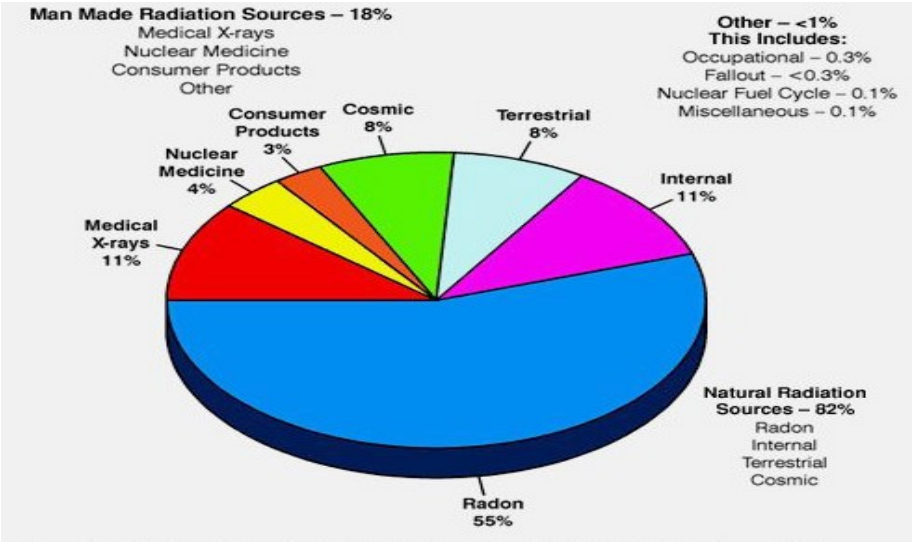

Figure 5. Ionizing radiation exposure to the public (Adapted from Ref. NCRP, 1987).

4. Effects of Radiation on Human Health

The harmful effects that radiation can have on human health have been known for a long time. These effects are radiation burns, radiation sickness, shortening of natural lifespan, cancer, and hereditary disorders. It is possible to observe death with high-dose exposure.

For ionizing radiation to cause biological damage in living things, the radiation energy must be absorbed by the cell. As a result of this absorption, ionization and excitation occur in the target molecules. These ionizations, which are the initiating effect of biological damage that may occur later, can cause breaks in the DNA chains that carry the genetic information of the cell and the production of chemical toxins within the cell. Repair activity begins immediately after the breaks. If the damage is not too extensive, these breaks in DNA can be repaired. However, errors may occur during this repair, and chromosomes containing incorrect code information may occur. If damaged DNA is not repaired properly, the cell will either survive with a defective (poorly functioning) metabolism or die. Many organs or tissues of the body can continue their normal activities despite the loss of significant numbers of cells (Yeyin, 2015).

When cell loss exceeds a certain number, damage to organs and tissues may occur. This can only be achieved by exposure to a radiation dose large

enough to cause the death of such a large number of cells. Such damages that occur in people who have received acute doses exceeding the effect threshold are called deterministic effects. In short, deterministic effects result in cell death, the threshold dose is high, and the severity of the effect increases with the dose.

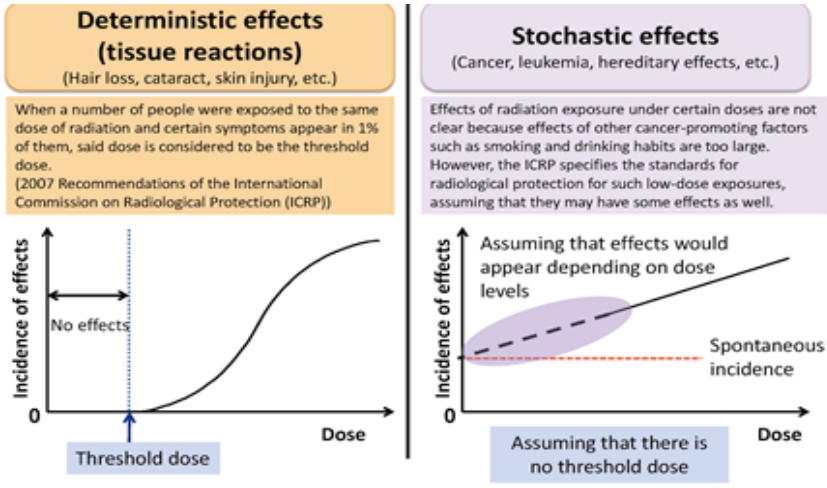

Figure 6. Biological effects of radiation on the human body (Adapted from Ministry of Environment Japan, 2005).

"Long-lasting" or "stochastic" effects occur at low radiation doses. Here, the stochastic effect is the probability of experiencing a disease in proportion to the amount of radiation received in previous years. Cells' self-repair mechanisms may be disrupted. Non-lethal DNA changes occur in some cells. These changes are passed on to subsequent cells through cell division. Diseases such as cancer or leukemia may occur years after irradiation (Yeyin, 2015). In Figure 6, the biological effects of radiation on the human body (stochastic effects and deterministic effects) are summarized.

4.1. Factors Affecting the Damage of Radiation

The biological damage that radiation will cause in the organism depends on parameters such as duration of exposure to radiation, dose rate, energy and type of radiation, the oxygen concentration in the environment, presence of some radioprotectors, the metabolic state of the cell, age, and health status of the person, as shown in Figure 7. As the duration of people's exposure to radiation increases, the effect of radiation on people increases in direct proportion.

However, if a person receives a certain amount of radiation dose at the same time, the effects will be different if they receive the same amount of radiation dose at certain intervals and for a certain period. Body tissues can renew themselves against damage caused by radiation received slowly or at regular intervals. However, this renewal opportunity may not be possible in the face of high radiation received in a short time. In general, as the duration of exposure to radiation increases, the harmful effect of radiation also increases (Gökoğlan et al., 2020).

It has been determined that body temperature, metabolic activities, and amount of oxygen are factors that increase sensitivity to radiation. Sensitivity to radiation also increases in cases where body temperature increases (feverish diseases, etc.), metabolic activities in the organism increase, and the oxygen concentration in the environment increases. Some chemicals increase sensitivity to radiation, while some chemicals decrease sensitivity.

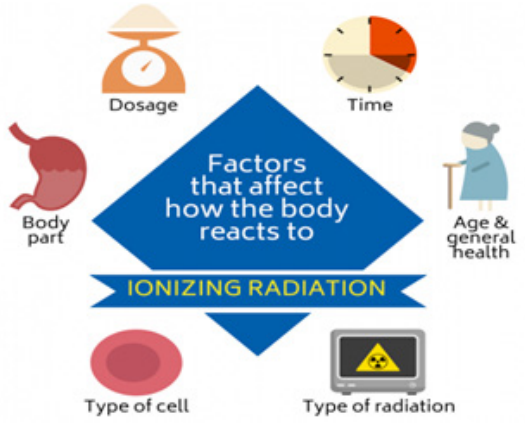

Figure 7. The factors that affect how the human body reacts to ionizing radiation (© 2019 Let's Talk Science).

Although limb parts such as hands and feet are exposed to higher doses of radiation, less damage occurs to these organs than, for example, blood. As we age, the body becomes less sensitive to the effects of radiation due to reduced cell division. Each person's radiation dose tolerance is different. The studies conducted are not sufficient to detect differences (Parlak et al., 2020).

5. Radiation Protection System

A radiation protection system is a set of precautions and measures implemented to ensure that individuals are protected as much as possible from

the negative effects of radiation. The main purpose of this system is to minimize radiation exposure and reduce potential health risks.

Radiation protection system can be applied in various fields and is important in different sectors, working environments, or activities where radiation sources are used. For example, those who work in nuclear power plants, healthcare personnel working in medical imaging and treatment applications, those working in industrial activities where radioactive materials are used, and those working in radiation-related research laboratories are an important part of the radiation protection system (Çimen et al., 2017).

There are three basic principles of radiation protection: time, distance, and shielding (Figure 8).

5.1. Time

Less radiation exposure can be received by reducing the time spent near a radiation source. For this reason, it is recommended to stay in the radioactive environment for as short a time as possible. When responding to a possible radiation accident, the amount of radiation the individual in the emergency response team will receive increases as the time they stay in the radiation area increases. Therefore, teams should be organized to work in shifts when necessary to limit the radiation dose to each individual (Parlak et al., 2020).

5.2. Distance

The second important factor in radiation protection is “distance” and is based on the principle that the further you stay from the radiation source during work, the less radiation you will be exposed to. The inverse square law works here. The inverse square law is valid for small point sources used in radiography. Although this rule cannot be used for radiation accidents in which radioactive substances are dispersed and scattered around, the amount of radiation can be significantly reduced by removing the radioactive source and materials contaminated with radioactive substances to a certain distance (Çimen et al., 2017).

5.3. Shielding

The higher the density of the material used in shielding, the greater its ability to stop radiation. High-density materials such as lead are generally used for shielding (Çimen et al., 2017). In a possible radiation accident, it is

not always possible to find dense materials such as lead in the accident area. For this reason, placing a vehicle, garbage pile or heavy material with dense content between the emergency response team and the radiation source may be an appropriate measure to reduce the radiation dose received at the scene of the accident. However, in many emergency situations, shielding is done with gloves, shoe covers, standard fire clothing, coats, jackets, or surgical protective materials used to prevent contamination. Such suits are sufficient to stop alpha and beta radiation but are ineffective to stop penetrating gamma radiation. As a result, shielding is not a protection method that can always be applied in the emergency response area. While searching for suitable shielding materials, emergency intervention should not be delayed, and the radiation dose received should be reduced by taking into account time and distance factors (www.epa.gov).

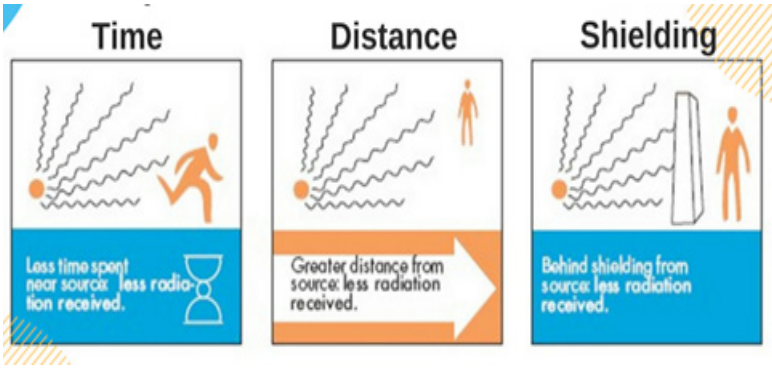

Figure 8. Three basic principles of radiation protection.
(Adapted from www.epa.gov/radiation/protecting-yourself-radiation)

6. Conclusion and Evaluation

The environmental and biological effects of radiation are a complex issue and need to be continually investigated. These studies will enable us to better understand the effects of radiation on human health and provide important information for a safer future. In this section, the possible effects of radiation from various sources on the environment, humans, and other living things, and methods of protection from these effects are examined.

From an environmental perspective, radiation has effects arising from its natural sources. Natural sources, especially sunlight and ground-based radiation, affect the level of radiation to which living things can be exposed. This should be taken into account when determining the effect of environmental radiation on

biological systems. The effect of radiation is based on the interaction of radiation with chemical systems. Radiation from visible light to ultraviolet light generally increases the energy state in a molecule from the lowest level to a higher level and is absorbed by the chemical system. This can make it colored and therefore visible. If the absorbed energy is greater than the visible range, the chemical system appears colorless.

From a biological perspective, the potential effects of radiation on health are quite significant. Radiation from outside the body passes through the skin and then enters tissue cells in the body. Exposure to high levels of radiation can cause cancer, genetic disorders, and other serious health problems. However, exposure to low levels of radiation is also thought to have long-term health effects, but these effects are less obvious and more difficult to study.

Radiation exposure can cause a variety of health effects, from mild to severe and even death. We can minimize the effects of radiation by protecting with dense materials such as lead, moving away from the radiation source, and limiting the duration of exposure.

The capacity of living organisms to repair damage caused by radiation is very limited. Therefore, to reduce the damage caused by radiation, it is of great importance to take safety precautions in nuclear power plants, to use medical practices such as radiation therapy correctly, and to manage radiation sources correctly.

References

Ağuş Y (2017) Radioactivity concentrations of the milk and dairy products. J BAUN Inst Sci Technol 19(2):169–176

Al-Hamarneh, I. F., Alkhomashi, N., & Almasoud, F. I. (2016). Study on the radioactivity and soil-to-plant transfer factor of (226)Ra, (234)U and (238)U radionuclides in irrigated farms from the northwestern Saudi Arabia. Journal of environmental radioactivity, 160, 1–7. https://doi.org/10.1016/j.jenvrad.2016.04.012

Aykamış, A., & Kılıç, A. M., (2009). Doğu Akdeniz Bölgesinde Bulunan Mersin-Ovacık-Kargıcak Kuvarsit Yataklarının Doğal Radyoaktivite Ölçümleri. *Ç.Ü.,* Mühendislik-Mimarlık Fakültesi Dergisi, vol.20, no.2, 42-51.

Baldık R., Aytekin H., Çelebi N., Ataksor B., Taşdelen M. (2006) Radon concentration measurements in the AMASRA coal mine, Turkey, Radiation Protection Dosimetry, Volume 118, Issue 1, April, Pages 122–125, https://doi.org/10.1093/rpd/nci374)

Bilgici Cengiz G, Göksu V, Ertap H (2017). Iğdır Yöresinde Çevresel Radyoaktivitenin Belirlenmesi. Iğdır Üniversitesi Fen Bilimleri Enstitüsü Dergisi, 7(2), 131 - 139.

Bilgici Cengiz, G. (2020). Determination of natural radioactivity in products of animals fed with grass: A case study for Kars Region, Turkey. Sci Rep, 10, 6939. https://doi.org/10.1038/s41598-020-63845-4

Bilgici Cengiz and Çağlar (2022). Transfer factors of natural radionuclides from soil to medicinal plants used by local people in Eastern Anatolia, Turkey. International Journal of Environment and Geoinformatics (IJEGEO), 9(2): 039-044, doi.10.30897/ ijegeo.956443

Bilgici Cengiz, G., & Caglar, I. (2022). Evaluation of lifetime cancer risk arising from natural radioactivity in foods frequently consumed by people in Eastern of Turkey. Journal of Radioanalytical and Nuclear Chemistry, *331*(4), 1847-1857.

Canbazoğlu C, Doğru M (2013). A preliminary study on ^{226}Ra, ^{232}Th, ^{40}K and ^{137}Cs activity concentrations in vegetables and fruits frequently consumed by inhabitants of Elazığ Region, Turkey. J Radioanal Nucl Chem 295(2):1245–1249

Caridi F, Belvedere A, D'Agostino M, et al. (2019). An investigation on airborne particulate radioactivity, heavy metals and polycyclic aromatic hydrocarbons composition in Calabrian selected sites, Southern Italy. Indian J Environ Prot. 39: 321-6.

Caridi, F., Paladini, G., D'Agostino, M., Marguccio, S., Belvedere, A., Belmusto, G., Stilo, G., Majolino, D., Venuti, V. (2023). Radon Specific Activity in Drinking Water and Radiological Health Risk Assessment: A Case Study. Appl. Sci., 13, 9660. https://doi.org/ 10.3390/app13179660

Çimen B, Erdoğan M, Oğul R. (2017). İyonlaştırıcı radyasyon ve korunma yöntemleri. S.Ü. FEN Fak Fen Derg, 43(2): 139-147.

Gökoğlan, E., Ekinci, M.H., Ozgenc, E., Ilem-Ozdemir, D., & Aşikoğlu, M. (2020). Radyasyon ve İnsan Sağlığı Üzerindeki Etkileri. Anatolian Clinic the Journal of Medical Sciences, 25(3): 289-294.

Görür FK, Keser R, Akçay N, Dizman S, As N, Okumuşoğlu NT (2012) Radioactivity and heavy metal concentrations in food samples from Rize, Turkey. J Sci Food Agric 92:307–312

Hashimoto, S., Komatsu, M., Miura, S. (2022). Radioactive Materials Released by the Fukushima Nuclear Accident. In: Forest Radioecology in Fukushima. Springer, Singapore. https://doi.org/10.1007/978-981-16-9404-2_1

Howard, B. (2021). Environmental Pathways of Radionuclides to Animal Products in Different Farming and Harvesting Systems. In: Naletoski, I., Luckins, A.G., Viljoen, G. (eds) Nuclear and Radiological Emergencies in Animal Production Systems, Preparedness, Response and Recovery. Springer, Berlin, Heidelberg. https://doi.org/10.1007/978-3-662-63021

Hutchison, S. G., & Hutchison, F. I. (1997). Radioactivity in everyday life. Journal of Chemical Education, 74(5), 501.

IAEA (2018) International Atomic Energy Agency, Radiation Protection and Safety in Medical Uses of Ionizing Radiation, IAEA Safety Standards Series No. SSG-46, Vienna (2018).

Issa S.A.M., Uosif M.A.M., Tammam M., Elsaman R. (2014). A Comparative Study of the Radiological Hazard in Sediments Samples from Drinking Water Purification Plants Supplied from Different Sources. Journal of Radiation Research and Applied Sciences, 7: 80-94.

Kaur, G., Singh, J. (2019). Effects of Radiation on the Environment. In: Kumar, V., Chaudhary, B., Sharma, V., Verma, K. (eds) Radiation Effects in Polymeric Materials. Springer Series on Polymer and Composite Materials. Springer, Cham. https://doi.org/10.1007/978-3-030-05770-1_1)

Küçükönder E. (2021). Kahramanmaraş İlinde Bina İçi Mevsimsel Radon Gazı Aktivitesi Ölçümü. Bitlis Eren Üniversitesi Fen Bilimleri Dergisi, 10(3), 891 - 901.

Kürkçüoğlu, M. & Bayraktar, G. (2014). Süleyman Demirel Üniversitesi›nde Bina İçi Radon Konsantrasyonlarının Nükleer İz Dedektörleri Kullanılarak Belirlenmesi. Süleyman Demirel Üniversitesi Fen Bilimleri Enstitüsü Dergisi. 16. 10.19113/sdufbed.52038.

Kürkçüoğlu, M. E. & Çine, A. (2017). Isparta İl Merkezindeki Okullarda Gama Ortam Doz Eşdeğeri Ölçümleri. Süleyman Demirel Üniversitesi Fen Bilimleri Enstitüsü Dergisi, 21 (2), 549-553. Retrieved from https://dergipark.org.tr/tr/pub/sdufenbed/issue/34634/382609

Mehta, S. R., Suhag, V., Semwal, M., & Sharma, N. (2010). Radiotherapy: Basic Concepts and Recent Advances. Medical journal, Armed Forces India, 66(2), 158–162. https://doi.org/10.1016/S0377-1237(10)80132-7

Ministry of Environment Japan (2005). Environmental Accounting Guideline. https://www.env.go.jp/en/policy/ssee/eag05.pdf

NCRP (1987) National Council on Radiation Protection and Measurement Report No. 93. Ionizing Radiation Exposure of the Population of the United States.

Neville, J. J., Palmieri, T., & Young, A. R. (2020). Physical Determinants of Vitamin D Photosynthesis: A Review. *JBMR Plus*, *5*(1). https://doi.org/10.1002/jbm4.10460

Nguyen, V. T., Vu, N. B., & Huynh, N. P. T. (2018). Gross alpha and beta radioactivity in food crops and surface soil from Ho Chi Minh City, Vietnam. Journal of Radioanalytical and Nuclear Chemistry, 315, 65-73.

NRC (1999) National Research Council (US) Committee on Evaluation of EPA Guidelines for Exposure to Naturally Occurring Radioactive Materials. Evaluation of Guidelines for Exposures to Technologically Enhanced Naturally Occurring Radioactive Materials. Washington (DC): National Academies Press (US); 1999. 2, Natural Radioactivity and Radiation. Available from: https://www.ncbi.nlm.nih.gov/books/NBK230654/

Parlak, Y, Uysal B, Kıraç F S, Kovan B, Demir M, Ayan A, Poyraz L, Özaslan İ A, et al. (2020) Radyasyon Güvenliği Kılavuzu: Genel Tanımlar ve Nükleer Tıp Uygulamalarında Radyasyondan Korunma Kuralları. Nucl Med Semin; 6(2):71-89. doi:10.4274/nts. galenos.2020.0009. google scholar

Peli´ c, M.; Mihaljev, Ž.; Živkov Baloš, M.; Popov, N.; Gavrilovi´ c, A.; Jug-Dujakovi´ c, J.; Ljubojevi´ c Peli´ c, D. (2023) The Activity of Natural Radionuclides Th-232, Ra-226, K-40, and Na-22, and Anthropogenic Cs-137, in the Water, Sediment, and Common Carp Produced in Purified Wastewater from a Slaughterhouse. Sustainability, 15, 12352. https://doi.org/ 10.3390/su151612352

Safarov, A., Safarov, A., Khasanov, S. et al. (2023). Evaluation of radon hazards at the rural settlements of Uzbekistan. Environ Monit Assess 195, 915 https://doi.org/10.1007/s10661-023-11493-2

Shaw, J., Dunderdale, J., & Paynter, R. A. (2007). A Review of consumer products containing radioactive substances in the European Union. Radiation Protection, 146, 11-14.

Thorne MC. Background radiation: natural and man-made. J Radiol Prot 2003; 23:29-42

Turhan, Ş., Gören, E., Uğur, F., Karataşlı, M. & Yeğingil, Z. (2018). Study of the radioactivity in environmental soil samples from Eastern Anatolia Region of Turkey. *Radiochimica Acta*, *106*(2), 161-168. https://doi.org/10.1515/ract-2017-2845)

UNEP (2016) Radiation: effects and sources, United Nations Environment Programme, ISBN: 978-92-807-3517-8, https://www.unscear.org/unscear/en/publications/booklet.html (last access: 15 September 2023).

UNSCEAR. (2000). United Nations Scientific Committee on the Effects of Atomic Radiation (UNSCEAR) 2000 Report, Volume I: Report to the General Assembly, with Scientific Annexes-Sources. United Nations.

UNSCEAR. (2008). Sources and Effects of Ionizing Radiation. United Nations Committee on the Effects of Atomic Radiation. Report to General Assembly with Annexes. Volume 1, Annex B, Exposures of the public and workers from various sources of radiation. United Nations, New York.

Vaz, P. (2015). Radiological protection, safety and security issues in the industrial and medical applications of radiation sources. Radiation Physics and Chemistry, 116, 48-55.

Vuruş, H. (2013). Adıyaman ili doğal zemin radyasyon düzeyinin belirlenmesi/Determination of natural background radiation level for Adiyaman province (PhD Thesis)

Yachiso G.T, Chaubey A. K. and Turi B. (2023) Transfer factor of radionuclides from soil to cereal crops around gold mining and evaluation of corresponding radiological hazard levels Oromia, Ethiopia, International Journal of Environmental Analytical Chemistry, DOI: 10.1080/03067319.2022.2158737

Watson, S. J., Jones, A. L., Oatway, W. B., & Hughes, J. S. (2005). Ionising radiation exposure of the UK population: 2005 review. Chilton, Oxon: Health Protection Agency

WHO (2009). World Health Organization, handbook on indoor radon: A public health perspective.

Wielopolski, L. (2013). The Ubiquity of Background Radiation and the Clinical Utility of Naturally Occurring Potassium-40 in Human Body (No. BNL-100806-2013-BOOK). Brookhaven National Lab.(BNL), Upton, NY (United States).

Yeyin, N. (2015, November). Biological Effects of Radiation/Radyasyonun Biyolojik Etkileri. In Nuclear Medicine Seminars 1(3), 139-144. Galenos Yayinevi Tic. Ltd.

www.epa.gov.https://www.epa.gov/radiation/protecting-yourself-radiation (Date of access:24. 09. 2023)

CHAPTER II

COMPILATION OF STUDIES ON THE EXAMINATION OF NATURAL RADIATION EMITTED FROM BUILDING MATERIALS FREQUENTLY USED IN TURKEY

Gülçin BİLGİCİ CENGİZ

(Assoc. Prof. Dr.), Kafkas University, Faculty of Science and Letters, Department of Physics, Kars, Turkey
E-mail:gulcincengiz@kafkas.edu.tr,
ORCID: 0000-0002-6164-3232

1. Introduction

Earth-based materials such as rocks, stones, and soil mainly contain uranium (^{238}U), thorium (^{232}Th) and their decay products, and radioisotopes such as potassium (^{40}K). Building materials contain low amounts of radioactive substances because they are produced from earth-sourced materials. Some industrial by-products also contain radionuclides from radioactive waste (Kristic et al. 2007). In studies conducted in different parts of the world, mostly using the gamma spectrometer method, the activity concentrations of ^{226}Ra, ^{232}Th, and ^{40}K radioisotopes in various building material samples have been reported (Çam Kaynar et al. 2015; Righi and Bruzzi, 2006; Sonkawade et al. 2008). Alpha and beta radiations emitted by ^{222}Rn and short-lived decay products, which originate from building materials used in home and workplace buildings and enter the body through the respiratory tract, cause internal irradiation (El-Taher 2012; TAEK, 2008). Since gamma rays emitted from building materials can travel long distances, people are constantly exposed to this radiation and face various health risks in the long term. Internal radiation occurs when the short half-life of ^{222}Rn gas, which is generally released in the uranium decay chain, mixes with the air and reaches the respiratory tract and lungs. Since the geological characteristics of the living area as well as the

building materials used in the building also affect the radiation dose, there are various studies on the evaluation of possible radiological hazards arising from the building materials used in the construction of home and workplace buildings (Ali et al. 1996; Faheem et al. 2008; Lu et al. 2012; UNSCEAR, 2000).

Much research has been carried out to specify the levels of natural radioactivity concentrations resulting from building materials used in different parts of Turkey. The results of these studies are compiled in this article for future reference.

2. Summary of the Results

Summaries of research carried out by several research teams to investigate the radioactivity of building materials used in Turkey are presented in this section.

Sarıkaya and Soykan determined the natural radioactivity levels of building materials used and produced in Uşak province and its surroundings using the HpGe detector and evaluated the results they found (Sarıkaya and Soykan, 2018). According to the results of their analysis, they reported that the equivalent radium activity (Ra_{eq}) of brick-tile products was 4.4 Bq/kg less than pumice block products. When they examined the activity concentration index (Iγ) values, they reported that brick–tile products have a 4.8% lower value than pumice block products. They stated that they thought the radioactivity differences between the two products did not constitute a significant difference.

NaI(TI) gamma spectroscopy was used in the study conducted by Mavi and his colleagues in 2010 on building materials used in Isparta, Turkey. Activity concentrations ranged from 17.91 Bq kg^{-1} to 58.88 Bq kg^{-1} for ^{226}Ra, from 6.77 Bq kg^{-1} to 19.49 Bq kg^{-1} for ^{232}Th, and from 65.72 Bq kg^{-1} to 248.76 Bqkg^{-1} for ^{40}K (Mavi and Akkurt, 2010).

In the study by Bilgici Cengiz et al., the radioactivity levels of some building materials used in Kars province and the radiological risks that may arise from the use of these materials were assigned. They measured the radioactivity concentrations of ^{226}Ra, ^{232}Th, and ^{40}K radioisotopes in different building materials used in Kars (limestone, clay, trass, gypsum, iron ore, cement) with an HPGe gamma-ray spectrometer system. They found the average radioactivity concentrations of ^{226}Ra, ^{232}Th, and ^{40}K radioisotopes to be 22.9 Bq kg^{-1}, 19.5 Bq kg^{-1}, 265.3 Bq kg^{-1}, and 1.7 Bq kg^{-1}, respectively. They calculated radiological hazard indices for building materials using the obtained values and reported the

building materials they examined did not pose a radiological risk and also could be used safely in the construction of buildings (Bilgici Cengiz et al., 2017).

In this research by Turhan et al., the activity concentrations of ^{226}Ra, ^{232}Th, and ^{40}K were measured using gamma-ray spectroscopy in 15 different building materials usually used in Osmaniye province. They have found the activity concentrations of ^{226}Ra, ^{232}Th, and ^{40}K varied from 2.5 ± 0.1 Bq kg^{-1} (marble) to 145.7 ± 4.4 Bq kg^{-1} (clay brick), 1.3 ± 0.1 (marble) to 154.3 ± 4.1 Bq kg^{-1} (marble), and 8.6 ± 0.2 Bq kg^{-1} (sand) to 1044.1 ± 70.3 Bq kg^{-1} (granite), respectively. They reported that the examined building materials were safe for residents to use in residential construction, as the estimated values of potential radiological hazard parameters were within the recommended safety limits or criterion values (Turhan et al., 2022).

In the research conducted by Erees et. al. (2006), ^{238}U, ^{232}Th and ^{40}K activity measurements of brick, sand, and cement materials used in Manisa province were made with the NaI (Tl) gamma spectroscopy system. The highest activity concentrations of ^{238}U, ^{232}Th, and ^{40}K are reported in the sand samples were 1559.10 Bq kg^{-1}, 142.48 Bq kg^{-1}, and 1711.47 Bq kg^{-1}, respectively. The radium equivalent activity was calculated based on their obtained activities. They stated that the highest Ra_{eq} value (945 Bq·kg^{-1}) was found in sand and gravel samples. They also calculated the doses received by residents living in Manisa from these building materials (Erees et al, 2006).

In this study, radioactivity levels and radiological hazard parameter values of 11 often used building materials in Samsun were evaluated with an HPGe detector. They compared their results with international limit values and stated that the materials examined in the study did not pose a radiological risk to human health (Tufan and Disci, 2013).

In the article by Damla et al., radiological measurements of four cement, marble, brick, sand, limestone, and gypsum samples used as building materials in Batman province were made using HPGe gamma spectroscopy. The concentrations of ^{226}Ra, ^{232}Th, and ^{40}K in their selected building materials range from 18 to 48 Bq kg^{-1}, 8 to 49 Bq kg^{-1}, and 68 to 477 Bq kg^{-1}, respectively. They compared the results they obtained with studies conducted for other provinces and internationally accepted limit values and stated that the measured samples did not carry radiological risk (Damla et al., 2010).

As a result of the research conducted by Turhan and Gürbüz; ^{226}Ra, ^{232}Th, and ^{40}K activity concentration values of 141 samples of 7 different cements taken from different cement factories were measured using HPGe gamma

spectroscopy. The average activity values found as a result of the analysis were published as 40.0 ± 27.1 Bq kg^{-1}, 28.0 ± 20.9 Bq kg^{-1}, and 248.3 ± 95.0 Bq kg^{-1} for ^{226}Ra, ^{232}Th, and ^{40}K, respectively. According to the results obtained, it was shown that there is no serious radiological risk in the use of Turkish cement in building construction (Turhan and Gürbüz, 2008).

Eren Belgin and Aycık collected samples of some frequently used construction materials from the main local raw material suppliers of Muğla and measured the activity concentrations of natural gamma-emitting radionuclides contained in these samples with a high-resolution gamma spectrometer. According to their results, the activity concentrations of ^{226}Ra, ^{232}Th, and ^{40}K radioisotopes in cement and bricks are higher than worldwide values. The Ra_{eq} values of the samples range from 0.69 to 208 Bq kg^{-1}, which is well below the internationally accepted value of 370 Bq kg^{-1} determined in the UNSCEAR report. They concluded that the materials they examined could be used in the interior and exterior construction of buildings (Eren Belgin and Aycık, 2015)

Hatungimana and his colleagues carried out a study to determine the concentration of natural radıoactıvıty in several building materials used in Izmır. The natural radioactivity in their chosen construction materials was analyzed using a NaI (T1) gamma scintillation detector. The activity concentrations of ^{226}Ra, ^{232}Th, and ^{40}K for the plaster materials they examined were ND to 48.5 ± 7.0 Bq kg^{-1}, ND to 41.0 ± 6.4 Bq kg^{-1}, and ND to 720.4 ± 26.8 Bq kg^{-1}, respectively. They found that radium equivalent activities ranged from 63.35 ± 8.0 to 149.62 ± 12.23 Bq kg^{-1}. According to their results, it can be concluded that plaster materials collected and examined from Izmir and its surroundings do not pose any significant radiation hazard (Hatungimana et al., 2020).

Kayakökü et al. (2016) collected pumice, ignimbrite, and perlite samples extracted from mines in Bitlis, and other building materials fabricated in factories in Bitlis, and measured the activity concentrations of ^{226}Ra, ^{232}Th, and ^{40}K in the construction material samples using NaI(Tl) detector. The radioactivity concentrations of ^{226}Ra, ^{232}Th, and ^{40}K ranged from 29.67 ± 5.9 to 228.27 ± 38.1 Bq kg^{-1}, 10.87 ± 5.4 to 95.57 ± 26.1 Bq kg^{-1} and 249.37 ± 124.7 to 2580.17 ± 266.9 Bq kg^{-1}, respectively. They reported that the Ra_{eq} values of construction material samples were within world standards (Kayakökü et al., 2016).

Activity concentrations in different building material samples in Ordu were measured using a coaxial HPGe detector by Çelik et al. (2009). The average of ^{226}Ra, ^{232}Th, and ^{40}K activity concentration values measured in building materials

such as sand, cement, brick, plaster, and limestone were found to be 34.5, 26.9, and 378.4 Bq kg^{-1}, respectively. From the measurements made, it was reported that radium equivalent activity, terrestrial absorbed dose, annual effective dose rate, external hazard indexes and internal hazard indexes were within acceptable limits. When they compared the results obtained with the ^{226}Ra, ^{232}Th, and ^{40}K activity concentrations of building materials from different countries given in the literature, the activity values of sand and cement samples were generally higher than other studies, while the ^{226}Ra, ^{232}Th, and ^{40}K activity concentrations of brick samples were found to be lower compared to other studies. They found that the activity concentrations of radionuclides in gypsum were consistent with data reported in the literature. They reported that the ^{226}Ra and ^{232}Th concentrations in limestone or lime were generally lower than other results they compared, while the ^{40}K activity concentration in the same material was comparable to other measurements (Çelik et al., 2009).

Çetinkaya et al. (2016) measured the natural radioactivity levels of samples frequently used as building materials such as ceramic tile, brick, concrete, gypsum, marble, and gas concrete taken from Kütahya province, with a NaI(Tl) gamma-ray spectroscopy system. They reported the average concentrations of all building samples as 29.1 ± 0.2, 11.8 ± 0.2, and 303.7 ± 0.7 Bq kg^{-1} for ^{226}Ra, ^{232}Th, and ^{40}K, respectively. They also declared that the obtained average Ra equivalent value of construction material samples was 69.4 Bq kg^{-1} (Çetinkaya et al., 2016).

The radioactivity levels of sand and cement samples used in Istanbul have been measured by using a NaI(Tl) gamma-ray spectrometer. Çam Kaynar et al. (2015) found the mean activity concentrations of ^{40}K, ^{238}U, and ^{232}Th in cement samples as 2.81, 91.41, and 18.38 Bq kg^{-1}, and for sand samples respectively. The average activity concentrations of the mentioned radionuclides were obtained as 452.46, 75.27, and 11.71 Bq kg^{-1}, respectively. They reported that the average Ra_{eq} value was 117.7 Bq kg^{-1} and 126.86 Bq kg^{-1} for cement and sand, respectively, and all their calculated Raeq values were lower than the maximum allowable value of 370 Bq kg^{-1} (Çam Kaynar et al., 2015).

Kucukomeroglu et al. (2009) study, activity concentration measurements of natural radionuclides (^{226}Ra, ^{232}Th, and ^{40}K) found in various building materials such as sand, cement, and marble in Bayburt Province were determined using gamma-ray spectrometry. Activity concentrations in building materials have been reported to range from 16 to 54 Bq kg^{-1} for ^{226}Ra, 10 to 21 Bq kg^{-1} for ^{232}Th, and 113 to 542 Bq kg^{-1} for ^{40}K. Calculated radium equivalent (Ra_{eq}) activity

values for the building materials they examined ranged from 40 to 93 Bq kg^{-1}, with an average of 75 Bq kg^{-1} (Kucukomeroglu et al., 2009).

3. Discussion

Many studies on measuring ^{226}Ra, ^{232}Th, and ^{40}K activity concentrations along with their mean values and Ra equivalent values for usually used constructing materials in Turkey using a gamma spectrometry system are tabulated in Table 1.

As seen in Table 1, ^{226}Ra, ^{232}Th, and ^{40}K activity concentrations were at the lowest values (12.0 Bq kg^{-1}, 5.0 Bq kg^{-1} 1, and 90.0 Bq kg^{-1}) in the sand samples of Osmaniye province. As a result of the investigations made on the sand samples of Manisa province, the highest activity concentration values of ^{226}Ra, ^{232}Th, and ^{40}K were reported as 1559.10 Bq kg^{-1}, 142.48 Bq kg^{-1}, and 1711.47 Bq kg^{-1}, respectively.

Maximum values of ^{226}Ra, ^{232}Th, and ^{40}K in cement samples were reported as 91.41 Bq kg^{-1} (Istanbul), 71±7 Bq kg^{-1} (Mugla) and 560±52 Bq kg^{-1} (Mugla), respectively, while minimum were reported 12,96 Bq kg^{-1} (Usak), 10.4 Bq kg^{-1} (Isparta), and 86.93 Bq kg^{-1} (Usak), respectively.

For marble samples the maximum values of ^{226}Ra, ^{232}Th, and ^{40}K were found as 30.0 Bq kg^{-1}, 58.0 Bq kg^{-1} and 297.20 Bq kg^{-1} in Osmaniye province. The minimum values of the mentioned natural radionuclides in gypsum were reported as 2.0 Bq kg^{-1}, 3.0 Bq kg^{-1} and 47.3 Bq kg^{-1} in Kars province, respectively.

Additionally, according to the reported results of the studies, the average of the ^{226}Ra, ^{232}Th, and ^{40}K activity concentrations of the brick samples examined in Bitlis province (123.9±21.3 Bq kg^{-1}, 42.6±15.6 Bq kg^{-1}, and 1160.4±139.8 Bq kg^{-1}, respectively) have a higher value than the average of the activity concentrations of natural radionuclides in the brick samples examined in other province.

Considering that the majority of buildings constructed in Turkey and in the world are made of concrete and brick, the results of the research on cement, marble, gypsum, brick, and sand materials are given in Table 1. According to the UNSCEAR (2000) report, the world mean of ^{226}Ra, ^{232}Th, and ^{40}K activity concentrations in the earth's crust are 32.0, 45.0, and 420.0 Bq kg^{-1}, respectively (UNSCEAR, 2000). As seen in Table 1, the average values of ^{226}Ra, ^{232}Th, and ^{40}K activity concentrations measured in structural material samples used in

some provinces are higher than the world average. The reason for this may be geologic genesis, geographic situations, soil kinds, climatic terms, and climate differences in the places where building materials are produced.

The maximum value of the radium equivalent activity index (Ra_{eq}) value was reported as 273.4±59.6 Bq kg^{-1} (brick), and the minimum value was reported as 0.1±0.08 Bq kg^{-1} (marble). The radium-equivalent activities for the reported building materials were also below the criterion limit of gamma-radiation dose of 370 Bq kg^{-1}. Therefore, the use of these materials in residential construction can be taken into account as secure for residents.

Table 1. Research results on the measurement of natural radioactivity and Ra_{eq} in various building material samples using different techniques

Materials studied	Technique	Research Area	Activity concentration (Bq kg^{-1})			Raeq (Bq kg^{-1})	References
			^{226}Ra	^{232}Th	^{40}K		
Cement	HPGe detector	Usak	12.96	12.21	86.93	37.13	Sarıkaya and Soykan, 2018
	NaI(Tl) detector	Isparta	26.1	10.4	129.7	51.03	Mavi and Akkurt, 2010
	HPGe detector	Batman	36±8	27±10	389±48	105 ±26	Damla et al., 2010
	HPGe detector	Kars	22.2	18.5	255.2	68.5	Bilgici Cengiz et al., 2017
	HPGe detector	Osmaniye	64	46	306		Turhan et al., 2022.
	NaI(Tl) detector	Kütahya	41.9	12.2	279.2	80.4	Çetinkaya et al.. 2016
	HPGe detector	Ordu	72	48	492	178.5 ± 10.2	Çelik et al., 2009
	HPGe detector	Muğla	31±3 75±7	45±4 71±7	410±40 560±52	152±16 208±20	Eren Belgin and Aycık, 2015
	NaI(Tl) detector	İzmir	31.0 ± 5.5	14.3 ± 3.8	155.8 ± 12.5	63.35	Hatungimana et al., 2020
	NaI(Tl) detector	İstanbul	91.41	18.38	2.81	117.7	Çam Kaynar et al., 2015
	HPGe detector	Bayburt	45 ± 5 54 ± 4	14 ± 3 15 ± 3	122 ± 6 211 ± 10	83 ± 8	Kucukomeroglu et al., 2009

Table 1. Research results on the measurement of natural radioactivity and Ra_{eq} in various building material samples using different techniques (Continue)

Sand	NaI(Tl) detector	Manisa	1559.10	142.48	1711.47		Erees and Çam Kaynar, 2006)
	HPGe detector	Batman	32 ± 4	22 ± 5	477 ± 42	100 ± 8	Damla et al., 2010
	HPGe detector	Osmaniye	12	5	90		Turhan et al., 2022
	HPGe detector	Ordu	42	42	804	164.9 ± 10.1	Çelik et al., 2009
	NaI(Tl) detector	İstanbul	75.27	11.71	452.46	126.86	Çam Kaynar et al., 2015
	HPGe detector	Bayburt	22 ± 3	21 ± 4	542 ± 24	93 ± 10	Kucukomeroglu et al., 2009
Marble	NaI(Tl) detector	Kütahya	2.5	<MDA	16.4	3.8	Çetinkaya et al.. 2016
	HPGe detector	Osmaniye	30.0	58.0	297.0		Turhan et al., 2022
	HPGe detector	Batman	18 ± 7	8 ± 4	68 ± 16	35 ± 14	Damla et al., 2010
	HPGe detector	Muğla	0.4±0.04 4.5±0.5	0.4±0.03	<MDL	0.1±0.08 5.0±0.6	Eren Belgin and Aycık, 2015
	HPGe detector	Bayburt	26 ± 3	10 ± 2	151.3 ± 8	52,6 ± 10	Kucukomeroglu et al., 2009
Gypsum	HPGe detector	Kars	2.0	3.0	47.3	9.9	Bilgici Cengiz et al., 2017
	NaI(Tl) detector	Isparta	27.5	15.6	200.2	65.34	Mavi and Akkurt, 2010
	HPGe detector	Batman	18 ± 10	17 ± 7	87 ± 4	49 ± 16	Damla et al., 2010
	HPGe detector	Osmaniye	45.0	12.0	102.0		Turhan et al., 2022
	HPGe detector	Ordu	17	14	99	44.6 ± 3.4	Çelik et al., 2009
	NaI(Tl) detector	Kütahya	7.3	4.0	55.2	17.3	Çetinkaya et al.. 2016

Table 1. Research results on the measurement of natural radioactivity and Ra_{eq} in various building material samples using different techniques (Continue)

Brick	HPGe detector	Usak	22,12	30,16	475,28	101,85	Sarıkaya and Soykan, 2018
	HPGe detector	Muğla	28±2 30±3	34±3 37±4	497±45 545±50	116±14 124±12	Eren Belgin and Aycık, 2015
	HPGe detector	Batman	21 ± 5	21 ± 5	364 ± 36	79 ± 8	Damla et al., 2010
	HPGe detector	Osmaniye	64.0	31.0	372		Turhan et al., 2022
	NaI(Tl) detector	Isparta	58.9	11.7	248.8	94.81	Mavi and Akkurt, 2010
	NaI(Tl) detector	Bitlis	123.9±21.3	42.6±15.6	1160.4±139.8	273.4±59.6	Kayakökü et al., 2016
	HPGe detector	Ordu	22	19	369	77.6 ± 5.3	Çelik et al., 2009
	NaI(Tl) detector	Kütahya	37.7	18.1	672.8	115.4	Çetinkaya et al.. 2016

4. Conclusion

The world is becoming increasingly polluted and as pollution increases, human health deteriorates. It is possible to protect humans and their universe by acting in the light of science and taking minimal precautions. The building materials used in the construction of workplaces and residences offered to people must first be produced by the standards during the production phase and used in accordance with the regulations during the construction of the buildings. It is clear that building materials produced and used following standards will protect people and the environment from harmful factors. In the light of the studies we have examined in this article, the harmful effects of building materials on human health will be better understood and human health will be protected by taking precautions.

As a result, in this article, the data reported on the results of a significant number of studies on natural radioactivity in construction materials used in Turkey have been compiled. An HPGe detector or a NaI (TI) detector measuring device was used by the research groups in question. The researchers who conducted the studies agreed in their article that careful selection of building materials used and the use of low-radioactivity materials in buildings would contribute to the reduction of important diseases such as cancer and lung diseases.

References

Ali, S., Tufail, M., Jamil, K., Ahmed, A., Klian, H.A., (1996). Gamma ray activity and dose rate of brick samples from some areas of North West Frontier Province (NWFP), Pakistan. Sci. Total Environ. 187, 247–252.

Bilgici Cengiz, G., Aras, İ., Ertap, H. & Karabulut, M. (2017). Kars İlinde Kullanılan Bazı Yapı Malzemelerindeki Doğal Radyoaktivite ve Radyolojik Tehlikelerin Değerlendirilmesi, Afyon Kocatepe Üniversitesi Fen Ve Mühendislik Bilimleri Dergisi, 17 (2), 406-414. Retrieved from https://dergipark.org.tr/en/pub/akufemubid/issue/43399/524643

Celik, N., Damla, N. and Cevik, U. (2010). Gamma ray concentrations in soil and building materials in Ordu, Turkey. Radiat. Eff. Defects Solids 165, 1–10 https://doi.org/10.1080/10420150903173270.

Çam Kaynar, S., Özbey, E., & Ereeş, F.S. (2015). Determination of radon exhalation rate and natural radioactivity levels of building materials used in Istanbul-Turkey. Journal of Radioanalytical and Nuclear Chemistry, 305, 337-343. https://doi.org/10.1007/s10967-015-3987-7

Çetinkaya, H., Manisa, K., & Işık, U. (2022). Radioactivity Content of Building Materials Used in Kütahya Province, Turkey. Radiation protection dosimetry, *198*(3), 167–174. https://doi.org/10.1093/rpd/ncac012

Damla, N., Cevik, U., Kobya, A.I. *et al.* (2010). Assessment of environmental radioactivity for Batman, Turkey. Environ Monit Assess, 160, 401–412. https://doi.org/10.1007/s10661-008-0704-9

El-Taher A (2012). Assessment of natural radioactivity levels and radiation hazards for building materials used in Qassim area Saudi Arabia. Romanian J Phys, 57(3– 4):726–735.

Erees F.S, Dayanıklı S.A, Çam S. (2006). Natural Radionuclides in the Building Materials used in Manisa City, Turkey. Indoor and Built Environment, 15(5):495-498. https://doi:10.1177/1420326X06069059

Eren Belgin, E. & Ayçık, G. (2015). 226Ra, 232Th, and 40K activity concentrations and radiological hazards of building materials in Mugla, Turkey. Mugla Journal of Science and Technology, 1 (2), 11-16. https://doi:10.22531/muglajsci.210004

Faheem, M., Mujahid, S.A. and Matiullah. (2008) Assessment of radiological hazards due to the natural radioactivity in soil and building material samples collected from six districts of the Punjab province Pakistan. Radiation Measurements 43, 1458–14

Hatungimana D, Taşköprü C, İçhedef M et al (2020) Determination of radon and natural radioactivity concentration in some building materials used in Izmir, Turkey. J Green Building 15:107–118. https://doi.org/10.3992/1943-4618.15.1.107

Kayakökü, H., Karatepe, Ş., & Doğru, M. (2016). Measurements of radioactivity and dose assessments in some building materials in Bitlis, Turkey. Applied Radiation and Isotopes, 115, 172–179. https://doi.org/10.1016/j.apradiso.2016.06.020

Krstić, D., Nikezić, D., Stevanović, N. and Vučić, D. (2007). Radioactivity of some domestic and imported building materials from South Eastern Europe. Radiation Measurements. 42, 1731–1736.

Kucukomeroglu, B., Kurnaz, A., Damla, N., Çevik, U., Çelebi, N., Ataksor, B., & Taşkın, H. (2009). Environmental radioactivity assessment for Bayburt, Turkey. Journal of Radiological Protection, 29, 417 - 428. https://doi.org/10.1088/0952-4746/29/3/006

Lu, X., Yang, G., Ren, C. (2012). Natural radioactivity and radiological hazards of building materials in Xianyang, China. Radiat. Phys. Chem., 81, 780–784.

Mavi, B. and Akkurt, İ. (2010). Natural radioactivity and radiation hazards in some building materials used in Isparta, Turkey. Radiation Physics and Chemistry 79, p:933–937

Righi, S., Bruzzi, L. (2006). Natural radioactivity and radon exhalation in building materials used in Italian dwellings. J. Environ. Radioact. 88, 158–170.

Sarıkaya, H. and Soykan, O. (2018). Uşak İli ve Çevresinde Kullanılan Yapı Malzemelerinin Doğal Radyoaktivitesinin Belirlenmesi. Türk Doğa ve Fen Dergisi, 7 (1), 35-40. Retrieved from https://dergipark.org.tr/tr/pub/tdfd/issue/37853/393607

Sonkawade RG, Kant K, Muralithar S, Kumar R, Ramola RC. (2008). Natural radioactivity in common building construction and radiation shielding materials. Atmos Environ 42:2254–2259.

TAEK 2008, Türkiyede Kullanılan Yapı Malzemelerindeki Doğal Radyoaktiviteden Kaynaklanan Radyasyon Dozunun Değerlendirilmesi, Tenik Rapor, 7

Tufan, M. Ç., & Disci, T. (2013). Natural radioactivity measurements in building materials used in Samsun, Turkey. Radiation protection dosimetry, 156(1), 87–92. https://doi.org/10.1093/rpd/nct047

Turhan, S., & Gürbüz, G. (2008). Radiological significance of cement used in building construction in Turkey. Radiation protection dosimetry, 129(4), 391–396. https://doi.org/10.1093/rpd/ncm454

Turhan, Ş, Kurnaz, A. & Karataşlı, M. (2022). Evaluation of natural radioactivity levels and potential radiological hazards of common building materials utilized in Mediterranean region, Turkey. *Environ Sci Pollut Res*. **29**, 10575–10584 https://doi.org/10.1007/s11356-021-16505-7

UNSCEAR (2000). Sources and effects of ionizing radiation. United Nations Scientific Committee on the Effects of Atomic Radiation, United Nations Publication, New York, USA.

CHAPTER III

INVESTIGATION OF HEIGHT DEPENDENCE FOR INDOOR ATMOSPHERIC RADON CONCENTRATION

Mehmet Ertan KÜRKÇÜOĞLU[1] & Özlem ÖNER[2]

1(Asst. Prof. Dr.) Süleyman Demirel University, Physics Department, 32260 Isparta, Türkiye
E-mail: m.ertan.kurkcuoglu@gmail.com
ORCID: 0000-0002-4694-1880
2(MSci Student) Süleyman Demirel University, Graduate School of Natural And Applied Sciences, 32260 Isparta, Türkiye
ozlemoner15@gmail.com
ORCID: 0000-0001-9350-9794

1. Introduction

It is known that half of the natural radiation that living things are exposed to throughout their lives is directly caused by radon (^{222}Rn) (UNSCEAR, 2000). In a research conducted in 1899, Ernest Rutherford found that the element thorium emitted a radioactive gas (Rutherford, 1900), and Pierre and Marie Curie also observed the emission of a radioactive gas from radium in the same year. During his research in Halle, Germany, in 1900, Friedrich Ernest Dorn came across that there was a gas accumulation in radium bulbs (Dorn, 1900), and thus radon gas was discovered (Partington, 1957). The term "radium emanation" was used for the first time in 1900 for ^{222}Rn referring to the gas released by radium-226, and this gas was accepted as a new element in 1912. There are three natural radioisotopes of radon; ^{222}Rn (from the uranium decay chain), ^{220}Rn (from the thorium decay chain), and ^{219}Rn (from the actinium decay chain). In 1923, the names of these radioisotopes were adopted as radon for ^{222}Rn (half-life 3.82 days), thoron for ^{220}Rn (half-life 55.6 seconds) and actinon for ^{219}Rn (half-life 3.96 seconds) (George, 2008; Mc Laughlin, 2012). ^{222}Rn, which

decays by emitting an alpha particle with an energy of 5.48MeV, is studied more intensively among these three natural radioisotopes due to its high abundance and relatively long half-life.

Radon is a colourless, odourless and tasteless monatomic gas under normal conditions. Radon (atomic number 86), the last member of group 8A of the periodic table, is the heaviest noble gas. The atomic radius of radon is 1.3×10^{-10} m. Its density is 9.73 g/l at 273 K and 1 atmosphere of pressure, and its molar volume at 273 K is 50.5 cm^3/mol. Radon, which is 100 times heavier than hydrogen, is about seven and a half times heavier than air, so it is more likely to accumulate near the ground. In addition, its specific heat is 0.091 J/g.K. It has almost no electrical conductivity and very low thermal conductivity (3.64×10^{-5} W/cm.K) (NCRP, 1988). If radon is cooled to temperatures below freezing point (-71 ºC), it will have a bright phosphorescence appearance that increases in yellowness proportionally with the decrease in temperature, while it can be observed in an orange-reddish colour as the air temperature increases. Due to its low electron affinity and high ionization energy, radon does not form chemical bonds with other elements, but it can form some compounds such as clathrate and mixed fluorides. It forms a metastable clathrate-hydrate ($Rn\text{-}6H_2O$), especially with water (Martinelli, 1993). Radon is partially soluble in water and can have a high solubility in organic liquids, except glycerine, which has less solubility than water. It can be easily absorbed by charcoal and silicone gel (Cigna, 2005).

Radon is undoubtedly present everywhere we live, in greater or lesser amounts. When radon gas is inhaled, it can be exhaled out of the body because it is inert (it does not form chemical bonds with the tissues in the respiratory system and with the particles in the air). However, the short-lived radon decay products (^{218}Po, ^{214}Pb, ^{214}Bi, and ^{214}Po) have static charges and can take part in chemical reactions. These radioisotopes, which can adhere to dust particles in the air, continue to decay after settling in the organs in the respiratory system. The radiation emitted during this process can change the DNA structure of living cells and lead to cancer formation (UNSCEAR, 1988; Al-Zoughool and Krewski, 2009).

Cancer is one of the most serious health problems that threaten human life. The International Agency for Research on Cancer (IARC) reports that among all deaths (63.17 million people) worldwide in 2020, approximately 9.96 million people died due to cancer and an estimated 19.3 million new cancer cases occurred. It is also stated that 18% of all cancer deaths in 2020 were caused by lung cancer (WEB-1). According to 2018 data on cancer cases recorded in

Türkiye, lung cancer ranks first among men with a rate of 21% and it ranks fifth for women with a rate of 6% (WEB-2). Epidemiological studies conducted to date show that there is a direct relationship between radon exposure and lung cancer formation (ICRP, 2010). The World Health Organization (WHO), and the USA Environmental Protection Agency (EPA) have classified radon gas as a "Class-A carcinogen" (EPA, 2005; WHO, 2009). Moreover, radon inhalation ranks second place after tobacco use on the list of the most dangerous carcinogens. WHO states that up to 14% of all lung cancer cases are caused by radon (WHO, 2005). For this reason, it is very important to determine indoor radon concentrations in enclosed spaces and take when necessary.

In general, indoor radon concentrations are observed in the range of 11-300Bq/m^3 (NCRP, 1988). In order to reduce the health risks, countries and various precautions organizations have advised some limitations for indoor radon concentrations. ICRP (International Commission on Radiological Protection) recommends that precautions be taken when the radon concentration in homes exceeds 300 Bq/m^3 and the radon level in workplaces exceeds 1000 Bq/m^3 (ICRP, 2014). WHO recommends that the radon concentration in enclosed spaces should be kept below 100Bq/m^3 in order to minimize the risk. If the radon level has to reach higher values due to country conditions, it is advised to take 300Bq/m^3 as the reference level for intervention (WHO, 2009). The permissible radon concentration values in Türkiye have been determined by the Turkish Energy, Nuclear and Mining Research Agency (TENMAK) as 400 Bq/m^3 for homes and 1000 Bq/m^3 for workplaces (WEB-3).

The main source of radon is the earth's crust. Radon gas, which is produced between rock layers as a result of natural processes, comes to the surface from the soil through various mechanisms and enters the building atmosphere through cracks in the floors and walls of buildings, as well as through installation gaps. There are many external factors that can affect indoor radon concentration: geological factors (rock structure, soil properties, etc.), meteorological parameters (humidity, pressure, temperature, altitude, etc.), building materials used in building construction, natural gas, water resources, age of the building, insulation of the building, and building usage habits (Porstendorfer et al., 1994; Baeza et al., 2003; Müllerova and Holý, 2010; Rafique et al., 2011; Kropat et al., 2014).

One of the parameters that affect the indoor radon level is height. Since radon, which is heavier than air, tends to accumulate on the ground, radon density is expected to decrease with increasing altitude. In the literature, there are many

national (Kürkçüoğlu et al., 2009; Bayraktar et al., 2009; Yılmaz Şen, 2009; Kürkçüoğlu et al., 2012; Akkurt, 2014; Çakmak, 2014; Kurt, 2015; Altınsöz et al., 2014). 2016; Aldemir, 2018; Çıtlak, 2018; Gül, 2019; Koçer et al., 2019; Erdoğan et al., 2020; Tamir Darcan, 2020; Küçükönder, 2021; Büyüksaraç et al., 2022) and international (Abu-Jarad vd., 1982; Khan vd., 1987; Pavlenko vd., 1997; Gallelli vd., 1998; Ioannides, 2000; Khan, 2000; Shaikh vd., 2003; Papaefthymio vd., 2003; Bahtijari vd., 2007; Papaefthymiou vd., 2007; Karpińska vd., 2008; Psichoudaki vd., 2008; Manousakas, 2010; Yarmoshenko vd., 2013; Afolabi vd., 2015; Vukotic vd., 2019; Vasilyev vd., 2020; De Maria vd., 2023) studies referring the relationship between indoor radon and altitude. Some of these studies were conducted in workplaces (Papaefthymiou et al., 2003; Bahtijari et al., 2007; Bayraktar et al., 2009; Kürkçüoğlu et al., 2009; Kürkçüoğlu et al., 2012; Çakmak, 2014; Afolabi et al., 2015; Kurt, 2015; Altınsöz et al., 2016; Aldemir, 2018; Çıtlak, 2018; Gül, 2019; Erdoğan et al., 2020; Tamir Darcan, 2020; Küçükönder, 2021), some in single-storey houses (Pavlenko et al., 1997; Büyüksaraç et al., 2022), some in multiple-storey buildings (Khan vd., 1987; Pavlenko vd., 1997; Gallelli vd., 1998; Khan, 2000; Ioannides, 2000; Papaefthymiou vd., 2003; Karpińska vd., 2008; Psichoudaki vd., 2008; Yılmaz Şen, 2009; Manousakas, 2010; Yarmoshenko vd., 2013; Akkurt, 2014; Çakmak, 2014; Koçer vd., 2019; Vukotic vd., 2019; De Maria vd., 2023), and some of them in skyscrapers (Abu-Jarad et al., 1982; Shaikh et al., 2003; Vasilyev et al., 2020). In the literature, there are some studies confirming that radon concentration decreases with increasing height (Pavlenko et al., 1997; Khan, 2000; Papaefthymiou et al., 2003; Shaikh et al., 2003; Papaefthymiou et al., 2007; Karpińska et al., 2008; Psichoudaki et al., 2008; Kürkçüoğlu et al., 2009; Yılmaz Şen, 2009; Manousakas, 2010; Kürkçüoğlu et al., 2012; Yarmoshenko et al., 2013; Akkurt, 2014; Afolabi et al., 2015; Kurt, 2015; Altınsöz et al., 2016; Aldemir, 2018 ; Çıtlak, 2018; Gül, 2019; Erdoğan et al., 2020; Küçükönder, 2021; Büyüksaraç et al., 2022), while some studies obtain results that are not compatible with this expectation (Abu-Jarad et al., 1982; Khan et al., 1987; Gallelli et al., 1998; Ioannides, 2000; Bahtijari et al., 2007; Karpińska et al., 2008; Bayraktar et al., 2008, Koçer et al., 2019; Vukotic et al., 2019; Tamir Darcan, 2020; Vasilyev et al., 2020; De Maria et al., 2023).

The present study aims to examine the relationship between indoor atmospheric radon concentration and height. For this, hourly radon measurements were carried out with electronic radon detectors (Airthings Wave radon detectors) in 9 rooms located on 3 different floors of the Department of Physics at Süleyman Demirel University between 1-30 April 2022.

2. Materials and Methods

2.1. Study Area

Located in the western part and inland part of the Mediterranean Region, Isparta province is the centre of the Lakes Region. The province lies between longitudes 30°20′ and 31°33′ East and latitudes 37°18′ and 38°30′ North, with an area of 8933 km^2 and an average altitude of 1050 meters. Neighboring Konya, Afyon, Burdur, and Antalya, the province has 13 districts including the central district, Aksu, Atabey, Eğirdir, Gelendost, Gönen, Keçiborlu, Senirkent, Sütçüler, Şarkikaraağaç, Uluborlu, Yalvaç and Yenişarbademli. The central district has the highest population and the district with the lowest population is Yenişarbademli. According to data for 2022, the total population of Isparta is 445.325 people. Since it is located in the transition zone between the Mediterranean climate and the continental climate, both climate characteristics are observed within the borders of Isparta. The annual average air temperature is around 12 °C (highest 38.7 °C and lowest -21.0 °C). A significant portion of precipitation occurs in the winter and spring seasons (69%). The average annual total rainfall in the city centre is 508.3 mm. The main structure of the soil in Isparta province is generally in calcareous form. The topsoil, which has a depth of 8-40 cm, has a clayey-calcareous granular and dispersible structure. The subsoil, which has the same structure as the topsoil, is generally coarser and clayey. Isparta province, which is an extension of the Western Taurus Mountains and has very high mountains up to 3000 meters in height, has a rugged structure. The province consists of 68.4% mountains, 16.8% plains and 14.8% plateaus. The province is in the first-degree earthquake zone, where the Isparta-Dinar-Çivril-Uşak earthquake line is located. There is a distribution with second-degree earthquake risk only in Sütçüler and Yenişarbademli districts, and third-degree earthquake risk in a narrow area on the eastern border of Sütçüler (WEB-4; WEB-5). Süleyman Demirel University, Department of Physics, located 10 km away from the city centre, was chosen for atmospheric radon measurements. The building where the Department of Physics is located is a 3-storey building with an area of 21300 m^2 on the East Campus and serves with 189 academic staff. The faculty has 40 classrooms, a computer laboratory for 50 students, 7 application and research laboratories, a seminar hall for each department, and a student cafeteria. Education and training activities continue with a total of 5476 students, both day and night (WEB-6). The location of the faculty building where the study was conducted is shown in Figure 1.

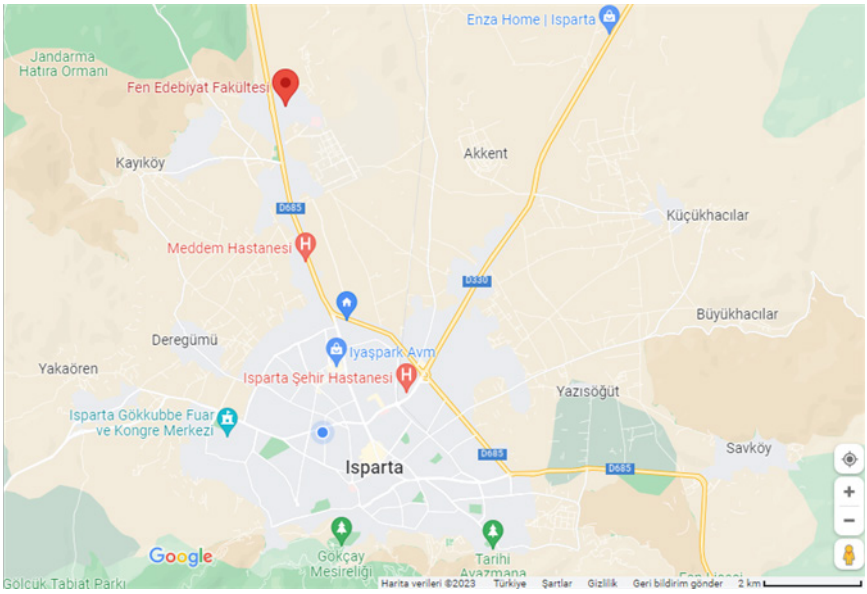

Figure 1. Map showing the location of the study area (Measurement point is marked with a red marker).

2.2. Measurement Device

Wave radon detector, produced by Airthings, is a low-cost device with a Bluetooth connection that stands out with its positive features such as measurement range, sensitivity, battery life, and data transfer ability. This electronic radon detector can also measure the humidity and temperature of the environment and visually indicate the radon level in the environment (with different coloured LED lights). In addition, it was preferred in this study due to its lightweight, portability, aesthetic appearance, and the possibility of free mobile application. The manufacturer recommends that the Wave detector not be placed near windows or in places where ventilation is provided, in order to evaluate radon and other parameters more accurately. Following the installation of the device, the first radon gas data can be obtained approximately 1 hour later. Some technical features of this portable device (Figure 2), which resembles a smoke detector, are summarized in Table 1.

Table 1. Basic features of Wave radon detector (WEB-7).

Radon Sampling	Passive diffusion chamber
Detection Method	Alpha spectrometry
Working Modes	Continuous radon monitoring: Long-term/Short-term monitoring
Measurement Range	0-20,000 Bq/m^3
Working Principle	Radon monitoring can be done with the iOS and Android applications by a continuous electrostatic collection of alpha particles.
Power Source	2 AA alkaline batteries: ~1.5 years
Connection Outputs	Wireless data transfer
Temperature and	4 °C - 40 °C
Humidity Range	Relative humidity: <85%
Weight	219 g (with batteries)
Dimensions	120 × 36 mm (diameter × height)
Connectivity	Ability to wireless data transfer via Bluetooth and Airthings Smartlink (Wi-Fi)
Monitoring	Radon data can be viewed on mobile phones and computers via Bluetooth connection.

Figure 2. Wave radon detector.

The system architecture used to obtain data from hourly measurements performed with the Wave radon detector is shown in Figure 3. The operation of the system can be explained as follows: The electronic detector placed at the measurement point measures the indoor radon concentration every hour. Using the Airthings Wave application installed on a smart phone, data can be downloaded to the mobile phone via Bluetooth connection or transferred to the internet database and saved on a PC with internet access. The obtained data then can be tabulated and examined with a spreadsheet program such as Excel.

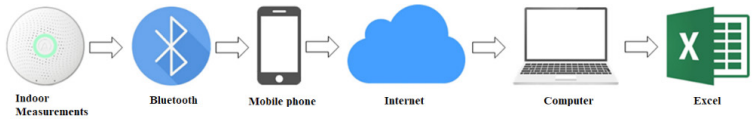

Figure 3. Data collection process for radon measurements.

2.3. Experimental Study

The experimental measurements were carried out between April 1 and April 30, 2022, in the faculty building where the Department of Physics is located. In the selection of the measurement points, 3 rooms on each floor were chosen in the 3-storey Physics Department by ensuring that the measurement points were on top of each other (Figure 4 and Figure 5). The photograph showing the floors of the department and marking the locations of the rooms, where the detectors were placed, is presented in Figure 4. Floor sketches of the Physics Department and the locations of the detectors placed at the measurement points are represented in Figure 5. The general characteristics of the rooms selected for radon measurements, the serial numbers of the electronic detectors placed at these measurement points, and the coding used in the study are given in Table 2. All radon detectors, one at each measurement point, were mounted at respiratory level, 1.5 meters above the floor and in order to obtain more accurate results, the measurement devices were not placed near radiators, electronic devices, doors or windows. The data of the hourly measurements performed during the study were recorded in accordance with the system architecture presented in Figure 3 and stored on a portable USB memory.

Figure 4. Rooms with measurement points on the floors in the Physics Department (The locations of the rooms, where the detectors are placed, are labelled in accordance with the sketch in Figure 5 and the coding given in Table 2).

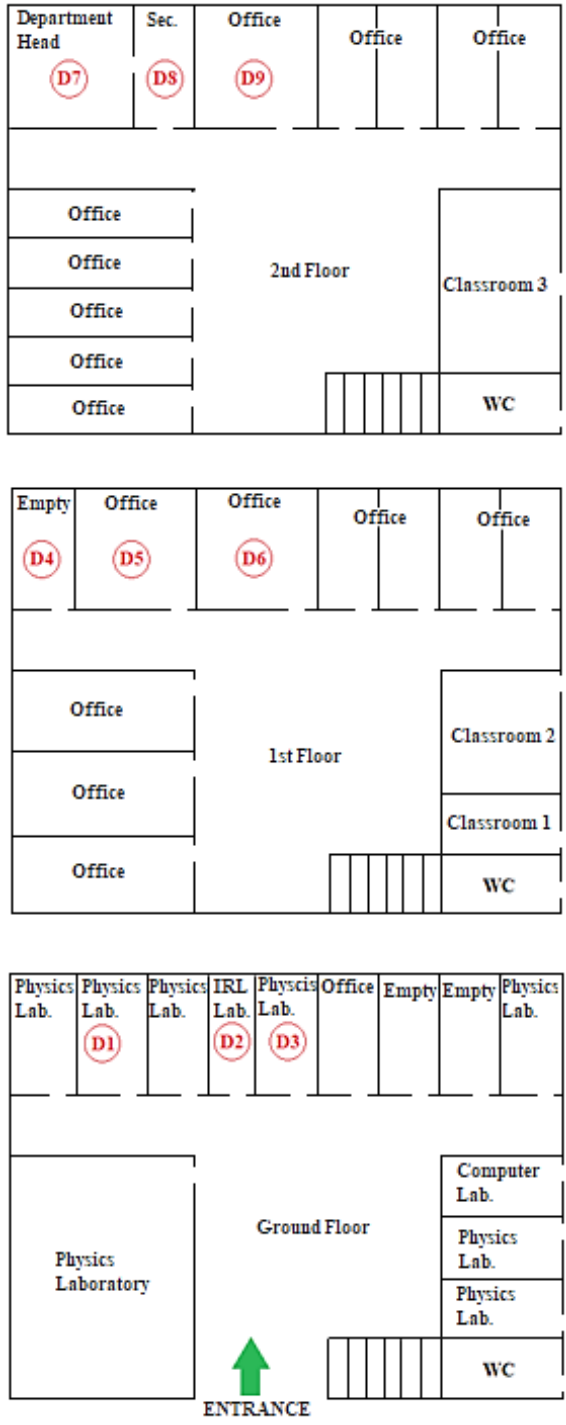

Figure 5. Display of measurement points on the floor sketches of the department (the coding matches with the codes in Figure 4 and Table 2).

Table 2. Information about the radon detectors used and the rooms where measurements were performed.

Detector's		Measurement Unit's			
Code	**Serial number**	**Room number**	**Number of doors**	**Number of windows**	**Area (m^2)**
D1	2950007481	Z-3	1	1	13.4
D2	2900262419	Z-5	1	1	13.7
D3	2950007518	Z-6	1	1	13.2
D4	2950006741	K1-4	1	1	19.7
D5	2950007488	K1-5	1	2	30.1
D6	2950007514	K1-6	1	2	30.1
D7	2950007493	K2-6	2	2	35.6
D8	2950007513	K2-7	2	1	14.4
D9	2950007495	K2-8	1	2	29.1

3. Results

5958 data were recorded for hourly radon measurements carried out simultaneously throughout the measurement process in 9 units of the Department of Physics at Süleyman Demirel University. The location information of the detectors used in the study and the descriptive statistical information of the measurement data obtained are presented in Table 3. The data were analysed statistically with the SPSS 29.0 program (WEB-8). Before starting the analysis, a normality test was applied to the data to determine whether the data had a normal distribution.

Since the number of data in the groups was more than 50, normality was examined with the Kolmogorov-Smirnov test and the data was considered to have a normal distribution since the significance value was found to be $p>0.05$. Since the data had a normal distribution and the groups were independent, statistically significant differences were detected for the measurements on the ground floor and the 1st floor using the one-way ANOVA test ($p<0.05$). However, it was found that there was no significant difference ($p>0.05$) between the measurements on the second floor (Table 3). The floor on which the measurement point was located was accepted as a criterion of the detector height, and the locations of the detectors were determined by GPS coordinates. The 662 measurement data taken per detector, descriptive statistics such as minimum (Min.), maximum

(Max.), and arithmetic mean (Mean) at the relevant measurement point, as well as p-values for each floor, are summarized in Table 3.

Table 3. Locations of measurement points and descriptive statistics of radon data (Coding of the detectors is compatible with the coding given in Figures 4 and 5, and Table 2).

Information about Detectors			**N**	**Descriptive Information on Measurement Data**			**p**
Code	**Location**	**Floor**		**Min. (Bq/m³)**	**Max. (Bq/m³)**	**Mean**	
D1	37.83042ºN 30.53260ºE	Ground floor	662	108	352	213	0.001
D2	37.83045ºN 30.53263ºE		63	599	271		
D3	37.83048ºN 30.53254ºE		11	102	53		
D4	37.83039ºN 30.53251ºE	First Floor	662	54	536	268	0.001
D5	37.83043ºN 30.53253ºE		30	235	95		
D6	37.83054ºN 30.53274ºE		27	342	129		
D7	37.83044ºN 30.53249ºE	Second Floor	662	21	213	103	0.623
D8	37.83042ºN 30.53248ºE		26	294	101		
D9	37.83049ºN 30.53266ºE		14	294	100		

N: number of measurements, p: significance value obtained as a result of one-way ANOVA test

It was observed that the atmospheric radon concentrations recorded by the detectors on the ground floor varied between 11Bq/m^3 and 599Bq/m^3. It is a phenomenon that can be encountered in the literature that atmospheric radon levels at measurement points close to each other in a building built on the same soil structure can be different from each other (Karakılıç et al., 2014). In addition to the fact that radioactive decay is a random process, there may be many different reasons that may lead to this result due to differences in

environmental parameters. In our study, it was found that the averages obtained from the radon measurements of the D1 and D2 detectors were in the same order, but the average obtained from the radon measurements of the D3 detector on the ground floor was found to be lower. It is thought that this situation may be related to the isolation of the room where the D3 detector is located. In addition, the measurements of the D1, D2 and D3 detectors placed on the ground floor were statistically analysed with one-way ANOVA test (Table 3) and it was determined that there was a statistically significant difference between the measurements on this floor ($p<0.05$). While the maximum radon concentration recorded by the detectors on the first floor increased to 536Bq/m^3, the lowest concentration detected during the measurement period was 27Bq/m^3. While the average radon levels in the rooms where the D5 and D6 detectors are located are relatively similar, a higher concentration is observed in the office where the D4 detector is located. This is thought to occur because this less frequently used office has lower natural ventilation than other rooms on the same floor. As a result of examining the radon measurements on the first floor using one-way analysis of variance test, it was found that there was a statistically significant difference ($p <0.05$) between the measurement data of D4, D5, and D6 detectors (Table 3). Radon concentrations ranging from 14 Bq/m^3 to 294 Bq/m^3 were observed with D7, D8, and D9 detectors taking measurements on the second floor. It is seen that the average radon levels in the rooms measured on the second floor are very close to each other (Table 3). The measurement data of D7, D8, and D9 detectors were statistically examined with one-way ANOVA test (Table 3) and it was determined that there was no statistically significant difference between the measurements on this floor ($p>0.05$).

In order to examine the behaviour of indoor radon concentration according to floors, descriptive statistics of the measurement data obtained for floors were determined with SPSS 29.0 (Table 4).

Table 4. Descriptive statistics of radon measurements for floors

Floor	N	Min.	Med.	Max.	Mean	p
		(Bq/m^3)				
Ground floor	1986	11	173	599	179	
First Floor	1986	27	132	536	164	0.001
Second Floor	1986	14	93	294	101	
Total	5958	11	116	599	148	-

N: number of measurements, p: significance value determined by one-way ANOVA test

The measurement data here has a normal distribution and since the groups are independent from each other, one-way ANOVA test was applied. Thus, it was revealed that there was a statistically significant difference ($p<0.05$) between all measurements of the floors (Table 4). The change in average radon concentrations depending on height (the floors) is visually presented in Figure 6.

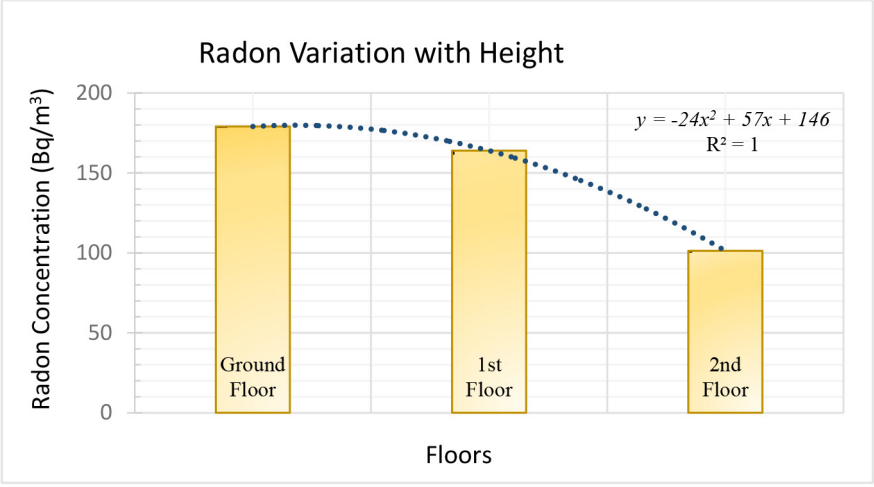

Figure 6. Indoor radon variation in the department building depending on the height of the floors.

For the recorded measurements in our study, it has been clearly demonstrated that radon decreases depending on the height as the floor height increases, and it has been shown in Figure 6 that this relationship can be successfully explained using a second-order polynomial fit ($R^2=1$). In order to examine the differences between floor measurements, the Tamhane test for the homogeneity of variance and the Post-hoc tests for the differences were applied, and the level of differences between the measurements was determined as $p=0.001$. Measurements with statistically significant differences and their comparisons are as follows; 1st Floor measurements < Ground Floor measurements, 2nd Floor measurements < Ground Floor measurements and 2nd Floor measurements < 1st Floor measurements ($p<0.05$). Additionally, it was also observed that, compared to atmospheric radon concentrations recorded at the measurement points on weekends, a decrease occurred on weekdays due to the use of these units, which could be related to natural ventilation.

4. Conclusion

Radon, among the most dangerous carcinogens, can be observed in different concentrations depending on the altitude in enclosed spaces where we spend most of our time. In this study, the variation of indoor atmospheric radon concentration depending on height was investigated by performing simultaneous hourly radon measurements in April 2022 (for approximately 4 weeks) with 9 electronic detectors placed in 3 rooms on the ground, first and second floors in the Physics Department of Süleyman Demirel University. During the measurement period, 1986 radon concentration data were taken per floor. When the averages obtained from the measurements were examined, it was found that the radon level on the ground floor was 179 Bq/m^3, the radon concentration on the first floor was 164 Bq/m^3, and the radon level on the second floor was 101 Bq/m^3. Approximately 41% of the 5958 hourly measurement data taken in total were found to be lower than the intervention level of 100 Bq/m^3 recommended by WHO. In addition, it was determined that only 9% of the measurements exceeded the intervention level of 300 Bq/m^3 recommended by ICRP for common spaces. However, none of the hourly radon concentration measurements exceeded the intervention level of 1000 Bq/m^3 recommended by TENMAK for workplaces. Measurement data were analysed with the SPSS 29.0 program, and as a result of one-way ANOVA tests, it was determined that there was a statistically significant difference between floor measurements ($p<0.05$). Comparisons were made between these measurements that had statistically significant differences. Accordingly, it was seen that the order of measurements of radon concentrations on each floor was as follows: 1st Floor measurements < Ground Floor measurements, 2nd Floor measurements < Ground Floor measurements and 2nd Floor measurements < 1st Floor measurements ($p<0.05$). Within the limits of the study, it was revealed that indoor atmospheric radon concentration decreased with increasing height. In order to minimize the health risk caused by radon; the insulation of the rooms where D1, D2 and D4 detectors are located can be reviewed, rooms with radon concentrations above 100 Bq/m^3 can be ventilated more frequently, and it can be suggested to identify risky areas by making more comprehensive measurements in the faculty building.

Acknowledgements

This research was supported by The Scientific and Technological Research Council of Türkiye (TÜBİTAK) under the 2209-A University Students Research

Projects Support Program with project number 1919B012106382. The authors would like to thank TÜBİTAK BİDEB (the Directorate of Science Fellowships and Grant Programmes).

References

Abu-Jarad, F., & Fremlin, J. H. (1982). The activity of radon daughters in high-rise buildings and the influence of soil emanation. *Environment International, 8*(1-6), 37-43.

Afolabi, O. T., Esan, D. T., Banjoko, B., Fajewonyomi, B. A., Tobih, J. E., & Olubodun, B. B. (2015). Radon level in a Nigerian University Campus. *BMC research notes, 8,* 1-6.

Akkurt, N. (2014). *Seasonal variation of radon concentrations in Eskişehir districts* (MSci Thesis in Turkish). Eskişehir Osmangazi University, Institute of Science and Technology, Department of Physics, Eskişehir.

Aldemir, K. (2018). *Measurement of radon levels in the primary Sschools in Batman* (MSci Thesis in Turkish). Batman University, Institute of Natural and Applied Sciences Physics Department, Batman.

Altınsöz, M., Alğın, E., Aşıcı, C. ve Soğukpınar, H. (2016). Radon concentration measurements at a university campus in Turkey. *Turkish Journal of Physics, 40*(1), 69-75.

Al-Zoughool, M., & Krewski, D. (2009). Health effects of radon: a review of the literature. *International journal of radiation biology, 85*(1), 57-69.

Baeza, A., Navarro, E., Roldan, C., Ferrero, J.L., Juanes, D., Corbacho, J.A., Guillen, F.J., (2003). Indoor radon levels in buildings in the autonomous community of Extremadura (Spain). *Radiation protection dosimetry, 103*(3), 263-268.

Bahtijari, M., Stegnar, P., Shemsidini, Z., Ajazaj, H., Halimi, Y., Vaupotič, J., & Kobal, I. (2007). Seasonal variation of indoor air radon concentration in schools in Kosovo. *Radiation measurements*, *42*(2), 286-289.

Bayraktar, G., Karakılıç, V., Karadem, A., & Kürkçüoğlu, M. E. (2009). Radon measurements at S.D.U. Sabancı dormitory by using CR-39 detectors, *X. National Nuclear Sciences and Technologies Congress,* 6-9 October 2009,291-301.

Büyüksaraç, A., & Kuluöztürk, M. F. (2022). Measurement of indoor seasonal and regional radon (^{222}Rn) gas activity in Çanakkale (Turkey). *Bitlis Eren University Journal of Science, 11*(3), 911-921.

Cigna, A.A. (2005). Radon in Caves. *International Journal of Speleology, 34*(1), 1-18, Italy.

Çakmak, M. A. (2014). *Measurement of radon activity concentrations of air indoors at various place and conditions in Samsun by active method (AlphaGUARD)* (MSci Thesis in Turkish). Ondokuz Mayıs University, Institute of Science, Samsun.

Çıtlak, K. (2018). *Determination of radon concentration in building in Sakarya University campus region* (MSci Thesis in Turkish). Sakarya University, Institute of Science, Sakarya.

De Maria, L., Sponselli, S., Caputi, A., Delvecchio, G., Giannelli, G., Pipoli, A., ... & Vimercati, L. (2023). Indoor Radon Concentration Levels in Healthcare Settings: The Results of an Environmental Monitoring in a Large Italian University Hospital. *International Journal of Environmental Research and Public Health, 20*(6), 4685.

Dorn, E., (1900). Die Von Radioaktiven Substanzen Ausgesandte Emanation. Abhandlungen Der Naturforschenden. *Gesellschaft zur Halle,* 23, 1-15.

EPA, (2005). Environmental Protection Agency. Citizen's Guide to Radon. *U.S. EPA* 402-K02-006, 11-16.

Erdoğan, M., Abaka, M., Manisa, K., Bircan, H., Kuş, C., & Zedef, V. (2020). Indoor radon activity concentration and effective dose rates at schools and thermal spas of Ilgın. *Nuclear Technology & Radiation Protection, 35*(4), 339-346.

Gallelli, G., Panatto, D., Lai, P., Orlando, P., & Risso, D. (1998). Relevance of main factors affecting radon concentration in multi-storey buildings in Liguria (Northern Italy). *Journal of environmental radioactivity, 39*(2), 117-128.

George, A. C. (2008, August). World history of radon research and measurement from the early 1900's to today. In *AIP Conference Proceedings* (Vol. 1034, No. 1, pp. 20-33). American Institute of Physics.

Gül, B. T. (2019). *Measurements of radon gas concentrations in buildings* (MSci Thesis in Turkish). Ankara University Institute of Nuclear Sciences, Ankara.

ICRP, (2010). International Commission on Radiological Protection. Lung Cancer Risk From Radon and Progeny, *ICRP* ref 4843-4564-6599 1, 20-23.

ICRP, (2014). International Commission on Radiological Protection. Radiological Protection Against Radon Exposure, *ICRP Publication 126. Annual, 43*(3), 5–73.

Ioannides, K. G., Stamoulis, K. C., & Papachristodoulou, C. A. (2000). A survey of ^{222}Rn concentrations in dwellings of the town of Metsovo in North-Western Greece. *Health physics, 79*(6), 697-702.

Karpińska, M., Mnich, Z., Kapała, J., Birula, A., Szpak, A., & Augustynowicz, A. (2008). Indoor Radon Concentrations in Concrete Slab Buildings Situated in Green Hills Housing Estate in Białystok, Poland. *Polish Journal of Environmental Studies, 17*(1).

Karakılıç, V., Bayraktar, G., Kürkçüoğlu, M., Haner, B., & Yılmaz, A. (2014). Radon Measurements at S.D.U. Information Center. *Süleyman Demirel University, Journal of Natural and Applied Sciences, 13*(3), 201-207.

Khan, A. J., Varshney, A. K., Prasad, R., & Tyagi, R. K. (1987). The indoor concentration of radon and its daughters in a multistorey building. *International Journal of Radiation Applications and Instrumentation. Part D. Nuclear Tracks and Radiation Measurements, 13*(1), 77-80.

Khan, A. J. (2000). A study of indoor radon levels in Indian dwellings, influencing factors and lung cancer risks. *Radiation measurements, 32*(2), 87-92.

Koçer, A.A. ve Kürkçüoğlu, M.E. (2019). An investigation on height dependence of atmospheric indoor radon concentration. *5th International Conference on Theoretical and Experimental Studies in Nuclear Applications and Technology,* Amasya, Turkey, 2-4 Mayıs 2019.

Kropat, G., Bochud, F., Jaboyedoff, M., Laedermann, J.-P., Murith, C., Palacios, M., Baechler, S., (2014). Major influencing factors of indoor radon concentrations in Switzerland. *Journal of environmental radioactivity*, 129, 7-22.

Kurt, A. (2015). *Determination of indoor radon concentrations at the elementary schools of Fatih district in İstanbul* (MSci Thesis in Turkish). İstanbul University, Institute of Graduate Studies in Science and Engineering, İstanbul.

Küçükönder, E. (2021). Seasonal indoor radon gas activity measurement in Kahramanmaraş province. *BEU Journal of Science, 10*(3), 891-901.

Kürkçüoğlu M., Haner, B., Yilmaz, A., & Toroğlu, İ. (2009). Radon measurements of Karaelmas campus central library. *Süleyman Demirel University Faculty of Arts and Science Journal of Science, 4*(2), 177-188.

Kürkçüoğlu, M. ve Bayraktar, G. (2012). Determination of indoor radon concentrations at Süleyman Demirel University by using nuclear track detectors. *Süleyman Demirel University Faculty of Arts and Science Journal of Science, 16*(2), 167-183.

Manousakas, M., Fouskas, A., Papaefthymiou, H., Koukouliou, V., Siavalas, G., & Kritidis, P. (2010). Indoor radon measurements in a Greek city located in the vicinity of lignite-fired power plants. *Radiation measurements, 45*(9), 1060-1067.

Martinelli G. (1993). Radon geochemistry and geophysics in deep fluids in Italy. In: Furlan G & Tommasino L (Eds.)- *Radon monitoring inrRadioprotection, environmental and Earth sciences.* World Scientific, pp.435-453.

Mc Laughlin, J. (2012, September). Radon: past, present and future. In Paper presented at the *First East European Radon Symposium–FERAS*.

Müllerova, M., Holý, K., (2010). Study of relation between indoor radon in multi-storey building and outdoor factors. Fifth International Summer School on nuclear physics methods and accelerators in biology and medicine. *AIP conference proceedings, 1204*(1), 161-162.

NCRP, (1988). Report Measurements of Radon and Radon Daughters in *Air, No.*.97, p.174.

Partington, J. R. (1957). Discovery of radon. *Nature, 179* (4566), 912-912.

Pavlenko, T. A., Los, I. P., Goritsky, A. V., & Aksenov, N. V. (1997). Exposure doses due to indoor ^{222}Rn in the Ukraine and basic directions for their decrease. *Radiation measurements, 28*(1-6), 733-738.

Papaefthymiou, H., Mavroudis, A. ve Kritidis, P. (2003). Indoor radon levels and influencing factors in houses of Patras, Greece. *Journal of Environmental Radioactivity, 66*(3), 247-260.

Papaefthymiou, H. ve Georgiou, C. D. (2007). Indoor radon levels in primary schools of Patras, Greece. *Radiation protection dosimetry, 124*(2), 172-176.

Porstendorfer, J., Butterweck, G., Reineking, A., (1994). Daily variation of the radon concentration indoors and outdoors and the influence of meteorological parameters. *Health Physics, 67*(3), 283-287.

Psichoudaki, M. ve Papaefthymiou, H. (2008). Natural radioactivity measurements in the city of Ptolemais (Northern Greece). *Journal of Environmental Radioactivity, 99*(7), 1011-1017.

Rafique, M., Rahman, S.U., Mahmood, T., Rahman, S., Matiullah, (2011). Assessment of seasonal variation of indoor radon level in dwellings of some districts of Azad Kashmir, Pakistan. *Indoor and built Environment. 20*(3), 354-361.

Rutherford, E., (1900). A radio-active substance emitted from thorium compounds. *The London, Edinburgh, and Dublin Philosophical Magazine and Journal of Science*, *49*(296), 1-14.

Shaikh, A. N., Ramachandran, T. V. ve Kumar, A. V. (2003). Monitoring and modelling of indoor radon concentrations in a multi-storey building at Mumbai, India. *Journal of environmental radioactivity, 67*(1), 15-26.

Tamir Darcan, M. (2020). *Measurement of indoor radon gas Kırklareli University Kayalı Campus* (MSci Thesis in Turkish). Kırklareli University, Institute of Science, Kırklareli.

UNSCEAR, (1988). United Nations Scientific Committee on the Effects of Atomic Radiation. Sources, Effects and Risks of Ionizing Radiation, *United Nations sales publication, Report No: E.88*.IX.7, 647p. New York.

UNSCEAR, (2000). United Nations Scientific Committee on the Effects of Atomic Radiation, Exposures from Natural Radiation Sources Annex B, 117-118, New York, USA.

Vasilyev, A., Yarmoshenko, I., Onishchenko, A., Hoffmann, M., Malinovsky, G., Marenny, A. ve Karl, L. (2020). Radon measurements in big buildings: Pilot study in Russia. *Radiation Protection Dosimetry, 191*(2), 214-218.

Vukotić, P., Zekić, R., Antović, N. M. ve Anđelić, T. (2019). Radon concentrations in multi-story buildings in Montenegro. *Nuclear Technology and Radiation Protection, 34*(2), 165-174.

WEB-1 IARC, (2020). International Agency for Research on Cancer, https://gco.iarc.fr/today/data/factsheets/cancers/39-All-cancers-fact-sheet.pdf.

WEB-2 TR Ministry of Health General Directorate of Public Health, (2022). https://hsgm.saglik.gov.tr/depo/birimler/kanser-db/Dokumanlar/Istatistikler/Kanser_Rapor_2018.pdf.

WEB-3 Government of the Republic of Türkiye. Access Date: 06.06.2022. (S.I.No. 37 published in the Official Gazette No. 23999 dated 24.03.2000, Regulation on Amending the Regulation on Amendments to the Radiation Safety Regulation No. 25598 Published in the Official Gazette), 2004. https://www.mevzuat.gov.tr/File/GeneratePdf?mevzuatNo=5272&mevzuatTur=KurumVeKurulusYonetmeligi&mevzuatTertip=5.

WEB-4 Isparta Provincial Directorate of Culture and Tourism, (2023). https://isparta.ktb.gov.tr/TR-71016/isparta.html.

WEB-5 TR Isparta Governorship, (2023). http://www.isparta.gov.tr/isparta.

WEB-6 Süleyman Demirel University, 2023. https://aday.sdu.edu.tr/bolum/fen-edebiyat-fakultesi.

WEB-7 Airthings; Wave Radon, (2023). https://www.airthings.com/wave-radon.

WEB-8 Süleyman Demirel University Department of Information Technology, 2023. https://bidb.sdu.edu.tr/tr/kolay-ulasim/lisansli-yazilimlar-14640s.html.

WHO, (2005). Radon and Cancer. *World Health Organization Fact Sheet,* No:91.

WHO, (2009). World Health Organization. *Handbook on Indoor Radon: A Public Health Perspective,* 94p.

Yarmoshenko, I., Onishchenko, A. ve Zhukovsky, M. (2013). Establishing a regional reference indoor radon level on the basis of radon survey data. *Journal of Radiological Protection, 33*(2), 329.

Yılmaz Şen, G. (2009). *Investigation of the effect of natural gas usage on indoor radon levels* (MSci Thesis in Turkish). Ege University, Institute of Science, Bornova, İzmir.

CHAPTER IV

RADIATION AND MOLECULAR OXIDATIVE STRESS

Aysel GUVEN[1] & Gülçin BILGICI CENGIZ[2]

[1](Assoc. Prof. Dr.), Başkent University,*
Vocational School of Healthcare Services, Ankara, Turkey
E-mail:ayselguven@hotmail.com,
ORCID: 0000-0001-7511-7105

[2](Assoc. Prof. Dr.), Kafkas University, Faculty of Science and Letters,
Department of Physics, Kars, Turkey
E-mail:gulcincengiz@kafkas.edu.tr,
ORCID: 0000-0002-6164-3232

1. Introduction

Radiation is a physical factor that always exists in nature, exists in different spectra in space, and affects living systems by releasing or transferring energy in the form of electromagnetic waves or particles. Radiation is divided into electromagnetic wave and particle type (CNSC, 2012).

Electromagnetic wave type radiation; It is a type of radiation with a certain energy but no mass. These are like waves of electric and magnetic energy that travel by vibrating. Electromagnetic waves (EM) are classified by three physical properties called wavelength λ (m), frequency f (Hz), and energy E (J or eV) depending on it (Kaya, 1997). This classification is called the electromagnetic spectrum (Figure 1).

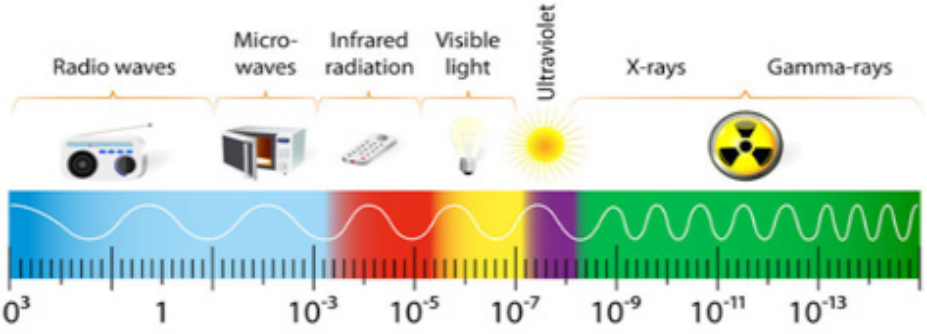

Figure 1: The electromagnetic spectrum
(https://www.google.com/search?q=elektromanyetik)

Today, sources of electromagnetic fields include radars, mobile phones, radio and television transmitters, various instruments used in medical and industrial applications, high voltage lines, microwave ovens, and electrical household appliances. Radiations are classified as ionizing and non-ionizing radiation according to their ability to penetrate the matter and remove electrons from the atoms or molecules that make up the body (NCRP, 2009). Radioactivity; refers to the amount of ionizing radiation emitted by a substance. In other words, it is expressed as the amount of decay of the radioactive substance in a certain time interval, that is, the substance emits alpha or beta particles, gamma rays, x-rays, or neutrons. The units of measure for radioactivity are Curie (Ci) and Becquerel (Bq) (Khan, 2017). Particle radiation, on the other hand, is tiny particles with a certain mass and energy that form the basic structure of a very fast-moving atom (Robert Percuoco, 2014)

Radiation interacts with atoms and molecules and transfers energy to the environment it passes through **(**Leroy, and Rancoita, 2011). Natural radiation consists of natural radioactive materials that have existed since the formation of the world and cosmic rays from space. Natural sources of radiation include soil, drinking water, air, radioisotopes in the Earth's crust, cosmic rays from outer space, and the food we eat. The natural radiation in the soil to which living things are exposed is formed as a result of ^{226}Ra, ^{232}Th, and ^{40}K radioactive serial elements and their decomposition products (Güven et al, 2023; Bilgici Cengiz, 2020). The dose rate that living things are exposed to is approximately 85% due to natural radiation and approximately 15% to artificial radiation (Karam and Leslie, 2005). As a result of the thinning of the ozone layer, Ultraviolet radiation

(UV-R) can reach the earth directly, and health and environmental effects due to this UV can occur.

Isotopes, which are in a stable state in nature, can be made radioactive by artificial means, and this phenomenon is called artificial radioactivity. Man-made radioactive sources, nuclear power plants, X-ray-producing devices, and some medical devices can be examples of artificial radiation sources (Oyar and Gülsoy, 2003).

As seen in Figure 2, it is possible to divide the radiation into two groups "ionizing" and "non-ionizing" radiations. Ionizing radiation can easily pass into matter and remove electrons from atoms or molecules (Özgüner and Mollaoğlu, 2006). Radiation exposure for medical purposes in the United States accounts for more than 95% of all man-made radiation exposures and accounts for half of all radiation exposures (Hricak et al., 2011). In the USA, the total radiation dose to which patients are exposed due to medical imaging has increased 6 times in the last 15 years (Mettler et al., 2009). An estimated 3.1 billion radiographic processes and 37 million diagnostic nuclear medicine applications are performed annually worldwide (Hricak et al., 2011).

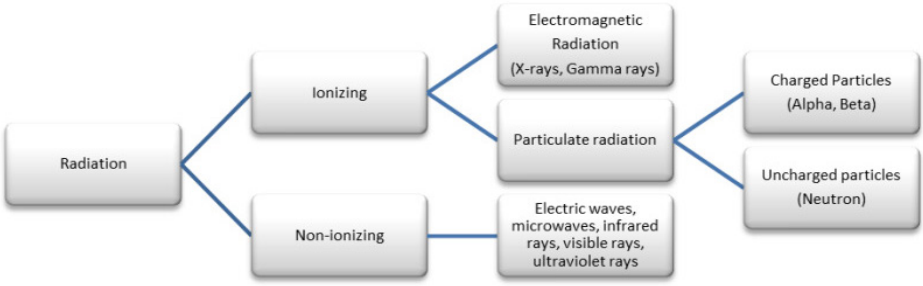

Figure 2. Classification of radiation

The most frequently exposed radiation sources are natural sources such as cosmic rays and radon in the earth's crust. Others are from human-made waste from nuclear reactors; x-ray, tomography, or mammography equipment used for medical diagnostic purposes; radiotherapy used in cancer treatment; and nuclear accidents caused by the use of nuclear weapons and nuclear testing. Wireless communication tools such as Wi-Fi and Bluetooth, base stations, mobile phones, and electronic devices emit EM radiation Since we are exposed to radiation from many sources in almost every aspect of life, the effects of radiation on human health have been an important research topic. Studies in this field have accelerated with decisive developments such as the nuclear war (Hiroshima and

Nagasaki atomic bomb attacks) and reactor accidents (Chernobyl disaster). The number of people working with radiation sources worldwide is approximately 23 million. About 10 million of them are exposed to artificial sources. Three out of every four workers exposed to artificial sources work in the medical sector; The annual effective dose per worker is 0.5 mSv (UNSCEAR, 2000). Low and/or high-dose radiation applications create effects at the cellular level by activating biochemical and molecular signalling pathways in the cell. (Hao et al. 2018; Poljak and Cvetkovic 2019).

Controversy over the biological effects of radiation has been a public health issue for the last 30 years. Various studies conducted with experimental animals have shown that various radiation exposures cause genotoxicity, hypersensitivity, and cytotoxicity and disrupt some cellular functions. It has also been reported that it negatively affects the digestive system, cardiovascular system, nervous system, endocrine system, and reproductive functions (Lagroye and Poncy, 1998; Açıkgöz, 2019). The main cellular mechanism reported in studies on radiation damage is the formation of intracellular reactive oxygen species (ROS) (Topbaş and Hasırcı, 2022). Nowadays, radiation is constantly received for the purpose of diagnosis, treatment, and research of various diseases, depending on the frequency of use of various devices with electromagnetic fields and materials developed with natural resources and technology. It can be said that the high frequency (300 Hz-10 MHz) electromagnetic fields created by these disrupt the oxidant-antioxidant balance of the human body, causing an increase in ROS such as superoxide anion, hydroxyl radical, hydrogen peroxide, and therefore oxidative effects.

2. Radiation and Reactive Oxygen Species (ROS)

It is known that free oxygen radicals are chemically active and play a role in the basis of many diseases. Radiation is one of the important reasons responsible for the formation of invisible free radicals. Radiation sources can excite and ionize materials by transferring their energy. Most free oxygen radicals are produced in low amounts in the body during normal aerobic metabolism, radiation exposure, and environmental pollution and cause damage to cells that can always be corrected (Genestra, 2007).

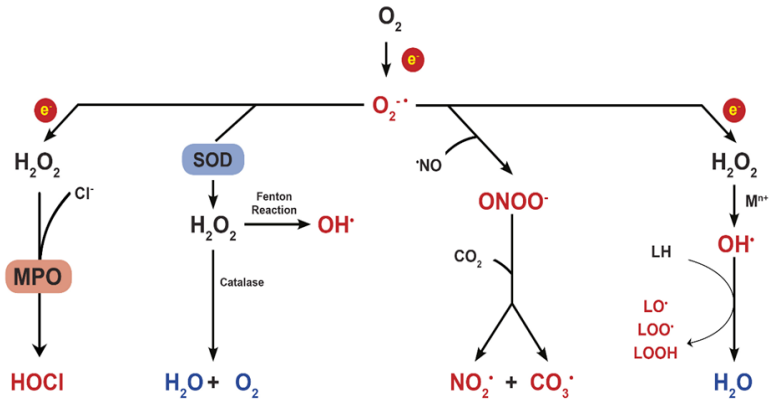

Figure 3. Reactive oxygen species (ROS)

Among the radicals, the most reactive type that attacks biological molecules is the hydroxyl radical. The radical with the strongest reactivity among ROS is hydroxyl (OH•), which is formed by the Fenton or Haber Weiss reaction (Figure 3). This begins when highly reactive radicals attack polyunsaturated fatty acids in cell membranes and remove a hydrogen atom from the methylene group (-CH2-). While this radical is synthesized from H2O2 as a result of the Fenton and Haber-Weiss reaction (in the presence of Fe+2 and Cu+), it is also formed as a result of exposure to water to high-energy ionising radiation (Colleen et al., 2007). The disruption of oxidative balance as a result of the increase in reactive oxygen species (ROS) formed during cellular metabolism, such as hydroxyl radical, superoxide radical and hydrogen peroxide, and the insufficiency of antioxidants that detoxify them, is defined as oxidative stress. Since the hydrogen atom contains only one electron, an electron is removed from the methylene group, leaving an unpaired electron on the carbon. Reactive oxygen species formed as a result of the increase in oxidative stress attack the double bond groups of intracellular lipid and protein structures and the double bonds of the bases in DNA and initiate chain oxidation reactions by breaking a hydrogen atom.

As a result, macromolecules such as intracellular lipids, proteins and DNA are damaged, resulting in cell damage or cell death (Figure 4). The most important pathological process associated with DNA damage is carcinogenesis, and oxidative damage is thought to play an important role in the initiation, progression and malignant transformation stages of carcinogenesis. The most common ROS in the organism is the lipid radical formed by the removal of hydrogen from the allyl group of unsaturated fatty acids. This structure first

reacts with oxygen to form the lipid peroxy radical, and then forms lipid hydroperoxides by making a chain reaction with lipids (Onat et al., 2002; Güven et al., 2021, Güven et al. 2003). High-frequency (300 Hz-10 MHz) electromagnetic fields disrupt the oxidant-antioxidant balance of the human body, causing an increase in ROS such as superoxide anion, hydroxyl radical, hydrogen peroxide, and therefore oxidative stress (Wang and Zhang, 2017). Our brain, which is the main organ of the central nervous system and where 20% of our body's oxygen consumption occurs, is more sensitive to oxidative stress because it has lower antioxidant capacity than other organs.

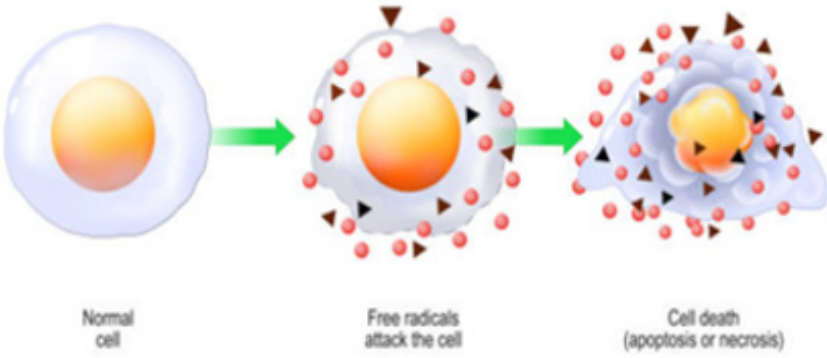

Figure 4: Effects of free radicals on the cell

Most intracellular regulatory changes after radiation occur through the interaction of classical signalling harmonizers between oxygen free radicals, DNA, and DNA double breaks (DSBs). Preservation of normal tissues may allow for increased radiation dose and increased tumour control. The cell component most affected by free radicals is lipids. However, almost all of the molecules that make up the cell are exposed to the harmful effects of free radicals. In particular, fatty acids and cholesterol in the cell membrane are attacked by free radicals, causing the release of lipid peroxidation products (Korkmaz, 2014; Güven and Alkış, 2018).

Radiation can seriously reduce the quality of life and life expectancy if precautions are not taken. The harmful effect of radiation results from the production of free radicals and reactive oxygen species (ROS). Reactive oxygen species, especially hydroxyl radicals, cause membrane lipid peroxidation, oxidation of cell proteins, and deoxyribonucleic acid (DNA). Additionally, ROS creates an inflammatory response cascade. Ultimately, it may cause cell death. Substances released from dead cells then increase inflammation by

stimulating endothelial and macrophage-like cells. The increased inflammatory response can cause long-term and irreversible tissue damage. Ionizing radiation directly interacts with DNA and proteins. The damaged cell tries to combat this harmful effect by activating the defence system. If exposure to ionizing radiation continues, the damage to DNA cannot be repaired and increases the risk of cancer. As a result of these effects; Hair loss, respiratory system diseases, gastrointestinal system bleeding, bleeding due to bone marrow suppression, and anaemia may occur. In addition, cancer may occur in the short or long term, depending on the pathogenesis of many diseases such as diabetes, cardiovascular diseases, neurological diseases, atherosclerosis, and inflammatory disorders, and most importantly, depending on the dose and dose rate of radiation. Studies have shown that low frequency and intensity pulsed electromagnetic field (PEMF) increases the permeability of cell membranes, promotes wound healing in soft tissues, and has a remarkable role in the treatment of symptoms of skin ulcers, neurodegenerative and ocular diseases (Wang and Zhang, 2017). The current study, unlike the literature, showed that 75 Hz, 1±0.2 mT PEMF exposure affected cell viability, ROS level, and antioxidant activity in U-87 MG human glioblastoma cells, in which oxidative stress was induced by treatment with high dose (0.1 mM) H2O2 for 30 min, 24 h, 48 h. It has been shown that it reduces the effect on the activity and/or amount of GPx and GSH, which are important molecules in the defence system.

Oxidative stress is a condition associated with many diseases such as myocardial infarction, neurodegenerative diseases, atherosclerosis, heart failure, and chronic liver and lung diseases. Modern society's constant exposure to radiation suggests that this can cause increased oxidative stress in cells and cellular damage through other mechanisms.

3. Effect of Radiation on Tissues

People absorb radioactive substances into their bodies from the food eat, the liquids drink, and the air breathe, and they are constantly exposed to radiation. When the human body is exposed to radiation, it accumulates energy in its body. The harmful effects of radiation to which a person is exposed vary depending on the person's weight, age, gender, and body structure. Since some organs differ in sensitivity compared to other parts and organs of the body, the effects of radiation on the living body also vary. Depending on these variables, the definition of equivalent dose or, in the case of the whole body, the effective

equivalent dose is used for the radiation dose that includes all these situations. The name of the equivalent dose or effective equivalent dose unit is Sievert (Sv) (Kaya et al., 1997). Some epidemiological findings (especially studies on post-atomic bomb survivors) show that for many types of cancer, the risk increases almost linearly with dose (Tamam et al., 2016). The risk of cell damage has been established at doses less than 100 mSv. There are risk assessments available in the range of 50-100 mSv. In the study where the levels of some antioxidants (GR, GPx, GST, SOD, CAT, GSH) in the brain and liver tissues of rats were evaluated, 0.434 (W/Kg) at 1 hour/hour, 0.433 (W/Kg) 5 days a week for 1 month), and the amount of GSH in the brain and liver tissues of rats exposed to 900, 1800, and 2100 MHz RF-EMA with a specific absorption rate (SAR) value of 0.453 (W/Kg), decreased significantly, especially in rats exposed to RF-EMA. 2100 MHz RF-EMA. It was determined that the amount of GSH in brain and liver tissues was lower than in other groups (Sharma et al. 2021). The type of radiation exposure, dose, and duration of exposure have been determined to be the main factors, and ionizing radiation has been proven to cause more serious effects than non-ionizing radiation. The effects occurring in different tissues and organs exposed to the same amount of radiation are not the same. Therefore, tissue and organ weight factors (WT) were determined (Sharma et al., 2021). The type of radiation exposed, dose, and duration of exposure have been determined to be the main factors, and it has been proven that ionizing radiation causes more serious effects than non-ionizing radiation. The effects occurring in different tissues and organs exposed to the same amount of radiation are not the same. Therefore, tissue and organ weight factors (WT) were determined. The effects on tissues and organs exposed to the same amount of radiation are different. Therefore, tissue and organ weight factors (WT) were determined. Tissue and organ weight factors according to the International Commission on Radiological Protection's (ICRP' actual determination are given in Table 1 (ICRP 2007).

Ionizing radiation can cause many diseases and cancer. Both physical and biological factors influence the pathophysiology of normal tissue damage after radiotherapy. There is no cell that is completely resistant to radiation. Among the structures that make up the cell, the nucleus and especially the chromosomes in the division stage are much more sensitive than the cell cytoplasm. Radiation can cause chromosomes to break, stick together, interlock, and curl. Chromosome breaks may reorganize, remain the same, or merge with another chromosome (Ugras et. al., 2010; Kim et al., 2017).

Table 1. Tissue weighting factors according to ICRP (ICRP 2007)

Tissue	Tissue weighting factor, wT	ΣwT
Bone-marrow (red), colon, lung, stomach, breast, remaining tissues(*)	0.12	0.72
Gonads	0.08	0.08
Bladder, oesophagus, liver, thyroid	0.04	0.16
Bone surface, brain, salivary glands, skin	0.01	0.04
	Total	1.00

(*) Remaining tissues: Adrenals, extrathoracic region, gall bladder, heart, kidneys, lymphatic nodes, muscle, oral mucosa, pancreas, prostate (♂), small intestine, spleen, thymus, uterus/cervix (♀)

Radiation causes damage to the tissues it interacts with, either directly or as a result of the interaction of free radicals with other elements in the cell. In the studies carried out; It is known that the negative effects of ionizing radiation on living tissue vary depending on the irradiation time and the dose exposed (Figure 5). High doses cause cell death by creating irreparable breaks in the DNA chain, while low doses pause cell division. As the dose increases, the time for division to begin is prolonged, the number of mitosis decreases, and abnormal mitotic patterns and degenerate cells appear (Ugras et al., 2010). In addition, the temperature increase in tissues due to exposure causes the opening of voltage-gated calcium channels in nerve cells and causes cellular death by changing the electrical activity in neurons (Pall 2013; Kim et al. 2017).

Today, many diagnostic and therapeutic applications such as traditional chemotherapy, radiotherapy applications, positron emission tomography (PET) imaging, immunotherapy, and molecular targeted therapy are successful in improving survival, control of local and distant metastasis, and quality of life. Radiation-induced lung disease may occur, especially after radiotherapy is applied for the treatment of breast, lung cancer, and other thoracic malignancies (Siegel et al., 2020; Rodrigues et al., 2004). Due to radiation toxicity, radiation dose is the limiting factor in conventional radiotherapy. With the development of new radiotherapy techniques such as intensity-modulated radiotherapy (IMRT), volumetric module arc therapy (VMAT), and proton therapy, the radiation exposure of healthy lung tissue is significantly reduced. It is known that in this way, the risk of developing radiation-related pneumonia (RIP) and radiation-related lung fibrosis (RILF) is reduced. The localization of the tumour (central, peripheral), as well as the technique and dose of radiotherapy, also affect lung toxicity (Kocak et al., 2005; Palma et al., 2013). Radiation nephritis;

It is a result of necrosis, atrophy, and sclerosis that occurs following exposure of the kidney to ionizing radiation. Studies have shown that radiation damage to the stomach in the acute period; has been reported that it is characterized by ulceration, perforation, atrophic gastritis, and a decrease in gastric acid secretion (Madrazo et al., 1975; Abdel-Salam et al., 2005). After the Chernobyl accident, many people were exposed to high doses of radioactive iodine in the first few hours. One of the most important health problems caused by radioactive iodine is childhood thyroid cancer.

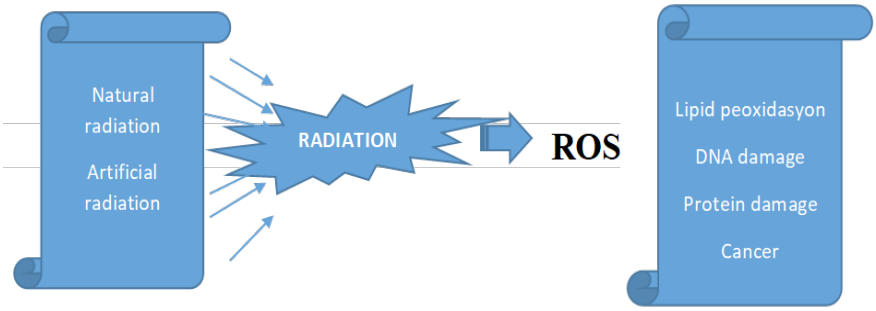

Figure 5. Damages caused by radiation-induced reactive oxygen species (ROS) to the human body

4. Conclusion

In people exposed to high radiation, skin cancer occurs when the radiation reaches the roots of the hair on the body, and cataracts occur when it reaches the eyes. The thyroid gland is vulnerable to radioactive iodine, which can destroy itself. Radiation taken through breathing or food causes lung and breast cancer. The digestive tract, stomach, and intestines suffer from many metabolic and pathological damages because of radiation. Radiation affects the ovaries in women and the testicles in men, and also causes the loss of white blood cells in the bloodstream, leaving the body vulnerable to infection. Radiation also directly triggers leukaemia and anaemia in children.

References

Abdel Salam, O. M., Hadajat, I., Bayomy, A. R., El-Shinawy, S. & Arbid, M. S. (2005). Acute effect of gamma irradiation on gastric acid secretion and gastric mucosal integrity in the rat. TheScientificWorldJournal, 5, 195–204. https://doi.org/10.1100/tsw.2005.25

Açıkgöz, Ş. (2019). Deneysel Düşük Doz Elektromanyetik Alanın Sıçan Testis ve Semen Dokularına Etkileri ve Kafeik Asit Fenetil Esterin Antioksidan Rolünün Araştırılması. Sakarya Üniversitesi, Tıp Fakültesi, Uzmanlık Tezi. (Mart 2019).

Bilgici Cengiz, G. (2020). Determination of natural radioactivity in products of animals fed with grass: A case study for Kars Region, Turkey. Scientific reports, 10(1), 6939.

Canadian Nuclear Safety Commission (CNSC). (2012). Introduction to Radiation. Minister of Public Works and Government Services Canada (PWGSC), December 2012 PWGSC catalogue number CC172-93/2012E, ISBN 978-1-100-21572-3, CANADA

Colleen, S., Marks, A.D., Lieberman, M. (2007). Marks' Temel Tıbbi Biyokimyası "Klinik Yaklaşım". 2. Baskı, Güneş Tıp Yayınları. Ankara.

Genestra M. (2007). Oxyl radicals, redox-sensitive signalling cascades and antioxidants. Cellular signalling, 19(9), 1807–1819. https://doi.org/10.1016/j.cellsig.2007.04.009

Güven, A., Erginsoy, S., & Kaya, N. (2003). Kazlarda karbon tetraklorür zehirlenmesinin biyokimyasal ve patolojik parametrelere etkisi. Kafkas Ü. Vet. Fak. Derg, *9*(2), 131-136.

Güven, A. ve Alkış, K. (2018). Hiperkolesterolemi Oluşturulmuş Farelerde Kefir ve Simvastatin Etkilerinin Araştirilmasi. Caucasian Journal of Science, 5 (2), 11-16. Retrieved from https://dergipark.org.tr/tr/pub/cjo/issue/42044/447725

Güven A, Nur G. and Deveci H.A. Liver Injury Due to Chemıcal Poisoning and Antioxidant Defence System, In Oxidative Stress and Antioxidant Defence System; Guven, A., Ed.; Livre de Lyon: Lyon, France, 2021

Güven, A., Cengiz, G. B., Çağlar, İ., & Ateş, S. (2023). Evaluation of radioactivity levels and radiological hazards of some endemic plants used as medicine in Ankara, Turkey. Applied Radiation and Isotopes. 200, 110939.

Hao, Y. H., Li, Z. H. A. O., & Peng, R. Y. (2018). Effects of electromagnetic radiation on autophagy and its regulation. Biomedical and environmental sciences, 31(1), 57-65.

Hricak, H., Brenner, D. J., Adelstein, S. J., Frush, D. P., Hall, E. J., Howell, R. W., McCollough, C. H., Mettler, F. A., Pearce, M. S., Suleiman, O. H., Thrall, J. H., & Wagner, L. K. (2011). Managing radiation use in medical imaging: a multifaceted challenge. Radiology, 258(3), 889–905. https://doi.org/10.1148/radiol.10101157

ICRP, 2007. The 2007 Recommendations of the International Commission on Radiological Protection. ICRP Publication 103. Ann. ICRP 37 (2-4).

Karam, P.A. and Leslie, S.A. (2005). Changes In Terrestrial Natural Radiation Levels Over The History Of Life. Radioactivity in the Environment, Volume 7, Pages 107-117 DOI:10.1016/S1569 4860(04)07011-1

Kaya, T., Adapınar B. and Özkan, R. (1997). Temel Radyoloji Tekniği. İstanbul: Nobel Yayın Dağıtım.

Khan, N. T. (2017). Radioactivity: an introduction to mysterious science. J Phys Chem Biophys. 7(254), 2161-2398.

Kim, J. H., Yu, D. H., Huh, Y. H., Lee, E. H., Kim, H. G., & Kim, H. R. (2017). Long-term exposure to 835 MHz RF-EMF induces hyperactivity, autophagy and demyelination in the cortical neurons of mice. Scientific reports, 7, 41129. https://doi.org/10.1038/srep41129

Kocak, Z., Evans, E. S., Zhou, S. M., Miller, K. L., Folz, R. J., Shafman, T. D. & Marks, L. B. (2005). Challenges in defining radiation pneumonitis in patients with lung cancer. International journal of radiation oncology, biology, physics, 62(3), 635–638. https://doi.org/10.1016/j.ijrobp.2004.12.023

Korkmaz A. Rat İnce Bağırsağında Oluşturulan Deneysel İskemik Reperfüzyon Hasarlanma Modelinde Gelişen Organ Hasarlanması Üzerine Vasküler Endotelyal Büyüme Faktörünün Etkisi. Doktora Tezi, Ankara: Gazi Üniversitesi, Sağlık Bilimleri Enstitüsü Fizyoloji Anabilim Dalı, 2014.

Lagroye, I., & Poncy, J. L. (1998). Influences of 50-Hz magnetic fields and ionizing radiation on c-jun and c-fos oncoproteins. Bioelectromagnetics, 19(2), 112–116.

Leroy, C., & Rancoita, P. G. (2011). Principles of radiation interaction in matter and detection. World Scientific.

Madrazo, A., Schwarz, G., & Churg, J. (1975). Radiation nephritis: a review. The Journal of urology, 114(6), 822–827. https://doi.org/10.1016/s0022-5347(17)67152-0

Mettler Jr, F. A., Bhargavan, M., Faulkner, K., Gilley, D. B., Gray, J. E., Ibbott, G. S. & Yoshizumi, T. T. (2009). Radiologic and nuclear medicine studies in the United States and worldwide: frequency, radiation dose, and comparison with other radiation sources—1950–2007. Radiology, 253(2), 520-531.

NCRP (2009), National Council on Radiation Protection and Measurements. Ionizing radiation exposure of the population of the United States. National Council on Radiation Protection and Measurements 2009; 160: 3-19.

Onat T. Emerk K. Sözmen E.Y. (2002). İnsan Biyokimyası. Yaşlanma Biyokimyası. Sözmen E.Y. Editor(s). Palme Yayıncılık. Ankara. pp. 665-674.

Oyar O, Gülsoy UK. (2003). Tıbbi Görüntüleme Fiziği: SDÜ Tıp Fakültesi, Ankara, Türkiye.

Özgüner, F., Mollaoğlu, H. (2006). Manyetik alanın organizma üzerindeki biyolojik etkileri. S.D.Ü. Tıp Fak. Derg, 13(1);38-41.

Pall M. L. (2013). Electromagnetic fields act via activation of voltage-gated calcium channels to produce beneficial or adverse effects. Journal of cellular and molecular medicine, 17(8), 958–965. https://doi.org/10.1111/jcmm.12088

Palma, D. A., Senan, S., Tsujino, K., Barriger, R. B., Rengan, R., Moreno, M., Bradley, J. D., Kim, T. H., Ramella, S., Marks, L. B., De Petris, L., Stitt, L., & Rodrigues, G. (2013). Predicting radiation pneumonitis after chemoradiation therapy for lung cancer: an international individual patient data meta-analysis. International journal of radiation oncology, biology, physics, 85(2), 444–450. https://doi.org/10.1016/j.ijrobp.2012.04.043

Poljak, D. ve Cvetkovic, M. (2019). On Exposure of Humans to Electromagnetic Fields– General Considerations. In: Garcia, A.C. (Ed.), Human Interaction with Electromagnetic Fields: Computational Models in Dosimetry. Elsevier, Slipt,. 1-20

Robert Percuoco, Chapter 1 - Plain Radiographic Imaging, Editor(s): Dennis M. Marchiori, Clinical Imaging (Third Edition), Mosby, 2014, Pages 1-43, ISBN 9780323084956, https://doi.org/10.1016/B978-0-323-08495-6.00001-4.

Rodrigues, G., Lock, M., D'Souza, D., Yu, E., & Van Dyk, J. (2004). Prediction of radiation pneumonitis by dose-volume histogram parameters in lung cancer--a systematic review. Radiotherapy and oncology: journal of the European Society for Therapeutic Radiology and Oncology, 71(2), 127–138. https://doi.org/10.1016/j.radonc.2004.02.015

Sharma, A., Shrivastava, S. & Shukla, S. (2021) Oxidative damage in the liver and brain of the rats exposed to frequency-dependent radiofrequency electromagnetic exposure: biochemical and histopathological evidence, Free Radical Research, 55:5, 535-546, https://doi.org/10.1080/10715762.2021.1966001

Siegel, R. L., Miller, K. D., & Jemal, A. (2020). Cancer statistics, 2020. CA: a cancer journal for clinicians, 70(1), 7–30. https://doi.org/10.3322/caac.21590

Tamam, C., Evrensel, M., ve Tamam, Y. (2016). Elekromanyetik Alanların İnsan Sağlığı Üzerinde Etkileri, Bilimsel Tamamlayıcı tıp, Regülasyon ve Nöralterapi Dergisi, 10(3), 19-24.

Topbaş M, Hasırcı Tuğcu Z.(2022) Ultraviyole radyasyon ve sağlık etkileri. Evci Kiraz ED, editör. İklim ve Sağlık. 1. Baskı. Ankara: Türkiye Klinikleri. p:35-42.

Ugras, M. Y., Kurus, M., Ates, B., Soylemez, H., Otlu, A., & Yilmaz, I. (2010). Prunus armeniaca L (apricot) protects rat testes from detrimental effects of low-dose x-rays. Nutrition research (New York, N.Y.), 30(3), 200–208. https://doi.org/10.1016/j.nutres.2010.03.001

UNSCEAR (2000). Sources and Effects of Ionizing Radiation, United Nations Scientific Committee on the Effects of Atomic Radiation 2000 Report, Volume I: Report to the General Assembly, with Scientific Annexes-Sources. United Nations.

Wang, H., & Zhang, X. (2017). Magnetic fields and reactive oxygen species. International Journal of Molecular Sciences, 18(10), 2175.

CHAPTER V

INVESTIGATION OF PHOTON RADIATION PERFORMANCE OF ELECTRONIC PERSONAL DOSEMETERS FOR TARLA

Mehmet Ertan KÜRKÇÜOĞLU[1] &Taylan GÖRKAN[2]

[1](Asst. Prof. Dr.), Süleyman Demirel University,
Physics Department, 32260 Isparta, Türkiye
E-mail:m.ertan.kurkcuoglu@gmail.com
ORCID: 0000-0002-4694-1880

[2](Dr), Süleyman Demirel University, Graduate School of
Natural and Applied Sciences, 32260 Isparta, Türkiye
E-mail: taylangorkan@gmail.com,
ORCID: 0000-0003-0411-3734

1. Introduction

TARLA (Turkish Accelerator and Radiation Laboratory in Ankara) is the first national free electron laser facility and was established to conduct research on materials science, nonlinear optics, semiconductors, biotechnology, medicine and photochemical processes. The facility is designed to produce free electron laser (FEL) pulses in the energy range of 10-40 MeV and bremsstrahlung radiation up to 30 MeV (Aksoy et al., 2018). When operating and dumping with accelerated electron beams at TARLA, high quantities of X-rays and gamma radiation may occur in FEL and bremsstrahlung units. According to the regulations, this amount of man-made radiation has to be supervised and controlled. The doses taken by the radiation workers have to be recorded and monitored for radiation protection and radiation safety concept. To minimize the health risks of ionizing radiation, the ICRP (International Commission on Radiological Protection) has recommended limits to the annual dose exposure for radiation workers (ICRP, 1991; ICRP, 2007).

Two types of personal dosimeters are used for individual monitoring in radiation applications: active (electronic) and passive dosimeters (Görkan, 2016). In passive dosimeters, dose exposure information is obtained as a result of various processes that require time, depending on the form of the dosimeter. Electronic dosimeters, on the other hand, offer real-time measurement and warn users with a dose rate alarm against unexpected radiation and sudden dose changes when the threshold value is exceeded. These opportunities offered by electronic dosimeters enable them to be ahead of passive dosimeters in high-radiation areas such as accelerator facilities (Takahashi et al., 2008; Suliman et al., 2010; Chiriotti et al., 2011; Görkan, 2016). At TARLA, active and passive systems are used together to monitor the annual doses received by the staff. OSL (Optically Stimulated Luminescence) dosimeter was chosen as passive dosimeter, and DMC 2000S type EPD (Electronic Personal Dosimeter) (MGP, 2011) was preferred as active dosimeter. Before routine use in a facility, dosimeters must be irradiated and tested in a laboratory with international standards. IEC (International Electrotechnical Commission) has published the IEC-61526 standard for testing personal dose equivalents Hp(10) and Hp(00.7) in electronic dosimeters (IEC, 2010). This standard is applicable for different types of radiation (X-rays, gamma-rays, neutrons and beta radiation), regardless of the detector type of dosimeters. Dosimeters can be tested in two ways: type testing and routine calibration (Oberhofer, 1991). Type testing of a dosimetry system is performed to determine the response variations of the dosimeters depending on the radiation type, energy and irradiation angle. Routine calibration is applied to normalize dosimeter measurements using a single source under special irradiation conditions. In the present study, the calibration test measurements on the Hp(10) performance of MGP DMC 2000S model electronic dosimeters for the irradiations at 10, 500 and 1000 μSv doses are examined.

2. Materials and Methods

2.1. TARLA Dosimetry System

DMC 2000S model electronic dosimeters (MGP, 2011) and LDM 220 model readers (MGP, 2003) from Mirion Technologies are used in TARLA (Figure 1). The dosimetry system of the facility consists of 55 EPDs, 2 dosimeter readers and the related software (dosimass and dosicare) compatible with Windows operating systems.

Figure 1. DMC 2000S electronic dosimeter (left) and LDM 220 dosimeter reader (right)

The electronic photon dosimeter can measure equivalent doses for gamma and X-rays in the energy range of 50 keV-6 MeV. The nuclear characteristics of the dosimeter are shown in Table 1. The LDM 220 is a compact dosimeter reader (hands-free) that communicates with the dosimeters of the DMC 2000S in pass-by data exchange mode. The reader detects dosimeters at a range of 20-30 cm with infrared waves. For monitoring and recording personal dose equivalents, the LDM 220 works by connecting to the USB port of the computer on which the necessary software packages are installed.

Table1. DMC 2000S characteristics Some nuclear characteristics of the DMC 2000S dosimeter

Radiation Types	Gamma and X rays
Detector	Silicon Diode
Energy Range	50 keV - 6 MeV
Measured Quantity	Hp (10)
Measurement Range	Equivalent Dose 1 μSv - 10 Sv Equivalent Dose Rate 1 μSv/h - 10 Sv/h
Response Time	< 5 s
Linearity	≤ ± 10% (for Hp(10) ≤ 1Sv/h) ≤ ± 25% (for 1Sv/h < Hp(10) ≤ 10Sv/h)

Dosimass and dosicare are the two main software of this dosimetry system. Dosimass is a software that allows storing, reading and changing the parameters of existing dosimeters, activating dosimeters and putting them in standby mode, checking historical data and providing solution suggestions for problems that may occur. Dosicare, on the other hand, is a database software where user data is created, dose and dose rate threshold values for alarms are determined, and the doses received by users are stored. In addition to the user manuals, detailed information about the components of the dosimetry system mentioned here can be found in the thesis written by Görkan (Görkan, 2016).

2.2. The Irradiation Process

14 dosimeters were irradiated with gamma radiation in the Calibration Laboratory of Ankara University Nuclear Sciences Institute which is a SSDL (Secondary Standard Dosimetry Laboratory) (Duruer, 2010; WEB, 2017). ^{137}Cs (622 keV), which is one of the sources recommended by ISO (ISO, 1996) and IEC (IEC, 2010), was used as a gamma radiation source. Dosimeters were irradiated together with the ISO water phantom to mimic human body. The water phantom is a 30×30×15 cm rectangular prism filled with pure water. The phantom is made using PMMA (polymethylmethacrylate) material. The thickness of the front surface is 2.5 mm and the thickness of all the other surfaces is 10 mm (ISO, 1999). While performing the measurement process in a real situation, dosimeters measure not only the direct radiation but also the backscattered radiation from objects and the users' own bodies. By placing the dosimeters on the water phantom, the radiation scattered back from the phantom is provided as if it were scattered from the human body, enabling the dosimeters to make more realistic dose measurements. The ^{137}Cs source is placed in a mechanism shielded with a steel-coated lead cylinder. The source is mounted on the stainless steel pipe inside the cylinder, and this pipe can be moved up and down by commands given from the computer in the control room. There is a window in the middle of the cylindrical shield, and when the moving mechanism brings the source to the level of this opening, the experimental setup is ready for the irradiation process.

Dosimeters were placed in pairs on the water phantom 1.5 m away from the ^{137}Cs source, as represented in Figure 2.

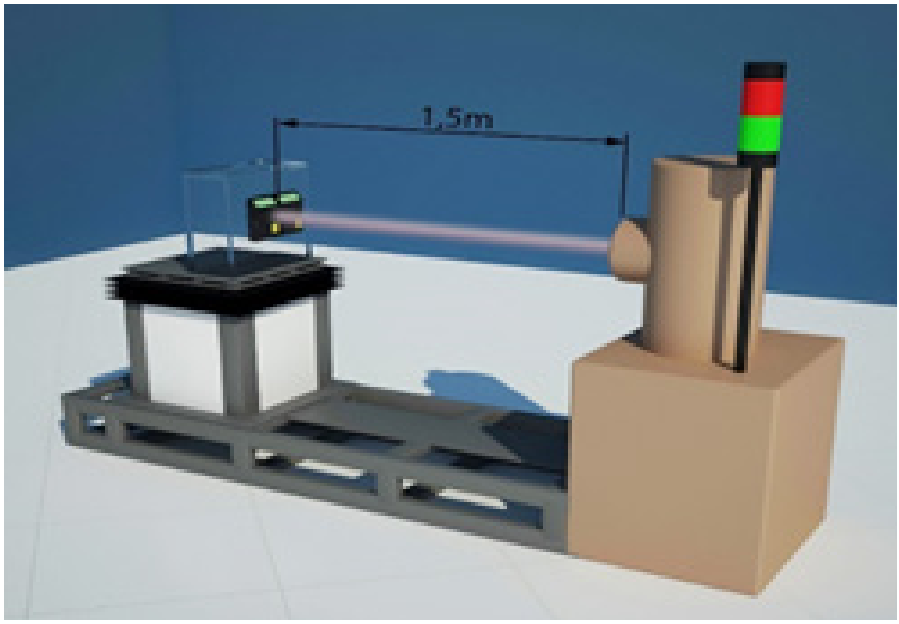

Figure 2. Representation of the experimental setup for the irradiation process

Dosimeters were irradiated at doses of 10 μSv, 500 μSv and 1000 μSv. In order to adjust the desired dose values, the distance between the source and the dosimeters was kept constant and the irradiation time was changed from the control unit (2 seconds for 10 μSv, 158 seconds for 500 μSv and 317 seconds for 1000 μSv).

When evaluating measurement results, the expression relative percent error is used to compare an experimental measurement value with the correct or expected value. Relative percent error, I(%) is given by

$$\mathrm{I\%} = \frac{\left(\mathrm{H_i} - \mathrm{H_t}\right)}{\mathrm{H_t}} \times 100 \cdot \; I(\%) = \left| \frac{\left(H_t - H_i\right)}{H_t} \right| \times 100\,, \tag{1}$$

where H_t is the expected dose value (true value) in μSv and H_i represents the measured value by a dosimeter in μSv. IEC has recommended that the percentage error for dosimeters irradiated with a ^{137}Cs source should not exceed (20+x)%. Here x is the uncertainty in the actual irradiated dose value and should not exceed 10% (IEC, 2010; Suliman et al., 2010). Therefore, it can be expected that the percentage error values of dosimeters should not exceed 30%. Since the measurements in the present study were performed for a single type

of dosimeter (DMC 2000S model dosimeters), it is not possible to know how much of the percentage error value is due to measurement and how much is due to irradiation error.

3. Results

In order to examine the Hp(10) performance of DMC 2000S devices, randomly selected 14 dosimeters were exposed to gamma radiation at 10, 500 and 1000 μSv doses in Ankara University Calibration Laboratory. The descriptive information of the dose measurements are presented in Table 2 (H_{iMin} indicates the minimum measurements, H_{iMax} stands for the maximum measurements, $\bar{H}_i$ is used for the mean values and the standard deviations of the measurements are represented by ΔH_i while I is the relative percent error).

When the measurement results were evaluated, it was revealed that the highest relative percentage error (20%) was observed in the lowest irradiation condition. In fact, only one dosimeter (7% of the measurements) resulted with 20% error, 8 dosimeters had 10% error and 5 dosimeters (36% of the measurements) provided exact measurements at 10 μSv exposure. When considering the conditions in radiation areas and the annual dose limitations for radiation workers, a dose of 10 μSv is quite low and therefore the error of 20% corresponds to a negligible value. Reflections from the phantom and from the objects in the laboratory can be considered to be less effective on dosimeters at 10 μSv exposure. On the other hand, the sensitivity of our EPDs is around 1 μSv, which possibly indicates that the contribution of instrumental error has become important.

Table 2. Hp(10) measurement results of DMC 2000S dosimeters for 10, 500 and 1000 μSv doses (*I* values were calculated for the averages by using Equation 1).

H_t (μSv)	N	H_{iMin} (μSv)	H_{iMax} (μSv)	$\bar{H}_i$ (μSv)	ΔHi (μSv)	I (%)
10	14	10.0	12.0	10.7	0.6	7.0
500	14	537.0	571.0	554.2	9.2	10.8
1000	14	1056.0	1127.0	1089.4	19.1	8.9

N: the number of dosimeters measured

For the irradiation test at 500 μSv, the lowest dose value recorded by the dosimeters was 537 μSv and the highest value was 571 μSv. The arithmetic mean of the measurements was around 554 μSv and all the dosimeters had readings greater than the irradiation dose. This may be because of the re-detection of the reflected radiation (from the phantom, walls and objects in the laboratory) by the dosimeters. For 500 μSv exposure, all of the personal dose equivalent measurement results were lower than the acceptable limitation for EPDs. It was found that the percentage error values of the dosimeters varied between 7% and 14%. Thus, it can be said that the contribution from the reflected radiation does not prevent the calibration test.

Among all Hp(10) measurements, the lowest error value (6%) was observed at 1000 μSv exposure, and the maximum relative percentage error recorded in this step was 13%. The arithmetic mean of the measurements was calculated as 1089.4 μSv, and no personal dose equivalent measurement level lower than 1056 μSv was observed (Table 2). These excesses in measurements may be due to scattered radiation, as seen in the 500 μSv exposure test, and background radiation, considering the irradiation time of 317 seconds.

Among the 14 EPDs tested, the dosimeter with ID number “859999” provided the highest measurement results for every irradiation condition. It is thought that this is caused by the instrumental error of the dosimeter. However, the percentage errors in the measurements of this dosimeter do not exceed 20%. For all 3 irradiation cases, on the other hand, the error values of the DMC 2000S dosimeters subjected to this study were determined to be lower than the (20+x)% limitation accepted for electronic dosimeters.

In addition, all measurement results regarding personal dose equivalents were examined for the linearity of the dosimeters (Figure 3). The x-axis (H_t) shows the actual dose values for the irradiation processes and the y-axis (H_i) represents the dose values measured by the dosimeters in Figure 3. When evaluated according to the applied irradiations, the graph shows that the measurement results obtained for 10 μSv exposure display a dispersion, while the other measurements overlap around 500 μSv and 1000 μSv. In Figure 3, both axes of the linearity graph are plotted on a logarithmic scale so that measurement differences can be noticed more easily.

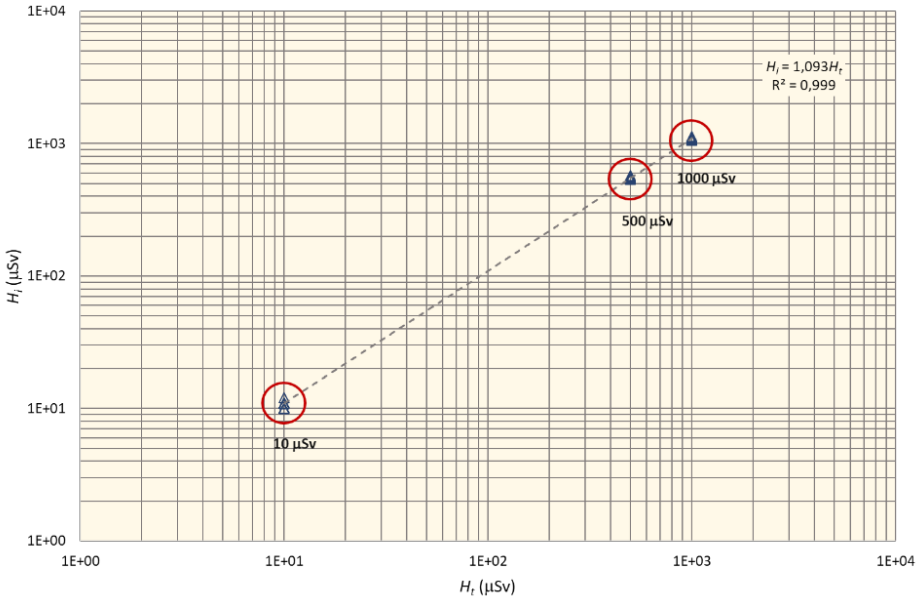

Figure 3. Linear response of DMC 2000S model dosimeters between 10 and 1000 µSv exposures

A linear fit relation was established assuming that the dosimeters did not record any readings in the absence of irradiation (H_i=1.093×H_t). This correlation is consistent with the linearity value of ≤ ±10% reported by the manufacturer for Hp(10) ≤ 1Sv/h (Table 1). R^2 value of this fit was found to be 0.999 and the fit formula could successfully explain that the measured values were slightly higher than the actual dose values (Figure 3). This may be due to a systemic error, which could be a combination of the background gamma radiation in the laboratory, the instrumental error of the dosimeters, and the extra readings caused by backscattering. Finally, it can be stated that the DMC 2000S dosimeters have a linear response in the range of 10 to 1000 µSv (Figure 3).

4. Conclusions

EPDs are important for accelerator facilities for several reasons such as radiation protection, safety compliance, dose optimization emergency response and so on. Accelerators produce ionizing radiation that can be harmful if exposure levels are not monitored and controlled. EPDs are designed to measure and record the radiation dose received by the staff working in and around the

accelerator facility. By wearing an EPD, personnel can be aware of the exposed radiation levels and take necessary precautions when necessary. Radiation safety regulations and guidelines require monitoring of ionizing radiation , which is taken by the personnel working in radiation areas. EPDs are very practical for measuring and documenting radiation doses. This data is important to ensure compliance with safety regulations and maintain a safe working environment. The use of EPDs to evaluate individual radiation doses is useful for dose optimization. By monitoring the radiation exposure of personnel, the locations or activities with higher radiation levels can be identified and appropriate arrangements to reduce exposure can then be considered such as changing work practices, implementing protective measures, or providing additional training and protective equipment. In an unexpected radiation situation or emergency, EPDs can provide real-time information about the radiation taken by personnel. This data is crucial for making decisions regarding evacuation, decontamination, and medical treatment. EPDs with alarm features also alert staff when radiation levels exceed predetermined thresholds. Thus immediate action can be taken. In general, EPDs store radiation dose measurements electronically, allowing historical data to be easily accessed and analysed. This data can be used for individual monitoring and for evaluation of the effectiveness of radiation protection. It also simplifies the generation of reports for regulatory compliance and controls.

In the present study, an electronic dosimeter system, which has been used by the radiation safety division of TARLA, was introduced. The photon radiation response of the electronic personal dosimeter DMC 2000S was examined. A set of 14 EPDs were exposed to gamma radiation at 10, 500 and 1000 μSv doses by using the ^{137}Cs (622 keV) source at the Secondary Standard Dosimetry Laboratory of Ankara University, Türkiye. It was shown that the measured Hp(10) values changed from 10 to 12 μSv for 10 μSv exposure. The measurements were varied between 537 and 571 μSv for 500 μSv exposure and ranged from 1056 to 1127 μSv for 1000 μSv exposure.

Within the limitations of this study, the responses of all the EPDs tested were found to meet dosimetric performance standards (i.e., all the percentage error values were lower than (20+x)%). The irradiation test results also revealed that the electronic dosimeters had a linear response to the doses between 10 μSv and 1000 μSv. Therefore, it can be concluded that DMC 2000S dosimeters can be used conveniently for high radiation applications as used in TARLA.

Acknowledgement

The present study includes a part of Dr. Görkan›s MSci thesis, which was financially supported by Süleyman Demirel University Scientific Research Projects Management Unit with Project Number 3881-YL1-14. The authors would like to thank Süleyman Demirel University.

References

Aksoy, A., Karsli, O., Aydin, A., Kaya, C., Ketenoglu, B., Ketenoglu, D., & Yavas, O. (2018). Current status of Turkish accelerator and radiation laboratory in Ankara: the TARLA facility. *Canadian Journal of Physics*, *96*(7), 837-842.

Chiriotti, S., Ginjaume, M., Vano, E., Sanchez, R., Fernandez, J.M., Duch, M.A., Sempau, J. (2011). Performance of several active personal dosemeters in interventional radiology and cardiology. *Radiation Measurements* 46 1266-1270.

Duruer, K. (2010). Preparation the protocol of calibration of photon detectors and personal dosimeters by using the X-rays and Cs-137 irradiator, (MSci Thesis in Turkish). Ankara University, Nuclear Sciences Institute, Ankara.

Görkan, T. (2016). *Investigation of the electronic dosimetry system for Turkish accelerator and radiation laboratory at Ankara, TARLA* (MSci Thesis in Turkish). Süleyman Demirel University, Graduate School of Natural And Applied Sciences, Isparta

IEC 61526. (2010). International Electrotechnical Commission, Radiation Protection Instrumentation, Measurement of personal dose equivalents Hp(10) and Hp(0.07) for X, gamma, neutron and beta radiations-direct reading personal dose equivalent meters, Geneva, Switzerland.

ICRP 60. (1991). Recommendations of the International Commission on Radiological Protection. ICRP Publication 60. Ann. ICRP 21(1-3).

ICRP 103. (2007). *Recommendations of the International Commission on Radiological Protection*. ICRP Publication 103. Ann. ICRP 37(2–4).

ISO 4037-1. (1996). *X and gamma reference radiations for calibrating dosimeters and dose rate meters and for determining their response as a function of photon energy, Part 1: Radiation characteristics and production methods.* International Organization for Standardization, Geneva, Switzerland.

ISO 4037-3. (1999). *X and gamma reference radiations for calibrating dosimeters and dose rate meters and for determining their response as a function of photon energy. Part 3: Calibration of area and personal dosimeters and the*

measurement of their response as a function of energy and angle of incidence. International Organization for Standardization, Geneva, Switzerland.

MGP Instrument, DMC 2000S, 2011, User's Manual.

MGP Instrument, 2003, LDM 210 - LDM 220, 2003, User's Manual

Oberhofer, M. (1991). *Advances in Radiation Protection*. Kluwer Academic Publishers GROUP, 376s, Netherland.

Suliman, I. I., Yousif, E. H., Beineen, A. A., Yousif, B. E., & Hassan, M. (2010). Performance testing of selected types of electronic personal dosimeters used in Sudan. *Radiation Measurements*, *45*(10), 1582-1584.

Takahashi, M., Sekiguchi, M., Miyauchi, H., Tachibana, H., Yoshizawa, M., Kato, T., Yamaguchi, A. (2008). Performance of the Hp(10) and Hp(0.07) measurable electronic pocket dosimeter for gamma- and beta-rays, *Journal of Nuclear Science and Technology, Supplement 5*, p. 225-228.

WEB 2014, http://ins.en.ankara.edu.tr/calibration-and-measurement-laboratory/ (Access: September 2014)

CHAPTER VI

A REVIEW ON THE GAMMA RAY ATTENUATION BEHAVIOURS OF SOME CHEMOTHERAPY DRUGS USED IN CANCER TREATMENT

İlyas ÇAĞLAR

(Lecturer) Kafkas University, Kazım Karabekir Vocational School of Technical Sciences, Department of Electricity and Energy, 36100 Kars, Turkey
E-mail: ilyas.caglar@kafkas.edu.tr
ORCID: 0000-0002-6958-8469

1. Introduction

Ionizing radiation is electromagnetic (such as X or gamma rays) or particle (such as neutrons or alpha particles) radiation that creates charged particles (ions) by removing electrons from the atoms or molecules in the matter it interacts with. Gamma rays are high-energy photons released by the unstable atomic nucleus, which remains excited as a result of radioactive decay (α or β decay), as it passes to the ground energy level. X-rays are high-energy photons produced by the rapid slowing down of a high-energy electron beam or by electron transitions in the inner orbits of atoms. As seen in Figure 1, X and gamma rays form the highest energy (shortest wavelength) part of the electromagnetic spectrum (TAEK, 2009; Çağlar, 2014).

Ionizing radiation sources can be examined under two main headings:

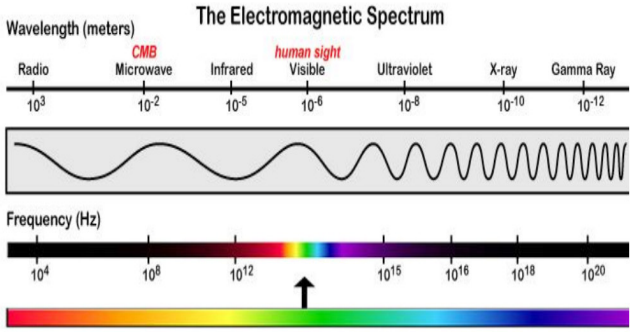

Figure 1. Electromagnetic Spectrum (Kot et al., 2014)

natural sources and artificial sources. Radionuclides such as ^{40}K, ^{238}U, ^{87}Rb and ^{232}Th with very long half-lives, which have existed in the earth's crust since the formation of the earth billions of years ago and have not yet completely decayed, cosmic rays coming from outer space and the sun, and radionuclides formed by cosmic rays constitute a significant part of the naturally occurring ionizing radiation (Coşkun, 2011; Cengiz and Çağlar, 2016; Bilgici Cengiz and Çağlar 2022). Natural radiation sources are found naturally in many environments such as soil, water, air, building material, food stuff, and etc. The main radionuclides of natural origin are ^{40}K, ^{238}U and ^{232}Th and various radionuclides that are their decay products (Bilgici Cengiz, 2020; Cengiz, and Öztanrıöver 2018). In addition, high-energy cosmic rays constantly produce new radioactive substances such as tritium (^{3}H) and carbon (^{14}C) in the upper layers of the atmosphere (Çağlar, 2014).

Radioactive fallout from nuclear bomb tests, fallout from nuclear reactor accidents such as the Chernobyl accident, radioactive substances released during the operation of nuclear reactors, and X-rays and artificial radioactive substances used in science, medicine, agriculture and industry are the main sources of artificial radiation (Çağlar, 2014). Radionuclides such as ^{239}Pu, ^{240}Pu, ^{241}Am, ^{90}Sr and ^{137}Cs, which spread into the environment through various processes, are the main sources of artificial ionizing radiation in the environment (Dang, et al.2021). In addition, x and gamma rays and various radionuclides used in medicine for imaging, diagnosis and treatment are other sources of ionizing radiation to which humans are exposed (Çağlar and Cengiz, 2021).

When an X-ray or γ-ray interacts with a target material, the photon may undergo attenuation, absorption, scattering, or transmission. Although there are many interaction mechanisms, three interaction types are of clinical importance in the interaction of radiation with matter in radiotherapy applications. These interaction mechanisms are Compton scattering, photoelectric effect and pair production (Mehta et al., 2010).

Cancer, one of the leading health problems of our age, is a disease that requires long-term treatment. It is defined as the uncontrolled division, proliferation and accumulation of cells in an organism. Surgery, chemotherapy and radiotherapy are commonly used methods in cancer treatment. In addition, different methods such as immunotherapy, hormone therapy and gene therapy are used depending on different types of cancer (Baykara, 2016). In the treatment of some diseases, chemotherapy and radiotherapy are applied simultaneously and this method is called chemoradiotherapy (Yorgun, and Kavaz, 2019). The

goal of radiotherapy is to destroy cancerous cells using X-ray, gamma ray or other types of ionizing radiation. However, while destroying cancerous cells, it is necessary to minimize the damage to healthy cells (Hosseinimehr, 2007). In radiotherapy applications, the damage caused by radiation to normal tissue depends on many factors such as the location and width of the treatment area, the total and daily dose to be applied, the age and general condition of the patient, and the quality of the treatment (Çelik, 2014).

The biological effects of radiation on living cells include injured or damaged cells, cell death, and improper cell repair resulting in biophysical changes (Painuli and Kumar, 2016). Ionizing radiations damage cells, tissues and organs through a series of molecular events such as photoelectric, Compton, pair production and Auger effects triggered by free radicals called reactive oxygen species (ROS). Superoxide anion (O_2^-), hydrogen peroxide (H_2O_2) and hydroxyl radicals (OH^-) are the main reactive oxygen species (ROS). Because these free radicals have unpaired electrons, they can easily interact with critical macromolecules such as DNA, proteins, or membranes, causing cell damage and potentially cell dysfunction and death (Fischer et al., 2018). Therefore, the study of gamma-ray absorption behaviour of chemotherapy drugs used in cancer treatment will be useful in chemoradiotherapeutic applications.

2. Gamma-ray Attenuation Parameters

Mass attenuation coefficient (μ_m), linear attenuation coefficient, half value layer, mean fere path, effective atomic number (Z_{eff}), effective electron density (N_e), are the basic parameters to evaluate the penetration and energy deposition of radiation in a given material. The widespread use of ionizing gamma and X-rays in science and technology increases the importance of knowledge of these radiological parameters. These radiological parameters depend mainly on the radiation energy, the chemical composition of the target material and the density of the material (Elmohrough et al., 2015; Ekinci et al., 2015)

The mass attenuation coefficient (μ_m) serves as a fundamental tool in calculating other attenuation parameters such as half-value thickness, mean free path, effective atomic number, effective electron density and etc. The μ_m values for any materials composed of different elements in varying proportions can be determined from the coefficients for the constituent elements by employing

mixture rule given in equation 1 (Jackson and Hawkes, 1981; Elmohrough et al., 2015; Alım et al., 2020):

$$\mu_m = \sum_i w_i (\mu_m)_i \quad (1)$$

where w_i is the weight fraction of element i and $(\mu_m)i$ is the mass attenuation coefficient of the i^{th} constituent element in a sample. The half value layer (HVL) represents the material thickness required to reduce the incident gamma photons intensity by one half and is calculated by using equation 2 (Sayyed, 2016; Yorgun and Kavaz, 2019; Aygun and Aygun, 2023):

$$HVL = \frac{0.693}{\mu} \quad (2)$$

where μ is the linear attenuation coefficient of the investigated material at a particular gamma energy.

The effective atomic number is a quantity used to visualize the interaction of gamma photons with the target material on the basis of atomic number. It depends on the incident gamma ray energy and the atomic diversity of the material. Z_{eff} is a parameter used to describe the atomic numbers of materials consisting of different elements at different energies. Z_{eff} values are given by the ratio of the total atomic cross section (σ_a) to the total electronic cross section (σ_e). The σ_a values are found using the m values of the samples with the following equation (Elmohrough et al., 2015; Çağlar et al., 2021):

$$\sigma_a = \frac{(\mu_m)_{sample}}{N_A \sum_i \frac{w_i}{A_i}} \quad (3)$$

where N_A is the Avogadro's number, A_i and w_i are atomic and fractional weights of the individual elements in the sample, respectively. Also, the total electronic cross section (σ_e) is calculated using following equation (Chanthima and Kaewkhao, 2013: Manjunatha, and Rudraswamy, 2011).

$$\sigma_e = \frac{1}{N_A} \sum_i \frac{f_i A_i}{Z_i} (\mu_m)_i \quad (4)$$

where f_i and Z_i are the fractional abundance and the atomic number of the individual elements in the sample, respectively. The Z_{eff} values for a given sample can be computed with the help of the following equation (Mostafa et al.,

2017; Elmohrough et al., 2015; Singh et al., 2018; Alım et al., 2020; Aygun et al., 2023):

$$Z_{eff} = \frac{\sigma_a}{\sigma_e} \tag{5}$$

In the studies we reviewed, gamma ray build-up factors of investigated drugs were calculated by applying GP fitting procedure in the following three steps.

1. Computation of equivalent atomic number (Z_{eq});
2. Computation of G–P fitting parameters
3. Computation of energy absorption and exposure build-up factors (EABF and EBF).

In the first step, the ratio of the Compton partial mass attenuation coefficient to the total mass attenuation coefficient for the examined materials is calculated for each interested energy value using the WinXCOM program. Then, Z_{eq} values are calculated by matching this ratio with the ratio of a pure element corresponding to the same energy with the following equation 6 (Harima et al, 1986; Şakar et al., 2020);

$$Z_{eq} = \frac{Z_1(\log R_2 - \log R) + Z_2(\log R - \log R_1)}{\log R_2 - \log R_1} \tag{6}$$

where Z_1 and Z_2 are the atomic numbers of the elements corresponding to the ratios R_1 and R_2, respectively. R is the ratio of $(\mu_m)_{Compton}$ and $(\mu_m)_{Total}$ and lies between R_1 and R_2.

In the second step, the obtained Z_{eq} values are used to calculate the G-P fitting coefficients (a, b, c, d, and X_k). G-P fitting coefficients for 23 elements (Z=4–92), water, air and concrete in the 0.015-15 MeV energy region up to 40 mfp are available in the ANSI/ANS-6.4.3 reference database. These coefficients are implemented to compute the G-P fitting buildup coefficients of selected materials using equation 7 (Raut et al., 2018; Ekinci et al., 2019; Şakar et al. 2020)

$$P = \frac{P_1(\log Z_2 - \log Z_{eq}) + P_2(\log Z_{eq} - \log Z_1)}{\log Z_2 - \log Z_1} \tag{7}$$

where P denotes G-P fitting parameters of investigated compounds. P_1 and P_2 are the values of G-P fitting coefficients taken from the ANSI/ANS-6.4.3 database corresponding to the Z_1 and Z_2 atomic numbers at particular gamma ray energy, respectively.

In the third step, the GP fitting coefficients obtained from equation 7 are used to estimate the gamma ray EABF and EBF factors. Taking into account the dose multiplication factor, the EABF and EBF factors of the examined drugs for the some standard gamma ray energies are calculated from equations 8-10; ((Harima etal.,1986; Raut et al., 2018; Ekinci et al., 2019).

$$B(E,X) = 1 + \frac{b-1}{K-1}(K^X - 1) \quad for\ K \neq 1 \tag{8}$$

$$B(E.X) = 1 + (b-1)X \qquad for\ K = 1 \tag{9}$$

$$K(E,X) = cx^a + d\frac{\tanh\left(\frac{x}{X_k} - 2\right) - \tanh(-2)}{1 - \tanh(-2)} \quad for\ x \leq 40mfp \tag{10}$$

In the above equations, x is the penetration depth in unit of mfp, b is the buildup factor for x= 1mfp, E is the incident gamma ray energy, and K (E, X) is the dose multiplication factor.

3. Results and Discussion

The X and gamma ray attenuation behaviours of some cancer drugs such as Tadocel, Fluro-5, Erbitux, Carboplatin, Temodal, Tamoxifen, Endoksan and Oxaliplatin were estimated with a study by Yorgun and Kavaz (2019). The mass attenuation coefficient (μ_m), half value layer (HVL) and effective atomic number (Z_{eff}) of these cancer drugs were experimentally determined for different gamma energies in the range of 13.81-59.54 keV obtained from ^{241}Am radioactive source by using Si(Li) detector. To check the usefulness of the experimental results, the theoretical values corresponding to these energies were determined using the WinXCOM software. It was reported that Oxaliplatin and carboplatin had higher μ and Z_{eff} values and lower HVL values among the cancer drugs examined. It was also seen that Tamoxifen has lower μ and Z_{eff} values and higher HVL values than others The EBF values for the selected drugs were calculated for 1, 10 and 40 mfp in the energy range of 0.15-15 MeV, and it was stated that

Oxaliplatin and Carboplatin had the lowest and tamoxifen had the highest EBF values.

In a study conducted by Kavaz et al. (2015) gamma ray energy absorption and exposure of buildup factors for Doxorubicin ($C_{27}H_{29}NO_{11}$), Vincristine ($C_{46}H_{56}N_4O_{10}$), Teniposide ($C_{32}H_{32}O_{13}S$), Azathioprine ($C_9H_7N_7O_2S$), Cyclosporine ($C_{26}H_{111}N_{11}O_{12}$), Etoposide ($C_{29}H_{32}O_{13}$), Cyclophosphomide $C_7H_{15}C_{l2}N_2O_2P$), Vinblastine ($C_{46}H_{58}N_4O_9$) and Bleomycin ($C_{55}H_{84}N_{17}O_{21}S_3$) were estimated by aid of the five-parameter geometric progression (G-P) fitting formula in the photon energy range 15keV–15 MeV up to penetration depths of 40 mean free path (mfp). They also computed effective atomic number and effective electron density for these chemotherapy drugs for the 1keV–10 GeV energy region. They observed that vinblastine has the minimum effective atomic number values while cyclophosphamide has the maximum values. It was reported that the calculated EABF and EBF values varied depending on the gamma ray energy and penetration depth, and that the EABF and EBF values obtained for the middle energy region were higher than those others energy region. It was also observed that the gamma ray build-up factors of azathioprine and cyclophosphamide were almost minimum for all penetration depths and incident gamma ray energy.

Radiation attenuation parameters such as mass attenuation coefficient (μ_m), effective atomic number (Z_{eff}) and electron density (N_e) for Tamoxifen ($C_{26}H_{29}NO$) drug were computed by Kanberoglu et al. in 2017 in the energy range from1 keV to 100 GeV via WinXCOM program. In addition, the variation of μ_m, Z_{eff} and N_e with incident photon energy were investigated in the study. It was reported that these parameters have different tendencies in low, medium and high energy regions depending on different interaction types (i.e. photoelectric absorption, Campton scattering and pair production (Kanberoglu et al., 2012).

The radiation attenuation parameters of some commonly used in chemotherapeutic drugs were investigated by Akman and Kaçal (2018) using WinXCOM program. The μ_m, μ, HVL, mfp, and Z_{eff} for Cisplatin ($Pt(NH_3)_2Cl_2$), Lomustine ($C_9H_{16}ClN_3O_2$), Chlorambucil ($C_{14}H_{19}Cl_2NO_2$) and Carmustine ($C_5H_9Cl_2N_3O_2$) were estimated for the energy range from1 keV to 100 GeV. The change of radiation absorption parameters depending on photon energy was also evaluated. While the highest values of μ_m, μ and Z_{eff} were found for low energies, the highest HVL and mfp values were found for medium photon energies. It was observed that Cisplatin had the largest μm, μ and Z_{eff} values and Chlorambucil had the smallest values. On the other hand, Cisplatin was

found to have smaller HVL and mfp values than other drugs. Therefore, it was concluded that Cisplatin has the best satiation attenuation feature among the selected drugs.

Çağlar and Cengiz (2021) estimated radiation absorption properties of some chemotherapy drugs using WinXCOM software package. The Z_{eff} and N_e of anastrozole ($C_{17}H_{19}N_5$), epirubicin ($C_{27}H_{26}NO_{11}$), gemcitabine ($C_9H_{11}F_2N_3O_4$), ifosfamide ($C_7H_{15}C_{l2}N_2O_2P$), methotrexate ($C_{20}H_{22}N_8O$) and paclitaxel ($C_{47}H_{51}NO_{14}$) were determined for a wide energy range corresponding to 1 keV - 100 GeV. They also examined the EABF and EBF build-up factors of these drugs using the GP Fitting procedure for some chosen energies in the range 0.015–15 MeV. Since ifosfamide contains phosphorus and chlorine, unlike other drugs, it has been stated that ifosfamide has larger Z_{eff} values than the other drugs. at a given gamma ray energy, it was observed that the build-up factors increased as the penetration depth increased and that ifosfamide had smaller gamma ray build-up values than the others at all energies except 15 MeV. Similarly, it has been emphasized that at a selected penetration depth, build-up values vary with photon energy and have the largest values at medium energies where Compton scattering is dominant. It was stated that the outcomes obtained from the work revealed that the chemical composition of the drugs, radiation energy and penetration thickness have an important role on the gamma ray absorption parameters, and that drugs containing elements with higher atomic numbers show better radiation attenuation properties.

Since radioprotective agents can reduce radiation damage when applied before irradiation, the energy absorption and exposure accumulation factors of Carnosin ($C_9H_{14}N_4O_3$), Melatonin ($C_{13}H_{16}\ N_2O_2$), Captopril ($C_9H_{15}NO_3S$), Interferon gamma ($C_{761}H_{12}0_6\ N_{214}O_{225}S_6$), Amifostine ($C_5H_{15}N_2O_3PS$), Tempol ($C_9H_{18}NO_2$), Orientin ($C_{21}H_{20}O_{11}$), Glutathione ($C_{10}H_{17}N_3O_6S$), Penicillamine ($C_5H_{11}NO_2S$) and Cysteine ($C_3H_7NO_2S$) were evaluated by Oto et al. (2016). Theoretical calculations were performed using 5-parameter GP fitting method in the 0.015–15 MeV energy region up to a penetration depth of 40 mfp. They reported that photon build-up factors depend on the photon energy and the interaction processes between the photon and the material. It has been emphasized that build-up factors are small at low and high energies and large at medium energies. This trend is ascribed to the fact that the photoelectric effect and pair production are the dominant interaction mechanisms at low and high energies, and Compton scattering is the dominant interaction process at medium energies. It also emphasized that build-up factors increase with the increase

in average free path. It was concluded that cysteine and amifostine are better compounds than others for gamma ray absorption applications.

The radioprotective effects of non-steroidal anti-inflammatory drugs (NSAIDs) were evaluated in terms of gamma ray build-up factors by Ekinci et al. (2014). The Z_{eff} and N_e of Aspirin ($C_9H_8O_4$), Paracetamol ($C_8H_9NO_2$), İbuprofen ($C_{13}H_{18}O_2$), Piroxicam ($C_{15}H_{13}N_3O_4S$), Diclofenac ($C_{14}H_{11}Cl_2NO_2$), Naproxen ($C_{14}H_{14}O_3$), Ketoprofen ($C_{16}H_{14}O_3$) and Aceclofenac ($C_16H_{13}Cl_2NO_4$) were computed for the energy zone of 1keV–100GeV. However, the gamma ray energy absorption (EABF) and exposure build-up factors (EBF) of these NSAIDs were estimated in the energy region of 15kev to 15MeV up 40mfp. It was stated that some elements with high Z, such as Cl, had a major contribution to the Z_{eff} values of the drugs examined in the study. For all the drugs studied, EABF and EBF values were smaller at low photon energies than at high photon energies. Maximum build-up factors were observed in the medium energy region. This energy-dependent trend in EABF and EBF is attributed to the fact that the photo-electric effect at low energies, pair production at high energies and Compton scattering at intermediate energies are the dominant types of interactions. In Compton scattering, the photons do not disappear completely, but their energy decreases, so that the photons remain in the material for a long time. For energy region lower than 1.5 MeV and at all penetration depths of interest, aceclofenac, diclofenac and piroxicam have lower gamma build-up factors than other compounds and are therefore attractive as radioprotective agents.

4. Conclusion

In this study, radiation absorption behaviours of various chemotherapy drugs used in the treatment of cancer disease were compiled from various research articles in the literature. It has been reported that the difference of element types in drugs and the number of atoms in the elements has a major impact on the photon interaction parameters. Generally, it is emphasized that drugs containing larger atomic elements are in particular with a better radiation absence. From the studies examined, it is clear that photon interaction parameters are strongly dependent on incoming photon energy. These parameters vary depending on the types of interaction (i.e. photoelectric absorption, Compton scattering and pair production) at different photon energy intervals. The mass absorption coefficient, linear absorption coefficient, effective atomic number,

and effective electron density values of chemotherapy drugs in the low energy region are greater than those in other regions. Similarly, HVL and mfp values at low energies are smaller than those at medium and high energies. Similarly, the EABF and EBF parameters have the largest values at medium energies and vary with penetration depth. In the evaluation carried out, it was observed that radiological parameters depend on the chemical composition of chemotherapy drugs, the incoming photon energy, and the types of interactions occurring between the drug samples and the photon. It is hoped that the outcomes of this review will be useful in radioprotection, medical diagnosis and radiotherapy applications.

References

Akman, F., Kaçal, M. R. (2018). Investigation of radiation attenuation parameters of some drugs used in Chemotherapy in Wide Energy Region. Journal of Radiology and Oncology, 2, 047-052.

Alım, B., Şakar, E., Baltakesmez, A., Han, İ., Sayyed, M. I., & Demir, L. (2020). Experimental investigation of radiation shielding performances of some important AISI-coded stainless steels: Part I. Radiation Physics and Chemistry, 166, 108455.

ANSI/ANS-6.4.3, 1991. Gamma Ray Attenuation Coefficient and Buildup Factors for Engineering Materials. Illinois: American Nuclear Society, La Grange Park.

Aygun, M., & Aygun, Z. (2023). A comprehensive analysis on radiation shielding characteristics of borogypsum (boron waste) by Phy-X/PSD code. Revista Mexicana de Física, 69; 040401-1.

Aygun, M., Aygun, Z., & Ercan, E. (2023). Radiation protection efficiency of newly produced W-based alloys: Experimental and computational study. Radiation Physics and Chemistry, 212, 111147.

Baykara, O. (2016). Kanser Tedavisinde Güncel Yaklaşimlar. Balıkesir Sağlık Bilimleri Dergisi, 5(3), 154-165.

Bilgici Cengiz, G., & Caglar, I. (2022). Evaluation of lifetime cancer risk arising from natural radioactivity in foods frequently consumed by people in Eastern of Turkey. Journal of Radioanalytical and Nuclear Chemistry, 331(4), 1847-1857.

Bilgici Cengiz, G. (2020). Determination of natural radioactivity in products of animals fed with grass: A case study for Kars Region, Turkey. Scientific reports, 10(1), 6939.

Cengiz, G. B., & Çağlar, İ. (2016). Determination of the health hazards and life time cancer risk due to natural radioactivity in soil of Akyaka, Arpaçay and Susuz areas of Kars, Turkey. International Journal of Scientific &Engineering Research, 7(3), 619-626.

Cengiz, G. B., & Öztanrıöver, E. (2018). Analysis of natural radioactivity levels in soil samples and dose assessment for Digor district, Kars, Turkey. Caucasian Journal of Science, 5(1), 30-39.

Chanthima, N., & Kaewkhao, J. (2013). Investigation on radiation shielding parameters of bismuth borosilicate glass from 1 keV to 100 GeV. Annals of Nuclear energy, 55, 23-28.

Coşkun, Ö. (2011). İyonize radyasyonun biyolojik etkileri. Teknik Bilimler Dergisi, 1(2), 13-17.

Çağlar, İ. (2014). Akyaka Arpaçay ve Susuz ilçelerinde doğal radyoaktivite seviyelerinin belirlenmesi (Master›s thesis, Fen Bilimleri Enstitüsü).

Çağlar, İ., Cengiz, G. B. (2021). Evaluation of radiation attenuation properties of some cancer drugs. Adıyaman University Journal of Science, 11(2), 503-522.

Çağlar, İ., Cengiz, G. B., & Bilir, G. (2021). Gamma radiation shielding properties of some binary tellurite glasses. Journal of Non-Crystalline Solids, 574, 121139.

Çelik, A. S. (2014). Radyoterapi sonucu gelişen yan etkiler ve hemşirelik yaklaşımı. Gümüşhane Üniversitesi Sağlık Bilimleri Dergisi, 3(3), 933-947.

Dang, H., Yi, X., Zhang, Z., Zhang, H., Lin, J., Zhang, W., ... & Wang, W. (2021). The level, distribution and source of artificial radionuclides in surface soil from Inner Mongolia, China. Journal of Environmental Radioactivity, 233, 106614.

Elmahroug, Y., Tellili, B., Souga, C. (2015). Determination of total mass attenuation coefficients, effective atomic numbers and electron densities for different shielding materials. Annals of Nuclear Energy, 75, 268-274.

Ekinci, N., Kavaz, E., Aygün, B., & Perişanoğlu, U. (2019). Gamma ray shielding capabilities of rhenium-based superalloys. Radiation Effects and Defects in Solids, 174(5-6), 435-451.

Ekinci, N., Kavaz, E., & Özdemir, Y. (2014). A study of the energy absorption and exposure buildup factors of some anti-inflammatory drugs. Applied Radiation and Isotopes, 90, 265-273.

Fischer, N., Seo, E. J., & Efferth, T. (2018). Prevention from radiation damage by natural products. Phytomedicine, 47, 192-200.

Harima Y, Sakamoto Y, Tanaka S, Kawai M (1986) Validity of the geometric progression formula in approximating gamma ray buildup factors. Nuclear Science and Engineering 94; 24-35.

Hosseinimehr, S. J. (2007). Trends in the development of radioprotective agents. Drug discovery today, 12(19-20), 794-805.

Jackson, D. F., Hawkes, D. J. (1981). X-ray attenuation coefficients of elements and mixtures. Physics Reports, 70(3), 169-233.

Kanberoglu, G. S., Oto, B., Gulebaglan, S. E. (2017). Gamma shielding properties of Tamoxifen drug. In AIP Conference Proceedings (Vol. 1815, No. 1). AIP Publishing.

Kavaz, E., Ahmadishadbad, N., Özdemir, Y. (2015). Photon buildup factors of some chemotherapy drugs. Biomedicine & Pharmacotherapy, 69, 34-41.

Kavaz, E., Perişanoğlu, U., Ekinci, N., Özdemır, Y. (2016). Determination of energy absorption and exposure buildup factors by using GP fitting approximation for radioprotective agents. International Journal of Radiation Biology, 92(7), 380-387.

Kot, P., Shaw, A., Jones, K. O., Cullen, J. D., Mason, A., Al-Shamma'a, A. I. (2014). The feasibility of using electromagnetic waves in determining the moisture content of building fabrics and the cause of the water ingress. International Journal on Smart Sensing and Intelligent Systems, 7(5), 1-5.

Manjunatha, H. C., & Rudraswamy, B. (2011). Computation of exposure build-up factors in teeth. Radiation Physics and Chemistry, 80(1), 14-21.

Mehta, S. R., Suhag, V., Semwal, M., & Sharma, N. (2010). Radiotherapy: Basic concepts and recent advances. Medical Journal Armed Forces India, 66(2), 158-162.

Mostafa, A. M. A., Issa, S. A., & Sayyed, M. I. (2017). Gamma ray shielding properties of PbO-B2O3-P2O5 doped with WO3. Journal of Alloys and Compounds, 708, 294-300.

Painuli, S., Kumar, N. (2016). Prospects in the development of natural radioprotective therapeutics with anti-cancer properties from the plants of Uttarakhand region of India. Journal of Ayurveda and integrative medicine, 7(1), 62-68.

Pawar, P. P., Bichile, G. K. (2013). Studies on mass attenuation coefficient, effective atomic number and electron density of some amino acids in the energy range 0.122–1.330 MeV. Radiation Physics and Chemistry, 92, 22-27.

Raut S. D., Awasarmol V. V., Shaikh S. F., Ghule B.G., Ekar S.U., Mane R. S., Pawar P. P. (2018) Study of gamma ray energy absorption and exposure

buildup factors for ferrites by geometric progression fitting method. Radiation Effects and Defects in Solids 173 (3-4); 429-438.

Sakar E., Ozpolat O.F., Alım B., Sayyed M., Kurudirek M. (2020) Phy-X/PSD: Development of a user friendly online software for calculation of parameters relevant to radiation shielding and dosimetry. Radiation Physics and Chemistry 108496; 1-12.

Sayyed, M. I. (2016). Bismuth modified shielding properties of zinc borotellurite glasses. Journal of alloys and compounds, 688, 111-117.

Singh, T., Kaur, A., Sharma, J., Singh, P. S. (2018). Gamma rays' shielding parameters for some Pb-Cu binary alloys. Engineering science and technology, an international journal, 21(5), 1078-1085.

TAEK (2009) Radyasyon, İnsan ve Çevre: İyonlaştırıcı radyasyon, etkileri ve kullanım alanları, güvenli kullanımı için uygulamada olan tedbirler. Ankara.

Yorgun, N. Y., & Kavaz, E. (2019). Gamma photon protection properties of some cancer drugs for medical applications. Results in Physics, 13, 102150.

CHAPTER VII

THE EFFECT OF THE ND_2O_3 ADDITION ON THE RADIATION SHIELDING PERFORMANCE OF THE TUNGSTEN TELLURITE GLASSES

Ömer KABAN[1] & İlyas ÇAĞLAR[2] & Gülçin CENGIZ[3] & Gökhan BILIR[4,*]

[1](Master Student), Department of Physics, Kafkas University, Türkiye
E-mail: omerkaban@hotmail.com

[2](Lecturer) Vocational School of Technical Sciences, Dept. of Electricity & Energy, Kafkas University, Türkiye
E-mail: ilyas.caglar@kafkas.edu.tr
ORCID: 0000-0002-6958-8469

[3](Assoc. Prof. Dr.), Department of Physics, Kafkas University, Türkiye
E-mail: cengizgulcin@gmil.com
ORCID: 0000-0002-6164-3232

[4](Assoc. Prof. Dr.),Department of Physics, Kafkas University, Türkiye*
E-mail: gbilirr@gmil.com
ORCID: 0000-0003-1963-0902

1. Introduction

Today's radiation technology is widely used in many fields like energy production, medical applications, space technologies, etc. High-energy ionizing radiations, besides their beneficial uses that make our lives easier, also cause irreparable damage to living tissues (Dong et al., 2019). For

this reason, different radiation shielding materials have been used to protect against radiation exposure since the discovery of radiation by Becquerel in 1896, and research on the different materials for their potential as a radiation shielding material has continued.

Recently, the radiation shielding properties of heavy metal oxide glasses have been intensively investigated because these glass systems offer properties such as non-toxicity, transparency in the visible region and good absorption of X- and gamma-rays. Among these glass systems, telluride-based glass systems are particularly notable for their better chemical resistance, higher dielectric constant, lower melting temperature, good thermal stability, mechanical strength and high transparency. In addition, telluride glasses are also a suitable material for shielding due to their wide transmission window (from the visible to the infrared region), lower phonon energies (800 cm^{-1}) compared to silicate glasses (1150 cm^{-1}) and high densities which provide better compactness of the glass and stronger radiation-shielding ability (Ersundu et al., 2018; Bilir et al., 2011; Bilir et al., 2011; Bilir et al., 2011; Bilir, 2015)/

In this context, we studied the effect of Nd_2O_3 doping on the radiation shielding performance of tungsten telluride glass systems with known radiation shielding properties. For this purpose, tungsten telluride glasses doped with Nd_2O_3 at 3 different concentrations were synthesized using melt quenching technique. The radiation shielding performance of the synthesized glass systems were studied both experimentally and theoretically by investigating the linear attenuation coefficients (μ), mass attenuation coefficients (μ_m), effective atomic numbers (Z_{eff}), and half value layer (HVL). All values, both measured and calculated, are compared with values for un-doped tungsten telluride glasses in the literature (Caglar et al., 2021).

2. Experimental Part

The traditional melt quenching technique was used to synthesize glass systems with a composition of (70-x) TeO_2-30WO_3-xNd_2O_3 (x=1, 3, 5). The starting reagents used for the synthesis were of at least 99.99% purity, TeO_2 - Alfa Aesar, WO_3 and Nd_2O_3 - Sigma Aldrich and used without any extra purification. The reagents in the amounts given in Table-1 were weighed using a precision balance and then mixed thoroughly in an agate mortar and transferred to a platinum crucible. Due to the presence of volatile components in the mixture, the platinum crucible was closed with a lid and heated to 800 $^{\circ}C$ in a

high temperature muffle furnace and kept at that temperature for an hour. The glass melt in the platinum crucible was then poured onto a stainless steel mold. The resulting glasses were heat treated at 200 ˚C to avoid thermal stresses.

The surfaces of the glass samples were ground and polished to obtain two parallel and smooth surfaces for gamma ray transmission measurements using different mesh size sand papers and felt.

The densities of synthesized glasses were measured by Archimedes' principle using ultrapure water as the buoyancy liquid and a high precision scale with a sensitivity of 10^{-4} g.

The details regarding the experimental setup for the radiation shielding parameters measurement, and theoretical calculations are given in elsewhere (Caglar et al., 2021; Bilir et al., 2022; Bilir et al., 2022; Cengiz et al., 2020).

Table 1. Glass Compositions and Some Physical Properties.

Glass Codes	Glass compositions % mole			Molar Mass M ($gmol^{-1}$)	Melting Temperature (˚C)	Density d (g/cm^3)	Molar Volume V_m (cm^3mol^{-1})	Thickness (mm)
	TeO_2	WO_3	Nd_2O_3					
TWNd1	69	30	1	183.041	800 - 850	5.351	34.21	3.05
TWNd3	68	30	3	186.578		5.399	34.56	2.68
TWNd5	65	30	5	190.12		5.421	35.07	4.00

3. Results and Discussions

The μ_m values of glass samples doped with Nd_2O_3 at different ratios were measured experimentally at 662, 1173 and 1332 keV gamma-ray energies. The theoretical mass attenuation coefficients (μ_m) of the glasses were calculated using the WinXCOM program at the experimentally measured energy values and in the energy interval of 0.015-15MeV. The obtained experimental and theoretical mass attenuation coefficients are tabulated in Table 2. It is obvious from results that the experimental results are in agreement with the theoretical results. Based on the experimental and theoretical results obtained for the investigated glasses, it can be concluded that the mass absorption coefficient values decrease with increasing energy of the gamma ray (Caglar et al., 2021). It is seen from the table that the mass attenuation coefficients are increased with increasing Nd_2O_3 dopant. From this point of view, when the density values of the glass samples are increased as a result of increasing amount of Nd_2O_3, the radiation protection is higher. The variation graph of the mass attenuation coefficients of the glass systems according to the incident photon energy is given in Figure 1.

Table 2. Theoretical and Experimental Mass Attenuation Coefficients at 662 keV, 1173 keV, and 1332 keV Energies.

Glass Code	Mass Attenuation Coefficient (cm^2/g)					
	662keV		1173 keV		1332keV	
	Experimental	Theoretical	Experimental	Theoretical	Experimental	Theoretical
TWNd1	0.0808±0.0025	0.0822	0.0495±0.0029	0.0550	0.0488±0.0028	0.0511
TWNd3	0.0814±0.0028	0.0823	0.0544±0.0033	0.0551	0.0521±0.0030	0.0512
TWNd5	0.0822±0.0019	0.0824	0.0549±0.0021	0.0552	0.0519±0.0021	0.0513

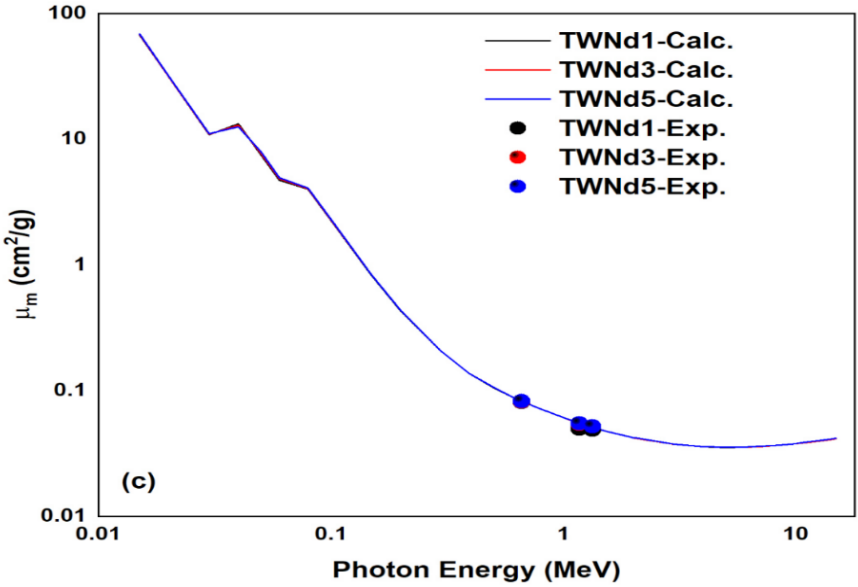

Figure 1. Variation of Mass Attenuation Coefficient Values of Glass Materials as a Function of Incident Photon Energy.

The linear attenuation coefficient (μ), which is the attenuation per unit length, was also determined experimentally at gamma ray energies of 662 keV, 1173 keV and 1332 keV for the glass systems studied. Experimental linear attenuation coefficients and theoretical linear attenuation coefficients are tabulated in Table 3. The obtained results are shown in Figure 2 together with the theoretical results. As can be seen from Figure 2, the variation of μ values with photon energy has the same trend as μ_m. It is clear that μ values depend on the photon energy and the chemical composition of the studied glasses.

Table 3. Theoretical and Experimental Linear Attenuation Coefficients at 662 keV, 1173 keV, and 1332 keV Energies.

Glass Code	Linear Attenuation Coefficient (cm^{-1})					
	662keV		1173 keV		1332keV	
	Experimental	Theoretical	Experimental	Theoretical	Experimental	Theoretical
TWNd1	0.4322±0.0136	0.4340	0.2647±0.0153	0.2947	0.2610±0.0149	0.2736
TWNd3	0.4397±0.0152	0.4445	0.2939±0.0177	0.2976	0.2814±0.0170	0.2763
TWNd5	0.4459±0.0103	0.4469	0.2977±0.0178	0.2990	0.2811±0.0115	0.2776

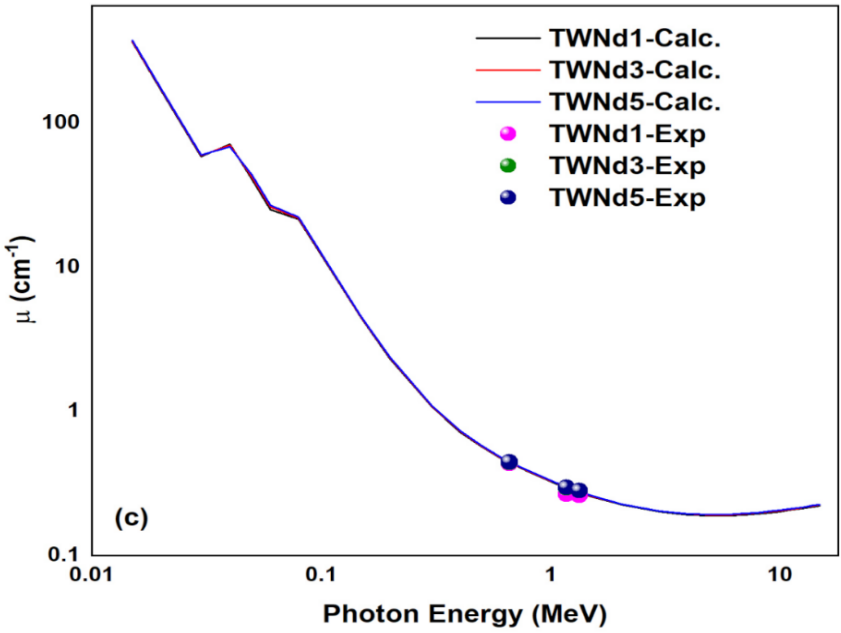

Figure 2. Variation of Linear Attenuation Coefficient Values of Glass Materials as a Function of Incident Photon Energy.

The half value layer (HVL) is a suitable parameter used to evaluate the gamma radiation shielding performance of materials. The HVL is known as the thickness required to halve the intensity of the incident gamma ray [8]. Glasses with smaller HVL values generally have higher gamma radiation shielding properties (Caglar et al., 2021; Bilir et al., 2022; Bilir et al., 2022). The measured and calculated HVL values are given in Table 4 and illustrated in the Figure 3. It is seen in Table 4 that HVL values decrease when the density of glass samples increases which can easily be attributed to the increasing densities of the glasses with the addition of the Nd_2O_3.

Table 4. HVL Values.

Glasses	HVL					
	662keV		1173keV		1332keV	
	Exp.	Calc.	Exp.	Calc.	Exp.	Calc.
TWNd1	1.6037±0.0505	1.5757	2.6186±0.1511	2.3520	2.6559±0.1515	2.5332
TWNd3	1.5765±0.0544	1.5594	2.3586±0.1423	2.3292	2.4635±0.1490	2.5088
TWNd5	1.5544±0.0358	1.5509	2.3286±0.1392	2.3180	2.4660±0.1007	2.4969

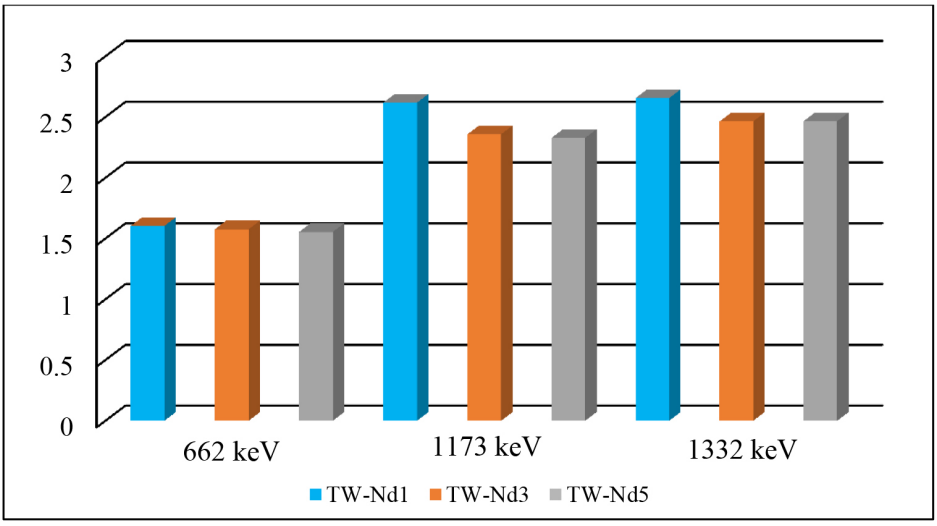

Figure 3. HVL Values of All Glass Systems.

As seen in Table 4, HVL values decreased when the density of glass samples increased. Since HVL by definition is the thickness of the sample required to stop the incoming gamma radiation by half, HVL values decrease as the amount of rare earth element increases as seen in Table 4 and Figure 3.

Effective atomic number is one of the important radiation shielding parameters. Glasses with higher Z_{eff} values have higher radiation shielding properties than others (Caglar et al., 2021; Bilir et al., 2022; Bilir et al., 2022). Z_{eff} values of the glasses we examined are given in Table 5. In addition, the variation graph of Z_{eff} values according to the energy of incident gamma photons is given in Figure 4. As can be seen from the Table 5 and Figure 4 that Z_{eff} values increase with increasing rare earth element amount. This is due to the fact that Nd element has a higher atomic number.

Table 5. Theoretical and Experimental Effective Atomic Numbers of Glasses

Glass Code	662keV		1173keV		1332keV	
	Exp.	Calc.	Exp.	Calc.	Exp.	Calc.
TWNd1	26.4030	26.8714	22.3494	24.8830	23.5973	24.7400
TWNd3	26.7808	27.0754	24.7591	25.0716	25.3857	24.9275
TWNd5	27.2081	27.2678	25.1358	25.2507	25.4197	25.1055

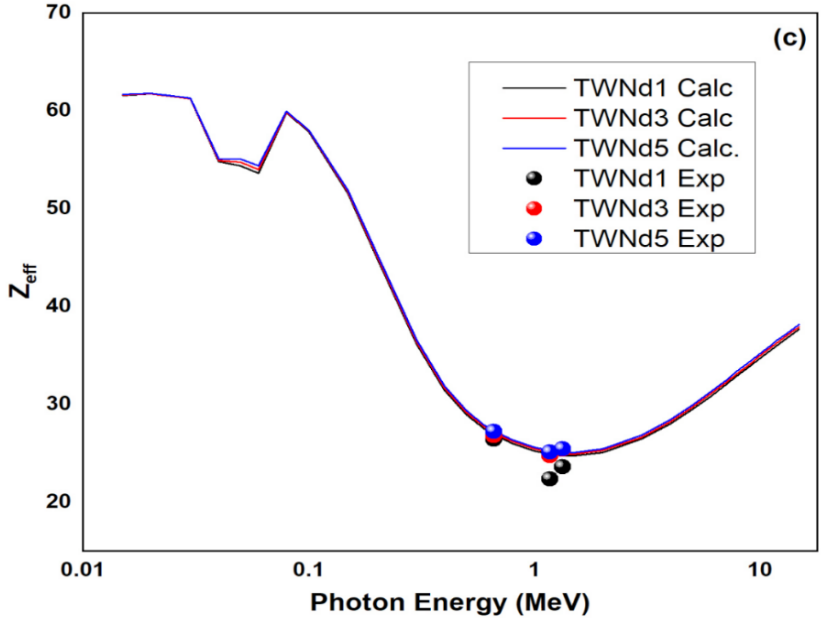

Figure 4. Variation of Z_{eff} Values of
Glass Materials According To Incident Photon Energy.

4. Conclusions

In this study, the radiation shielding properties of tungsten telluride glasses doped with Nd_2O_3 were investigated. The studied glass systems were successfully synthesized using conventional melt quenching technique. The mass attenuation coefficients, linear attenuation coefficients, half-value layer and effective atomic number values of the synthesized glass systems were determined both theoretically and experimentally. Increasing linear and mass attenuation coefficients, Z_{eff} values and decreasing HVL values showed that Nd_2O_3 doping enhances the radiation shielding properties of tungsten telluride glasses. The obtained shielding parameters of the studied glass systems are found to be compatible with those of undoped tungsten tellurite glasses given in

the literature (Caglar et al., 2021). The improved radiation shielding properties as a result of Nd_2O_3 doping are attributed to the higher atomic number of the element Nd compared to Te and W and increased glass densities. Especially TWNd5 glass showed superior radiation shielding properties among the studied glass systems and this glass system can be recommended as a candidate for shielding material in medical, industrial and nuclear applications.

Acknowledgement

This study was supported by the Scientific Research Projects Coordination Unit of Kafkas University with project numbered 2022-FM-65.

REFERENCES

Dong, M. G., Agar, O., Tekin, H. O., Kilicoglu, O., Kaky, K. M., & Sayyed, M. I. (2019). A comparative study on gamma photon shielding features of various germanate glass systems. *Composites Part B: Engineering*, *165*, 636-647.

Ersundu, A. E., Büyükyıldız, M., Ersundu, M. Ç., Şakar, E., & Kurudirek, M. J. P. N. E. (2018). The heavy metal oxide glasses within the WO3-MoO3-TeO2 system to investigate the shielding properties of radiation applications. *Progress in Nuclear Energy*, *104*, 280-287.

Bilir, G., Ozen, G., Tatar, D., & Öveçoğlu, M. L. (2011). Judd–Ofelt analysis and near infrared emission properties of the Er3+ ions in tellurite glasses containing WO3 and CdO. *Optics Communications*, *284*(3), 863-868.

Bilir, G., Mustafaoglu, N., Ozen, G., & DiBartolo, B. (2011). Characterization of emission properties of Er3+ ions in TeO2–CdF2–WO3 glasses. *Spectrochimica Acta Part A: Molecular and Biomolecular Spectroscopy*, *83*(1), 314-321.

Bilir, G., & Ozen, G. (2011). Optical absorption and emission properties of Nd3+ in TeO2–WO3 and TeO2–WO3–CdO glasses. *Physica B: Condensed Matter*, *406*(21), 4007-4013.

Bilir, G. (2015). Synthesis and spectroscopy of Nd3+-doped tellurite-based glasses. *International Journal of Applied Glass Science*, *6*(4), 397-405.

Çağlar, İ., Cengiz, G. B., & Bilir, G. (2021). Gamma radiation shielding properties of some binary tellurite glasses. *Journal of Non-Crystalline Solids*, *574*, 121139.

Bilir, G., Bilgici Cengiz, G., Çağlar, İ., & Ertap, H. (2022). Photon radiation shielding properties of germanate glass systems containing Bi2O3, PbF2, and B2O3. *International Journal of Applied Glass Science*, *13*(4), 729-737.

Bilir, G., Çağlar, İ., Cengiz, G. B., & Ertap, H. (2022). Synthesis of transparent binary germanate glasses and determination of their shielding performance against the gamma radiation. *Radiation Effects and Defects in Solids*, *177*(7-8), 768-782.

Cengiz, G. B., ÇAĞLAR, İ., & BİLİR, G. (2020). Gamma radiation shielding properties of natural glass obsidian. *Eskişehir Technical University Journal of Science and Technology A-Applied Sciences and Engineering*, *21*(4), 539-553.

CHAPTER VIII

SYNTHESIS OF MOO_3 MODIFIED ANTIMONY GLASSES AND ASSESSMENT OF THEIR GAMMA RADIATION SHIELDING PERFORMANCE

İlyas ÇAĞLAR[1]& Gülçin Bilgici CENGİZ[2]& Gökhan BİLİR[3] & Hüseyin ERTAP[4]

[1](Lecturer), Kafkas University, Kazım Karabekir Vocational School of Technical Sciences, Department of Electricity and Energy, 36100 Kars, Turkey
E-mail: ilyas.caglar@kafkas.edu.tr
ORCID: 0000-0002-6958-8469

[2](Assoc. Prof. Dr.), Kafkas University, Faculty of Science and Literature, Department of Physics, 36100 Kars, Turkey
E-mail: gulcincengiz@kafkas.edu.tr
ORCID: 0000-0002-6164-3232

[3](Assoc. Prof. Dr.), Kafkas University, Faculty of Science and Literature, Department of Physics, 36100 Kars, Turkey
ORCID: 0000-0003-1963-0902
E-mail: gbilirr@gmail.com

[4](Assoc. Prof. Dr.), Kafkas University, Faculty of Science and Literature, Department of Physics, 36100 Kars, Turkey
E-mail: huseyinertap@gmail.com
ORCID: 0000-0003-3896-6188

1. Introduction

The shielding materials for protection from the hazardous effects of ionizing radiation always stand as the main challenge for researchers since the discovery of the radiation and its applications like energy

harvesting, space technologies, nuclear medicine, etc. Radiation exposure has inevitable bad consequences for human beings and all living beings. Therefore, many materials have been used as shield materials for protection from the hazardous effects of the radiation and the search still continues for the non-toxic, light, flexible, and cost-effective radiation shielding materials to replace traditional shielding materials.

In recent years, heavy metal oxide glasses with characteristic properties like wide transparency interval in the visible to the mid-infrared range, good stability against devitrification, high thermal, mechanical and chemical durability, low melting temperatures, high refractive index, good non-linear optical characteristics, the high solubility of rare-earth ions, low phonon energies (Bilir et al., 2011a; Bilir et al. 2011b; Bilir and Ozen, 2011; Bilir et al., 2015), have attracted considerable attention for exploitation as for luminescent host materials and radiation shielding materials. Therefore, heavy metal oxide glasses, which includes more than 50% of a heavy metal cation, paved new routes on the way of materials for radiation shielding purposes. Many heavy metal oxide glass systems, like telluride (Çağlar et al., 2021), germanate (Bilir et al., 2022a; Bilir et al., 2022b), bismuth borate (Alajerami et al., 2020) etc., modified with different network modifiers, have been widely investigated both experimentally and theoretically in the literature for radiation shielding purposes. Most of these studied glass systems have shown good gamma-ray attenuation properties compared to the commercially available shielding materials (Çağlar et al., 2021; Bilir et al., 2022a; Bilir et al., 2022b; Alajerami et al., 2020). Among these glass systems, antimony oxide (Sb_2O_3) based glass systems are one of the major classes of heavy metal oxide glasses, and its glass-forming ability was firstly predicted by Zachariasen (1932). Antimony glasses are characterized by some unique properties like all heavy metal oxide glasses are (Zachariasen, 1932; Nalin et al., 2001; Ouannes et al., 2013; Soltani et al., 2009; Soltani et al., 2013). All these excellent properties of antimony-based glasses make them a good candidate for radiation shielding purposes besides they are already a good host material for photonics applications. In this respect, we have studied the gamma radiation shielding properties of antimony glasses modified with different amounts of MoO_3. To do so, we have measured the linear attenuation coefficient, mass attenuation coefficient, half-value layer, and effective atomic number values of the glasses at gamma-ray energies of 662, 1173, and 1332 keV in a narrow-beam transmission geometry and employed WinXCOM (Gerward et al., 2004) software to verify those measured parameters.

2. Experimental Part

Antimony oxide-based glasses modified with MoO_3 in different molar ratios (10 – 30%) were synthesized using the conventional melting and quenching method. The starting reagents (Sb_2O_3 and MoO_3) with the purities not less than 99 % were purchased from Sigma Aldrich and used without any further purification. The appropriate molar amounts of the oxide powders were mixed thoroughly in an agate mortar and transferred into quartz crucibles with a lid for the melting process. The glass melts were obtained by melting the mixtures using a muffle furnace (Protherm PLF150 model) at temperatures given in Table 1. The glass melts were then casted onto a brass plate and pressed by another one. The obtained glass samples were then ground and polished well to form two parallel surfaces to perform the gamma-ray transmission experiments.

The densities of synthesized glasses were measured by Archimedes' principle using ultrapure water as the buoyancy liquid and a high precision scale with a sensitivity of 10^{-4}g. The densities of the samples are also given in Table 1.

In order to verify the vitreous nature of the synthesized materials, XRD measurements were performed using a Philips PW 1830/40 model X-Ray Diffractometer (Cu Kα radiation) in the 40 kV and 30 mA settings in a 2θ interval of 2°–70° with a scanning step of 0.01°.

The details regarding the experimental setup for the radiation shielding parameters measurement, and theoretical calculations are given in our earlier works (Çağlar et al., 2021; Cengiz and Çağlar, 2020).

3. Results and Discussion

In this study, we synthesized and investigated the gamma radiation shielding properties of some antimony-based glasses. Experimentally measurements were performed for energies of 0.662, 1.173 and 1.332 MeV obtained from ^{137}Cs and ^{60}Co radioactive sources, respectively. Theoretical calculations for the same gamma ray energies were performed using the WinXCOM program. In order to comprehensively evaluate the usability of the studied glasses as radiation shielding, the radiation shielding parameters of the studied glasses were compared with those of some standard armor materials. The shielding parameters of RS-253 G18 glass (Kaur et al., 2019) and ordinary (OC), hematite-serpentine (HS), and steel-magnetite (SM) concretes (Bashter, 1997) were calculated for the studied energies with the help of the WinXCOM program.

Figure 1 shows the XRD pattern of the SbMo20 sample. The pattern only consists of an amorphous hump which is the indicator of the glassy nature of the sample, no crystalline phase is seen in the pattern.

Table 1. The glass code, composition, molar mass, molar volume, melting temperature, density, and thickness of the synthesized glasses

Sample Code	Glass Compositions mole %		Molar Weight M (g mol^{-1})	Melting Temperature (°C)	Thicknesses (mm)	Density d (g/cm^3)	Molar Volume V_m (cm^3 mol^{-1})
	Sb_2O_3	MoO_3					
SbMo20	80	20	262	700 – 750	1.18	4.898	53.49
SbMo30	70	30	247.25		1.91	4.858	50.90
SbMo40	60	40	232.49		1.60	4.837	48.06

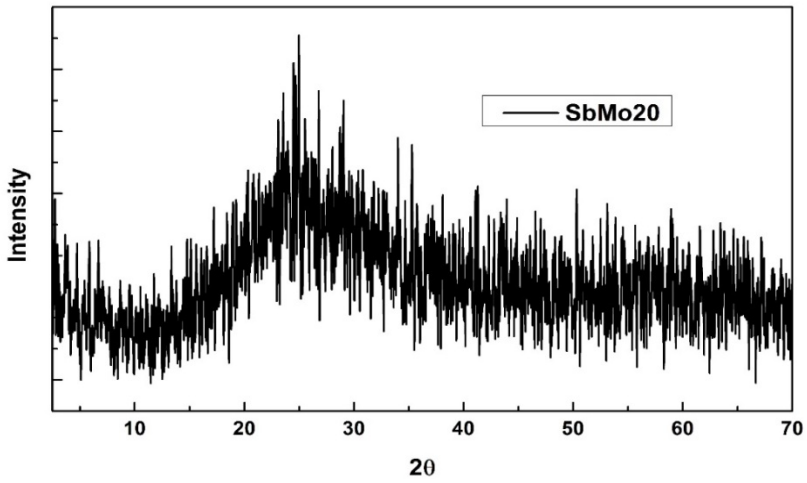

Figure 1. XRD patterns of SbMo20 glass sample.

The experimentally measured mass absorption coefficients (μ_m) of the investigated antimony-based glasses are given in Table 2 together with the theoretical results. At 6.62 MeV, the maximum and minimum μm values were found for SbMo20 and SbMo40 samples, respectively. At 1.173 and 1.332 MeV gamma energies, the highest μ_m values were found for SbMo40, while the smallest value was found for SbMo20 glass. It is clear from the experimental and theoretical results that the μ_m values vary depending on the increase in the

amount of molybdenum oxide in the synthesized glasses. At 0.662 MeV gamma energy, a decrease in μ_m values was observed with the increase in the amount of MoO_3. At 1.173 and 1.332 MeV gamma energies, μ_m values slightly increase with the increase in the amount of molybdenum oxide.

Table 2. Experimental and theoretical mass attenuation coefficients (μ_m) of the synthesized antimony based glasses at 0.662, 1.173, and 1.332 MeV gamma-ray energies.

Glass Codes	Mass Attenuation Coefficients (cm^2/g)					
	0.662 MeV		1.173 MeV		1.332 MeV	
	Experimental	Theoretical	Experimental	Theoretical	Experimental	Theoretical
SbMo20	0.0763 ± 0.0037	0.0760	0.0530 ± 0.0040	0.0539	0.0495 ± 0.0038	0.0503
SbMo30	0.0759 ± 0.0023	0.0759	0.0542 ± 0.0031	0.0540	0.0499 ± 0,0030	0.0504
SbMo40	0.0755 ± 0.0028	0.0758	0.0557 ± 0.0037	0.0541	0.0500 ± 0,0033	0.0505

Table 3 lists the experimental and theoretical μ results of the synthesized antimony-based glasses. As with μ_m values, it is clear from table 3 that there is agreement between the theoretical and experimental results of μ values. It was observed that the experimental and theoretical μ values of the glasses synthesized at all gamma-ray energies decreased slightly with the increase in the amount of molybdenum oxide. This decrease can be explained by the decrease in the density of the glasses with the increase in the amount of molybdenum oxide. Contrary to the mass attenuation coefficient results, it can be clearly seen from Table 2 that SbMo20 glass has higher μ values than other samples at all experimentally studied gamma energies.

Table 3. Experimental and theoretical linear attenuation coefficients (μ) of the synthesized antimony based glasses at 0.662, 1.173, and 1.332 MeV gamma-ray energies.

Glass Codes	Linear Attenuation Coefficient (cm^{-1})					
	0.662 MeV		1.173 MeV		1.332 MeV	
	Experimental	Theoretical	Experimental	Theoretical	Experimental	Theoretical
SbMo20	0.3736±0.0182	0.3720	0.2627±0.0196	0.2639	0.2425±0.0094	0.2464
SbMo30	0.3688±0.0111	0.3687	0.2620±0.0143	0.2622	0.2423±0.0088	0.2448
SbMo40	0.3650±0.0138	0.3667	0.2610±0.0142	0.2616	0.2419±0.0094	0.2444

The variation of experimentally measured and theoretically calculated μ results of the investigated glasses against photon energy from 15keV to 15 MeV is plotted in Figure 2. It can be seen from Figure 2 that the linear attenuation coefficient for all glasses has a similar behaviour with the incident photon energy. The results showed that the sample coded SbMo20 had the highest μ values at all photon energies. This case can be attributed to the elemental composition and material characteristics of the SbMo20 sample. Because materials with higher atomic numbers and higher density provide more effective shielding against gamma radiation (AbuAlRoos et al. 2019).

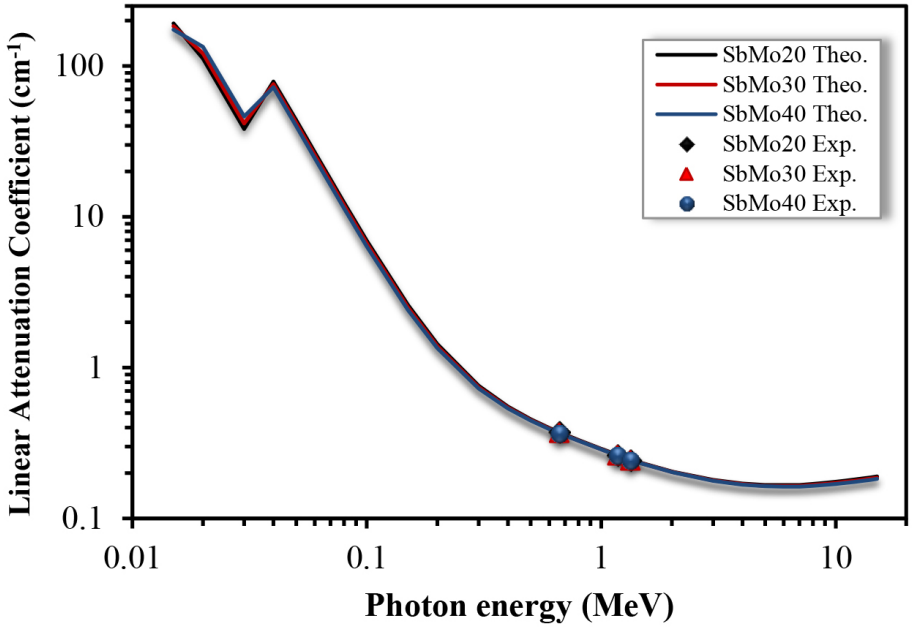

Figure 2. Experimental and theoretical μ values antimony based glasses as a function of gamma-ray energy.

As seen in Figure 2, in the low energy region up to 0.8 MeV, the μ values decrease dramatically with the increase in photon energy. In addition, with the increase of MoO_3 modifier concentration from 20% mol to %40 mol in glass samples, μ values decrease proportionally. These changes can be explained by the fact that photoelectric absorption is the dominant interaction type at low energies. The interaction cross section for photoelectric absorption varies with the photon energy as $E^{-3.5}$ and with the atomic number as Z^4 (Alım et al., 2020; Al-Buriahi et al., 2021; Kaky et al., 2020). On the other hand, some discontinuous

peaks were observed in the low photon energy region. These discontinuous peaks can be attributed to the k absorption edges of Mo and Sb corresponding to 20.00 and 30.49 keV, respectively. In the 0.8-5 MeV energy range, μ values tend to decrease more slowly against the increase in photon energy, and the elemental composition of the glasses has less effect on μ values. This is due to Compton scattering gradually becoming the dominant interaction mechanism in this region. Because the Compton scattering cross section changes inversely to the photon energy (E^{-1}) and linearly with the atomic number Z (Alım et al., 2020; Al-Buriahi et al., 2021; Kaky et al., 2020). At energies greater than 5 MeV (i.e. in the high energy region), pair production becomes the dominant interaction type and μ values increase slowly with increasing photon energy up to 15 MeV.

Fort the studied gamma ray energies, the comparison linear attenuation coefficients of the investigated antimony-based glasses with those of standard armor materials are given in Figure 3,4 and 5. It was observed that the μ values of the examined samples were quite higher than the values of RS-253 G18, OC and HS materials at all gamma energies. On the other hand, the values of the SM material are very close to the μ values of the glasses studied.

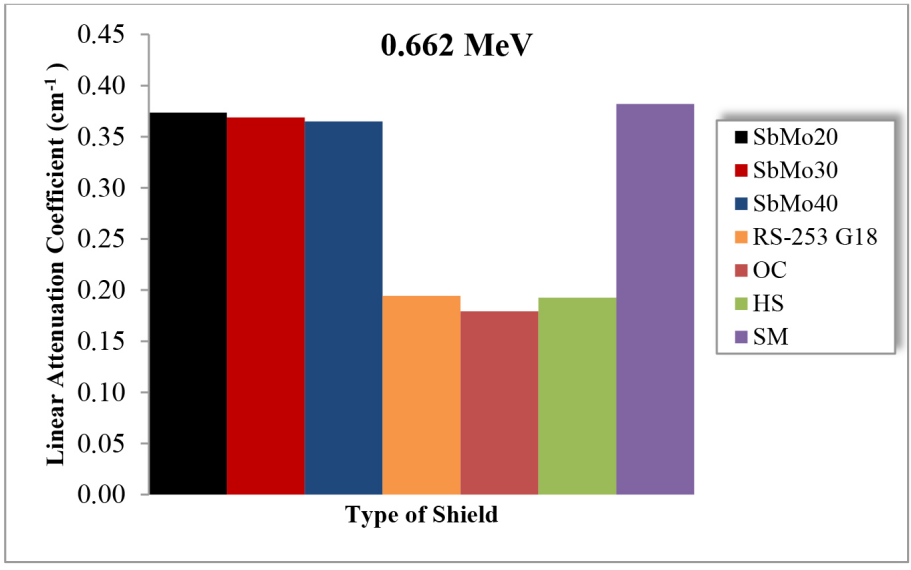

Figure 3. The comparison of the experimental μ values for studied glasses with those of standard shielding materials at 0.662 MeV.

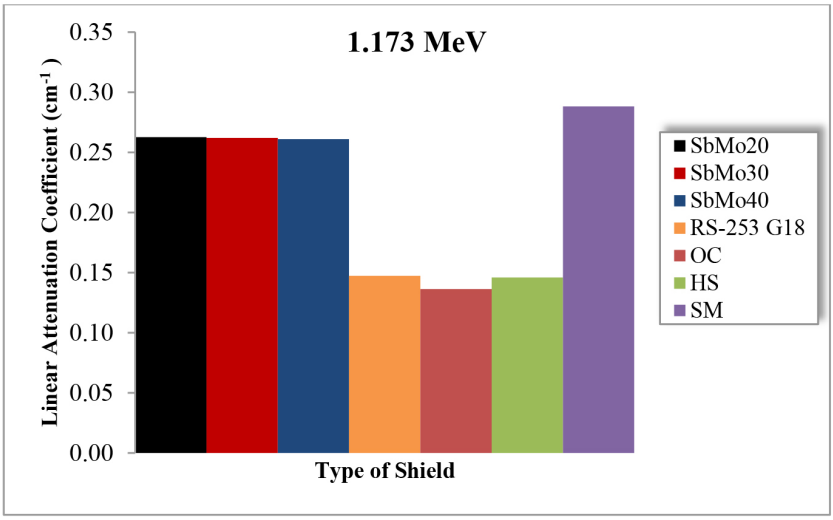

Figure 4. The comparison of the experimental μ values for studied glasses with those of standard shielding materials at 1.173 MeV.

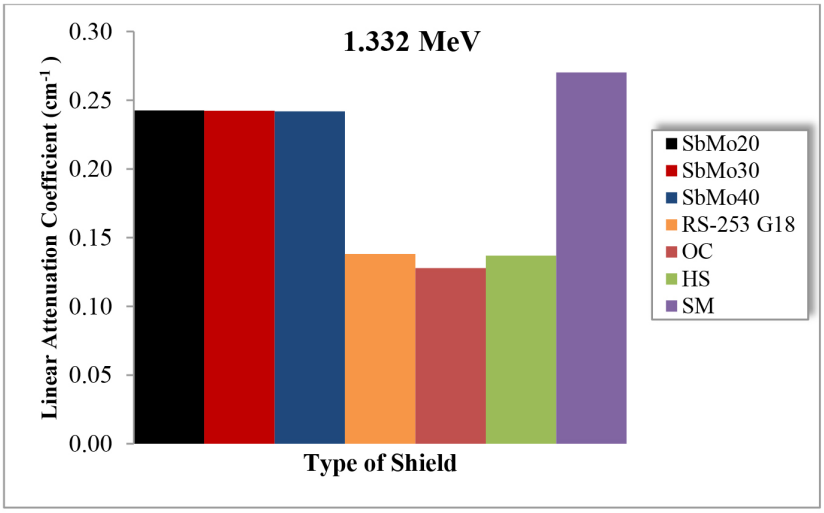

Figure 5. The comparison of the experimental μ values for studied glasses with those of standard shielding materials at 1.332 MeV.

The half value layer (HVL) is one of the most used parameters to evaluate the penetration ability of radiation into materials and the radiation shielding performance of materials (Waly et al., 2018). The half value layer is defined as the thickness of a material required to halve the gamma-ray intensity interacting with the material (Yaykaşlı et al. 2022). It has been reported that materials with lower HVL values have higher shielding performance (Aygun and Aygün,

2021; Aygun and Aygün, 2023). Fort the investigated antimony-based glasses, experimental HVL values range from 1.855±0.090 to 1.899±0.072 cm for 0.662 MeV, 2.638±0.197 to 2.655±0.145 cm for 1.173 MeV and 2.858±0.113 to 2.865±0.118 cm for 1.332 MeV, respectively. In Figures 6, 7 and 8, the experimental HVL results obtained for the synthesized glasses were compared with those of the standard armor materials we mentioned above.

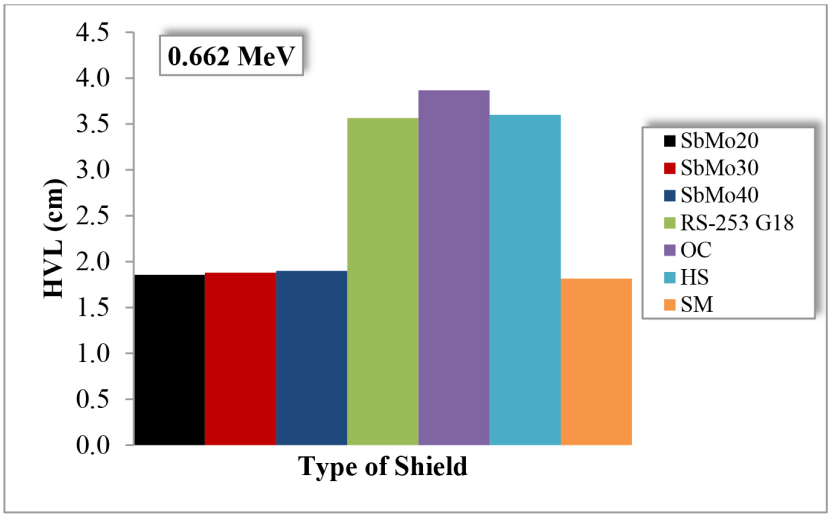

Figure 6. The comparison of the experimental HVL values for studied glasses with those of standard shielding materials at 0.662 MeV.

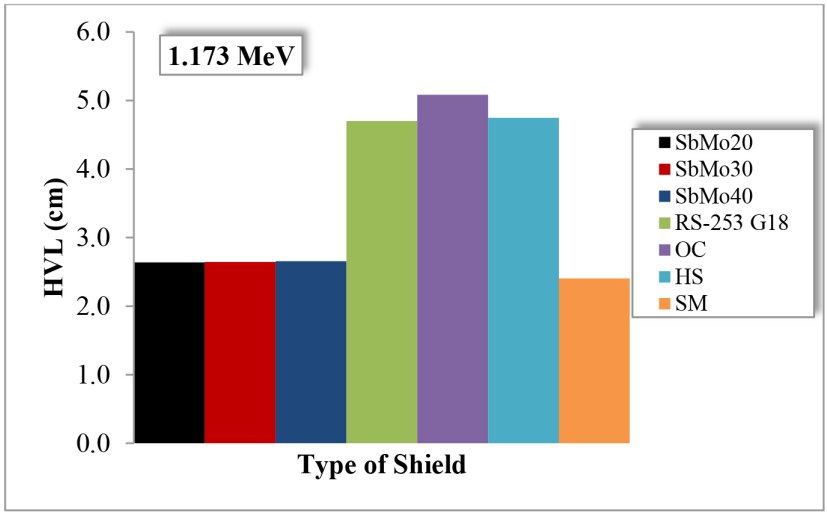

Figure 7. The comparison of the experimental HVL values for studied glasses with those of standard shielding materials at 1.173 MeV.

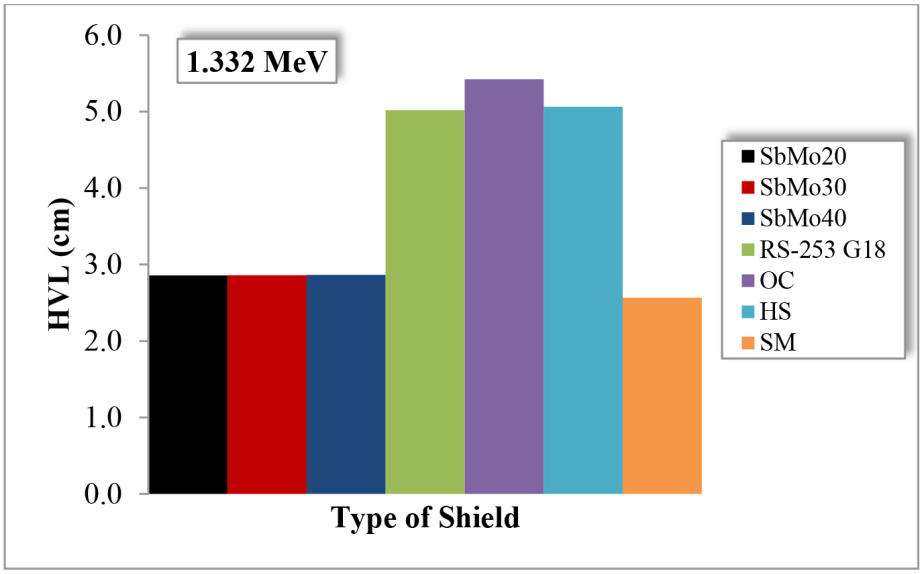

Figure 8. The comparison of the experimental HVL values for studied glasses with those of standard shielding materials at 1.332 MeV.

The HVL values of RS-253 G18, OC, HS and SM were also found as 3.566, 3.867, 3.599 and 1.814 cm for 6.62 MeV, 4.701, 5.083, 4.746 and 2.405 cm for 1.173 MeV and 5.017, 5.423, 5.064 and 2.565 cm for 1.332 MeV, respectively. When Figures 6, 7 and 8 are evaluated together, it is seen that HVL values increase with increasing gamma ray energy, as expected based on the values of linear attenuation coefficients. In addition, it is clear that there is an increase in HVL values with the increase in MoO_3 concentration. As can be seen from these figures, the experimental HVL values of the studied glasses at all gamma ray energies are considerably smaller than those of RS-253 G18 glass and OC and HS. Furthermore, the HVL values of SM concrete are slightly smaller than those of the glass we analysed.

The effective atomic number (Z_{eff}) is one of the important parameters to be taken into account when evaluating the ability of materials to protect against ionizing radiation. The Z_{eff} values for the synthesized glasses were found theoretically and experimentally at 6.62, 1.173 and 1.332 MeV photon energies. For a more detailed evaluation, the Z_{eff} values of the studied glasses were calculated in the energy range of 15 keV to 15 MeV and are present graphically in Figure 9.

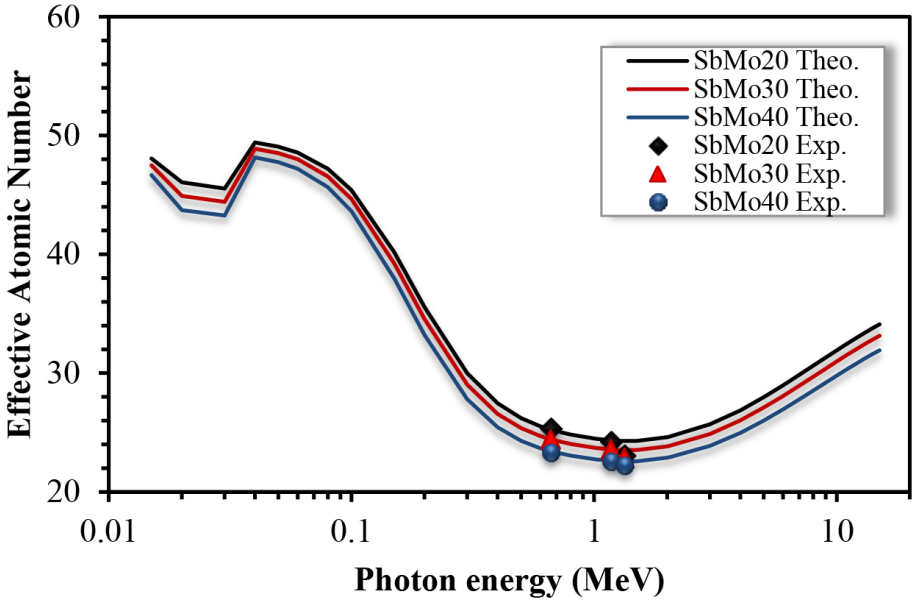

Figure 9. Experimental and theoretical Z_{eff} values antimony based glasses as a function of gamma-ray energy.

As can be seen in Figure 9, Z_{eff} values are quite high in the low energy region and decrease dramatically with increasing photon energy up to 0.8 MeV. Two sudden jumps are observed at energies of about 20.00 and 30.49 keV, corresponding to the absorption edge of Mo and Sb, respectively. In the middle energy region, corresponding to the energy range from 0.8 MeV to 5 MeV, Z_{eff} values decrease more slowly with increasing photon energy. At energies greater than 5 MeV, Z_{eff} values increase slowly with increasing photon energy.

The Z_{eff} values of RS-253 G18, OC, HS and SM were found to be 10.056, 8.631, 9.203 and 15,508 for 6.62 MeV, 10.026, 8.626, 9.178 and 15.448 for 1.173 MeV and finally 10.025, 8.627, 9.181 and 15.452 for 1.332 MeV, respectively. On the other hand, the comparison of the Z_{eff} values of antimony-based glasses with those of standard armor materials for 6.62, 1.173 and 1.332 MeV gamma energies given in Figures 10, 11 and 12 respectively.

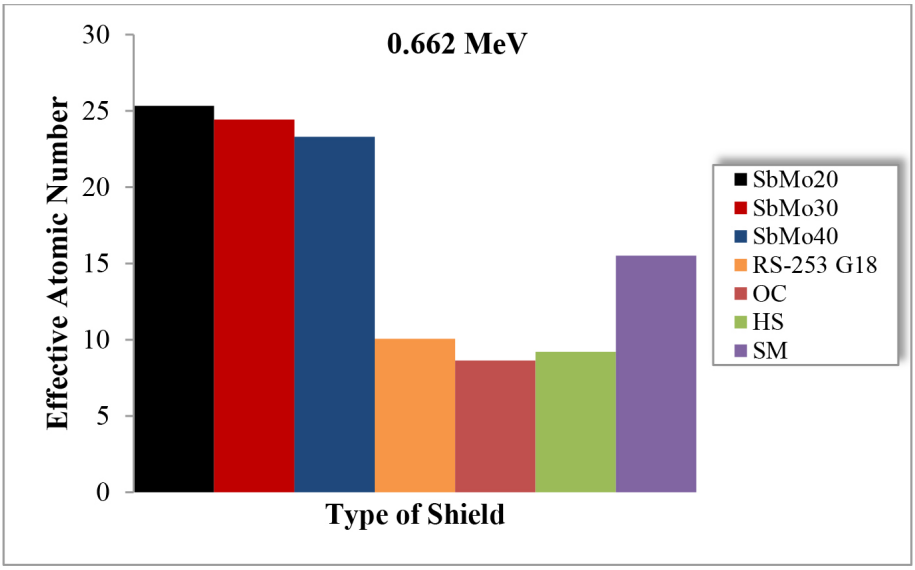

Figure 10. The comparison of the experimental Z_{eff} values for studied glasses with those of standard shielding materials at 0.662 MeV.

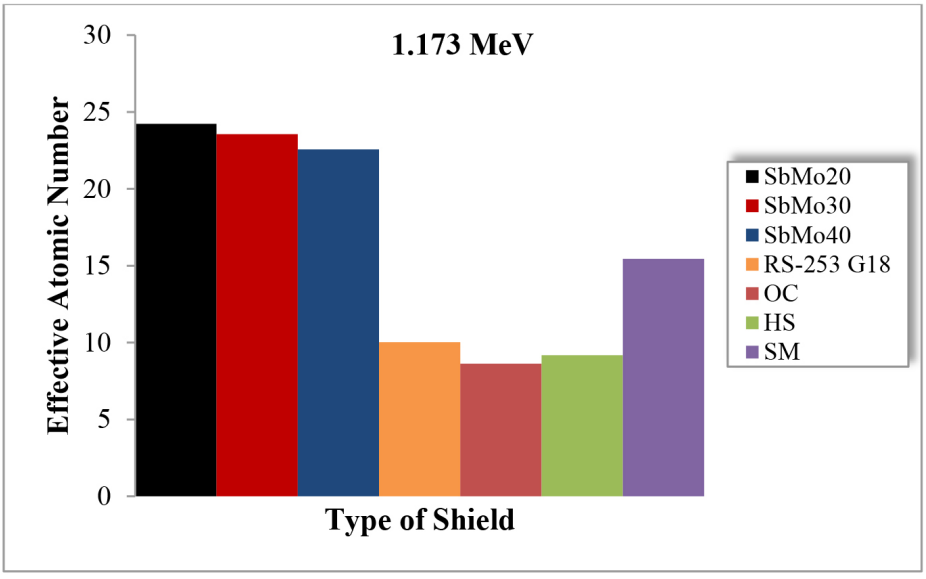

Figure 11. The comparison of the experimental Z_{eff} values for studied glasses with those of standard shielding materials at 1.173 MeV.

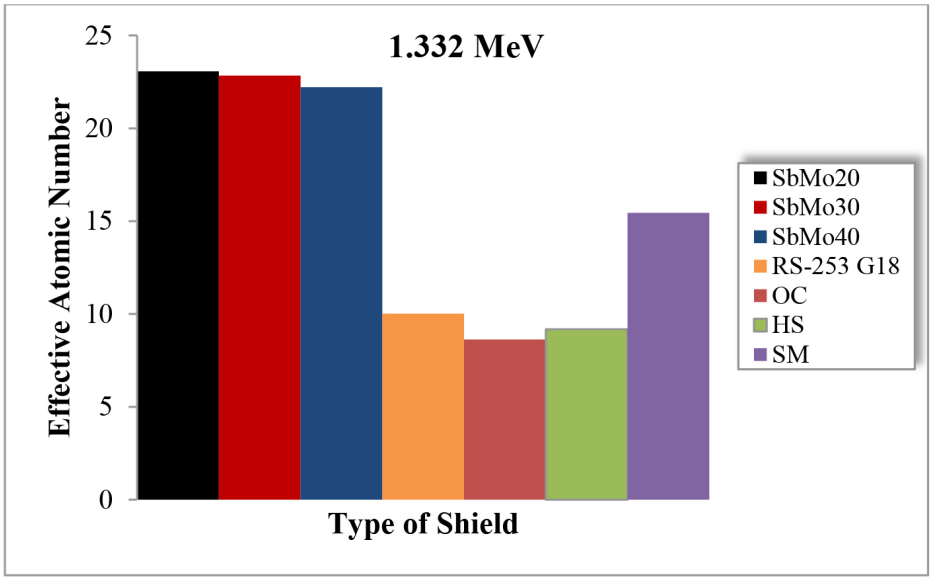

Figure 12. The comparison of the experimental Zeff values for studied glasses with those of standard shielding materials at 1.332 MeV.

When the Z_{eff} results of the antimony based glasses we synthesized were compared with those of the standard materials, it was observed that the Z_{eff} values of all samples were considerably higher than those of RS-253 G18, OC, HS and SM at 0.662, 1.173 and 1.332 MeV gamma energies. This reveals that the glasses we synthesized can be used as armor materials against ionizing radiation.

4. Conclusion

Today, radiation is widely used in various advanced technologies such as medical, nuclear and industrial applications (Lakshminarayana et al., 2020). This large-scale use of radiation can pose many health risks to those working with radiation, patients, and the public exposed to radiation (Al-Buriahi, 2023). In this context, many researchers have focused on developing radiation shielding materials to protect people from the harmful effects of ionizing radiation. In this study, we produced antimony oxide-based glasses containing different molar ratios of MoO_3 using the traditional melt-quenching method and experimentally investigated their gamma radiation absorption performance. Experimental investigations were performed for 0.662, 1.173 and 1.332 MeV gamma energies

emitted from ^{137}Cs and ^{60}Co radioactive point sources, respectively. Theoretical calculations were also carried out through the WinXCOM program. According to the theoretical and experimental findings, it was concluded that the MoO_3 concentration is of great importance for the radiation shielding properties and that the sample exhibiting the highest density and the lowest MoO_3 concentration has better shielding capacity for gamma rays than the others. In addition, when the results obtained are compared with some commonly used standard shielding materials, it is seen that the synthesized glasses can be recommended for gamma radiation shielding applications.

References

AbuAlRoos, N. J., Amin, N. A. B., Zainon, R. (2019). Conventional and new lead-free radiation shielding materials for radiation protection in nuclear medicine: A review. Radiation Physics and Chemistry, 165, 108439.

Alajerami, Y. S., Drabold, D., Mhareb, M. H. A., Cimatu, K. L. A., Chen, G., Kurudirek, M. (2020). Radiation shielding properties of bismuth borate glasses doped with different concentrations of cadmium oxides. Ceramics International, 46(8), 12718-12726.

Al-Buriahi, M. S., Alzahrani, J. S., Olarinoye, I. O., Mutuwong, C., Elsaeedy, H. I., Alomairy, S., Tonguç, B. T. (2021). Effects of reducing PbO content on the elastic and radiation attenuation properties of germanate glasses: a new non-toxic candidate for shielding applications. Journal of Materials Science: Materials in Electronics, 32(11), 15080-15094.

Al-Buriahi, M. S. (2023). Radiation shielding performance of a borate-based glass system doped with bismuth oxide. Radiation Physics and Chemistry, 207, 110875.

Alım, B., Şakar, E., Baltakesmez, A., Han, İ., Sayyed, M. I., Demir, L. (2020). Experimental investigation of radiation shielding performances of some important AISI-coded stainless steels: Part I. Radiation Physics and Chemistry, 166, 108455.

Aygun, Z., Aygün, M. (2021). A theoretical study on radiation shielding characteristics of magnetic shielding alloys, Ni80Fe15Mo5 and Ni77Fe14Cu5Mo4, by determining the photon attenuation parameters in the energy range of 15keV-100GeV. Karaelmas Fen ve Mühendislik Dergisi, 11(2), 165-173.

Aygun, Z., Aygün, M. (2023). Evaluation of radiation shielding potentials of Ni-based alloys, Inconel-617 and Incoloy-800HT, candidates for high

temperature applications especially for nuclear reactors, by EpiXS and Phy-X/PSD codes. Journal of Polytehnic, 26(2): 795-801.

Bashter, I. I. (1997). Calculation of radiation attenuation coefficients for shielding concretes. Annals of nuclear Energy, 24(17), 1389-1401.

Bilir, G., Bilgici Cengiz, G., Çağlar, İ., Ertap, H. (2022a). Photon radiation shielding properties of germanate glass systems containing Bi2O3, PbF2, and B2O3. International Journal of Applied Glass Science, 13(4), 729-737.

Bilir, G., Çağlar, İ., Cengiz, G. B., Ertap, H. (2022b). Synthesis of transparent binary germanate glasses and determination of their shielding performance against the gamma radiation. Radiation Effects and Defects in Solids, 177(7-8), 768-782.

Bilir, G., Mustafaoglu, N., Ozen, G., DiBartolo, B. (2011a). Characterization of emission properties of Er^{3+} ions in TeO_2–CdF_2–WO_3 glasses. Spectrochimica Acta Part A: Molecular and Biomolecular Spectroscopy, 83(1), 314-321.

Bilir, G., Ozen, G. (2011). Optical absorption and emission properties of Nd^{3+} in TeO_2–WO_3 and TeO_2–WO_3–CdO glasses. Physica B: Condensed Matter, 406(21), 4007-4013.

Bilir, G., Ozen, G., Tatar, D., Öveçoğlu, M. L. (2011b). Judd–Ofelt analysis and near infrared emission properties of the Er^{3+} ions in tellurite glasses containing WO_3 and CdO. Optics Communications, 284(3), 863-868.

Bilir, G. (2015). Synthesis and spectroscopy of Nd3+-doped tellurite-based glasses. International Journal of Applied Glass Science, 6(4), 397-405.

Cengiz, G. B., Çağlar, İ. (2020). Assessment of Mass Attenuation Coefficient, Effective Atomic Number and Electron Density of Some Aluminum Alloys. Caucasian Journal of Science, 7(2), 109-122.

Çağlar, İ., Cengiz, G. B., Bilir, G. (2021). Gamma radiation shielding properties of some binary tellurite glasses. Journal of Non-Crystalline Solids, 574, 121139.

Gerward, L., Guilbert, N., Jensen, K. B., Levring, H. (2004). WinXCom—a program for calculating X-ray attenuation coefficients. Radiation physics and chemistry, 71(3-4), 653-654.

Kaky, K. M., Sayyed, M. I., Mhareb, M. H. A., Abdalsalam, A. H., Mahmoud, K. A., Baki, S. O., Mahdi, M. A. (2020). Physical, structural, optical and gamma radiation attenuation properties of germanate-tellurite glasses for shielding applications. Journal of Non-Crystalline Solids, 545, 120250.

Kaur, P., Singh, K. J., Thakur, S., Singh, P., Bajwa, B. S. (2019). Investigation of bismuth borate glass system modified with barium for structural

and gamma-ray shielding properties. Spectrochimica Acta Part A: Molecular and Biomolecular Spectroscopy, 206, 367-377.

Lakshminarayana, G., Kumar, A., Lira, A., Dahshan, A., Hegazy, H. H., Kityk, I. V., Park, T. (2020). Comparative study of gamma-ray shielding features and some properties of different heavy metal oxide-based tellurite-rich glass systems. Radiation Physics and Chemistry, 170, 108633.

Nalin, M., Poulain, M., Poulain, M., Ribeiro, S. J., Messaddeq, Y. (2001). Antimony oxide based glasses. Journal of non-crystalline solids, 284(1-3), 110-116.

Ouannes, K., Lebbou, K., Walsh, B. M., Poulain, M., Alombert-Goget, G., Guyot, Y. (2017). Antimony oxide based glasses, novel laser materials. Optical Materials, 65, 8-14.

Soltani, M., Hamzaoui, M., Houhou, S., Touiri, H., Bediar, L., Ghemri, A., Petkova, P. (2013). Physical Characterization of Sb2O3-M2O-MoO3 (M= Li, K) New Glasses. Acta Physica Polonica A, 123(2), 227-229.

Soltani, M. T., Djouama, T., Boutarfaia, A., Poulain, M. (2009). New heavy metal oxide glasses based on Sb2O3. In J. Optoelectron. Adv. Mater. Symp (Vol. 1, pp. 339-342).

Waly, E. S. A., Al-Qous, G. S., Bourham, M. A. (2018). Shielding properties of glasses with different heavy elements additives for radiation shielding in the energy range 15–300 keV. Radiation Physics and Chemistry, 150, 120-124.

Yaykaşlı, H., Eskalen, H., Kavun, Y., Gögebakan, M. (2022). Microstructural, thermal, and radiation shielding properties of Al50B25Mg25 alloy prepared by mechanical alloying. Journal of Materials Science: Materials in Electronics, 33(5), 2350-2359.

Zachariasen, W. H. (1932). The atomic arrangement in glass. Journal of the American Chemical Society, 54(10), 3841-3851.

ISBN 978-2-38236-641-7